TRANSIENT ELECTRIC BIREFRINGENCE OF MACROMOLECULAR SYSTEMS

by

P.J. RUDD, B.Sc.

This thesis was submitted in fulfilment
of the requirements for the degree of
Doctor of Philosophy
Brunel University

February 1974.

To

My wife, Sheilagh, and

son, Andrew James.

My Parents.

ABSTRACT

The transient electric birefringence method, i.e. the transient Kerr effect, has been employed to study the optical, electrical and geometrical properties of three macromolecular systems. An apparatus is described in which the birefringence could be measured when d.c. electric field pulses (of duration 1 μs to 5 s and strength up to 50 KV/cm) and a.c. electric field pulses (of duration greater than 5 ms, of frequency up to 20 kHz, and strength up to 3 KV/cm) were applied to solutions of macromolecules.

Both the linear and quadratic optical systems have been employed to measure the induced birefringence. A theoretical analysis and review of the errors implicit in such measurements is given, with suggested alignment and calibration procedures.

For the first time in electro-optic work, a data-logging system and computer program have been developed and employed, and enabled the automatic recording of transient responses with subsequent high speed data analysis.

Measurements have been made on a polypeptide poly - β - benzyl - l - aspartate in two solvents. These show how the method can be used to study a rigid macromolecule.

A novel investigation was made on the interaction of an anionic surfactant, sodium dodecyl sulphate, with a flexible polymer, polyvinylpyrrolidone. The large variation of Kerr constant observed with addition of surfactant indicated a great potential use of this method for studying polymer surfactant interactions.

An aqueous suspension of the bacteria E. coli was also studied, but changes in turbidity and not birefringence were the origin of the observed effects. Novel practical methods of investigation, and turbidity calculations carried out with the aid of a computer enabled size parameters and electrical properties to be determined for E. coli. For the first time such results were in agreement with electro-optic light scattering measurements.

CONTENTS

CHAPTER 1

Transient electric birefringence of macromolecular systems; a physical interpretation and historical background.

The optical behaviour of some materials can be altered if they are subjected to an electric field. If transient electric fields are applied then the rate of change of the optical effect can be observed. Transient electro-optic methods can therefore allow the electrical, optical and geometrical properties of macromolecules in solution to be simultaneously determined. Of such methods, transient electric birefringence, i.e. the Kerr effect, is the longest established, most understood and generally most applicable and sensitive method.

It was John Kerr who in 1875[1] discovered that a normally isotropic system such as a glass or a liquid would become doubly refracting when placed in an electric field. For instance in the absence of an electric field both the solute and the solvent molecules in a solution are randomly orientated by virtue of Brownian motion. On application of a uniform electric field electrically assymmetric molecules will become partially orientated with respect to the field direction. If the individual molecules are optically assymmetric or even if the molecules only have an elongated shape, the solution itself may become doubly refracting. Moreover because the molecules are randomly distributed about the field direction and not along it, the solution acts as a uniaxial birefringent medium with its optic axis in the

field direction.

Molecules have generally a permanent dipole moment and an anisotropy of polarisation which gives rise to a dipole moment in an electric field. Both the permanent and induced electric dipole moments of a molecule generally increase with the size of the molecule. Correspondingly, the contribution to the total birefringence of the solution is much greater for the large macromolecules than for the small solvent molecules. This does not mean that the effect of the solvent can at all times be neglected but rather that small concentrations of solute macromolecules can be studied.

The actual quantity called the birefringence, Δn, is given by

$$\Delta n = n_{//} - n_{\perp}$$

where $n_{//}$ and $n_{\perp}$ are the refractive indices of the medium as measured for light polarised with its electric vector parallel and perpendicular respectively to the field direction on which it is incident normally.

Kerr discovered that it was related to the electric field strength, E, at low values by the relation

$$\Delta n = B\lambda E^2$$

where λ is the wavelength of the incident light in vacuo.

The Kerr constant, B, is a product of the optical anisotropy factor and a term involving the values of the permanent dipole moment and electrical polarisability of the molecule. The magnitude of the Kerr constant can therefore

only be used to determine the optical anisotropy factor if the electrical term has been determined using other methods such as dielectric techniques. Correspondingly the magnitude of the electrical term can be determined only if methods such as flow birefringence or depolarisation of scattered light have furnished a value for the optical anisotropy factor.

However the saturation of birefringence with increasing field strength can be used to separately determine both terms. This is true even if full orientation of the macromolecules, where the magnitude of the birefringence is solely dependent on the optical anisotropy factor, has not been reached. This method has been used in the present work on a polypeptide in Chapter 5.

Prior to 1950[2,3] continuous d.c. electric fields were almost always employed with optical arrangements which could be manually adjusted to compensate for and hence measure the steady induced birefringence. By far the largest amount of measurements were performed on gases and liquids.[4] However for work on highly conducting systems, such as colloids and viruses in aqueous solution, alternating fields were used. The results obtained were, to a large part, uninterpretable, but at least relaxation effects could be observed and information gained about particle size, as this important molecular parameter is related to the rate of orientation of a molecule in a viscous medium.

About 1950 two sets of workers[5,6] began to orientate molecules with single shot pulses of d.c. voltage and of sufficient time duration for the birefringence to reach its

steady state value. The geometrical properties of the macromolecules could be determined from the rate of decay of birefringence after the termination of the pulse. It was this latter feature which proved to be a great advance for the method. To observe the accompanying rapid changes in birefringence two optical systems were and have been employed with a photoelectric detecting system. An aspect of the present work, which is described in Chapter 3, has been to determine the errors introduced by misalignment of the optical systems and hence to give simple but accurate alignment procedures. By the nature of the method data can be quickly amassed. Previous methods of analysis have been laboriously slow but in the present work data-logging equipment and computer analysis have meant rapid interpretation of results, as shown in Chapter 4.

In the past the transient birefringence method has been successfully employed on a large number of macromolecular systems.[7,8,9] One important class of system which has so far received very poor attention by workers in this field is the interaction of surfactants with macromolecules. Work on such a system is reported in Chapter 6 and demonstrates a great potential use of the method.

Changes in other optical properties such as absorption,[9] optical activity,[10] depolarisation of fluorescence,[11] and light scattering[12] may all occur when the molecules orientate in the applied field. When they do some correction should be applied to the birefringence results. One material

studied herein was a suspension of the bacteria E. coli. It is shown that in this case the amount of light scattered accounts for the observed effects. The work in Chapter 7 describes practical methods and a theoretical analysis which allow useful information to be obtained in such a situation.

Throughout this thesis c.g.s. units are used in accord with the common practice in electro-optic studies. To comply with the current desire for rationalisation a conversion table to S.I. units is presented in Appendix 2.

References

1) Kerr (J.), Phil. Mag. 50, 337, 1875.

2) Beams (J.W.), Rev. Mod. Phys. 4, 133, 1932.

3) Le Fevre (C.G.), Le Fevre (C.G.) In 'Techniques of Organic Chemistry', 3rd Edition, Part III, Ed. Weissberger, Pub. Interscience.

4) International Critical Tables Vol. 7, 109.

5) Benoit (H.), Ann. de Phys. (Paris) 6, 561, 1951.

6) O'Konski (C.T.), Zimm (B.H.) Science 111, 113, 1950.

7) O'Konski (C.T.), In 'Encyclopaedia of Polymer Science and Technology', Ed. N. Bikales, vol. 9, p.551 pub. Wiley.

8) Watanabe (H.) In 'Physical Principles & Techniques of Protein Chemistry' Ed. S. Leach, pub. Academic Press, ch. 7, 1969.

9) Fredericq (E.), Houssier (C.), 'Electric Dichroism and Electric Birefringence' pub. Clarendon Press, Oxford, 1973.

10) Baily (E.D.), Jennings (B.R.), J. Colloid Int. Sci. 45, 177, 1973.

11) Fredericq (E.), Houssier (C.), Biopolymers, 11, 2281, 1972.

12) Jennings (B.R.), British Polymer J. 1, 252, 1969.

CHAPTER 2

A resumé of Kerr effect theory as applied to macromolecular solutions.

Introduction

This chapter introduces the theory and equations relevant to the experimental observations described later. Where suitable equations do not exist a brief outline of the present state of the theory is given.

Experimental quantities.

The birefringence of a solution, Δn, is related to the observed phase difference via the relationship

$$\Delta n = \frac{\lambda \delta}{2\pi l} \qquad (1)$$

where λ is the wavelength IN VACUO

and l is the path length in the medium.

The Kerr constant, B, is given by

$$B = \lim_{E \to 0} \frac{\Delta n}{\lambda E^2} = \lim_{E \to 0} \frac{\delta}{2\pi l E^2} \qquad (2)$$

where E is the applied field strength.

For solutions it is usual to employ the specific Kerr constant, K_{sp}.

$$K_{sp} = \frac{\text{Bsolute}}{C} = \lim_{E \to 0} \left(\frac{\delta}{2\pi l E^2 C}\right) \qquad (3)$$

where Bsolute is determined from the equation

$$B_{solution} = B_{solvent} + B_{solute} \qquad (4)$$

Theories however require the value of K at infinite dilution, i.e. the intrinsic Kerr constant, $[K]$, to be determined.

$$[K] = \lim_{c \to 0} (K_{sp}) \qquad (5)$$

where C is the concentration of solute expressed in gms. per c.c. of solution. Concentration expressed as a percentage in this thesis is given by

$$\frac{\text{weight of solute in gms.}}{\text{volume of solvent in ccs.}} \times 100 \qquad (6)$$

and is, to a first approximation, equal to C.

Theory for rigid insulating particles in a non-conducting medium.

Consider primarily the following:

1) Molecules whose electrical and optical axes coincide, which have axial symmetry (see Fig. 1) and whose largest dimension is smaller than the wavelength of light.

2) A solution which is dilute and monodisperse.

The birefringence of an ordered array of molecules in solution as determined by Peterlin and Stuart[1] is

$$\Delta n = \frac{2\pi C \bar{\nu} (g_1 - g_2)}{n} \Phi \qquad (7)$$

where $\bar{\nu}$ is the partial specific volume of the macromolecules,

n is the refractive index of the unorientated solution,

$(\varepsilon_1 - \varepsilon_2)$ is the optical anisotropy factor

and Φ is the orientation function.

Now $\varepsilon_1 - \varepsilon_2$ can be the resultant of two contributions. The first arises from the intrinsic anisotropy of the molecules' optical structure. The second, giving rise to form birefringence, is due to the difference in refractive index of solvent and solute. If such a difference does not exist, then $\varepsilon_1 - \varepsilon_2$ is entirely dependent on the initial factor. The validity of the standard calculations of the intrinsic birefringence and the form birefringence using equations derived by Peterlin[1] and Wiener[2] respectively is in some doubt.[3,4]

The orientation function is a result of the interaction of the applied electric field and the electrically anisotropic molecules. O'Konski et Al[5] have determined its value at arbitrary field strength for molecules having a permanent moment coincident with the symmetry axis.

At low fields, they showed that

$$\Phi = \frac{1}{15}(b'^2 + 2c)E^2$$

with $b' = \mu'/kT = \mu^{B}/kT$

$$c = (\alpha_1 - \alpha_2) / 2kT$$

where μ' is the apparent dipole moment of the macromolecule in solution, and has been related to the actual dipole moment

via the internal field function B_1. B_1 is a function of the shape of the molecule, as shown in ref. 11, as well as the dielectric constants of molecule and solvent.

$\alpha_1 - \alpha_2$ is the electric polarisability of the molecule. It could also be written in the form $\alpha_1' B_1 - \alpha_2' B_2$ where α' refers to the actual intrinsic polarisability of the molecular material. The factors B again take account of the actual internal field acting on the molecule.

It can be noted that $g_1 - g_2$ is the optical polarisability per unit volume and is dimensionless. Correspondingly $g_1 - g_2$ is dependent on the internal field functions, as defined at optical frequencies, and is likewise dependent on the shape of the molecule.

The intrinsic Kerr constant is therefore given by

$$[K] = \frac{2\pi\bar{\nu}}{15\, n\lambda} (g_1 - g_2)(b'^2 + 2c) \qquad (8)$$

For arbitrarily high fields the complex algebraic result was presented in a graphical form. This allows $(g_1 - g_2)$, μ', and $\alpha_1 - \alpha_2$ to be separately determined.(6)

In practice, an experimental graph of

$$(\delta/E^2) \Big/ (\delta/E^2)_{E \to 0} \quad \text{v} \quad \log E^2$$

is compared with theoretical graphs(7) of

$$15\,\phi(\beta,\gamma) / (\beta^2 + 2\gamma) \quad \text{v} \quad \log (\beta^2 + 2\gamma)$$

where $\beta = b'E$ and $\gamma = c\,E^2$,

in order to obtain the three quantities above.

At infinitely high fields

ϕ equals unity such that

$$\delta_1 - \delta_2 = \frac{\Delta n_s}{2\pi C \bar{\nu}}$$

where Δn_s is the corresponding value of the birefringence. Conversely the graph Δn v $^1/E^2$ yields the value of Δn_s on extrapolation of $^1/E^2$ to zero.

These equations were further extended to the case $\alpha_1 - \alpha_2 < 0$ by Shah[8] and to a completely assymmetric molecule having a permanent moment at any arbitrary orientation by Holcomb and Tinoco.[9]

Transient electric birefringence

Application of a rectangular field pulse results in the solution becoming birefringent. The magnitude of the birefringence rises to a steady state value during the length of the pulse. On removal of the applied field the birefringence decays to its original value of zero.

The theory proposed by Benoit[10] attempted to describe the observed transients. His assumptions regarding the solute molecules to be investigated were that they must be smaller than the wavelength of light, monodisperse, in dilute solution, and possess axial symmetry with electrical, optical and hydrodynamic axes coincident.

For the rise of birefringence

Benoit solved the diffusion equation

$$\frac{df}{dt} = D\nabla^2 f - \frac{D}{kT} \text{ div } f\,\mathbf{M}$$

where f is the angular distribution function,

M is the torque acting on the particles

and D is the rotary diffusion constant for motion of the symmetry axis about the transverse axis.

at low fields in terms of a series of Legendre polynomials. The distribution function then allowed him to determine the optical polarisability parallel and perpendicular to the field and hence the birefringence.

For low fields

$$\frac{\Delta n(t)}{\Delta n(t \to \infty)} = 1 - \frac{3r}{2(r+1)} \exp(-2Dt) + \frac{(r-2)}{2(r+1)} \exp(-6Dt) \qquad (9)$$

where $r = b'^2/2c$

$\Delta n(t \to \infty)$ is the steady state value of the birefringence. Tinoco[11] extended this equation to the case of a dipole moment not along the symmetry axis. The result included the rotary diffusion constant for rotation of the transverse axis about the symmetry axis.

Nishinari and Yoshioka[12] have considered the rise process at arbitrary field strength and developed a method by which b' and c can be determined independently.

<u>For the decay</u>

The birefringence at a time t after the removal of the field was determined by Benoit to be

$$\frac{\Delta n(t)}{\Delta n(t=0)} = e^{-6Dt} \qquad (10)$$

A result which was valid for arbitrary field strength and even if $\Delta n(t \rightarrow \infty)$ was not attained during the pulse. For ellipsoidal molecules which do not possess either geometric symmetry or optical symmetry about axis 1, Ridgeway[13] has shown that the decay is a function of two exponentials.

Interpretation of D in terms of the dimensions of the particles can be made if prior knowledge is available regarding the particle's shape.

For long cylindrical rods Burgers[14] has given the equation

$$D = \frac{3\,kT}{8\pi z_o a^3}\left[\ln\left(\frac{2a}{b}\right) - 0{\cdot}8\right] \qquad (11)$$

where $2a$ is the length of the rod,

b is the radius of the rod,

and z_o is the viscosity of the solvent.

For a prolate ellipsoid, Perrin[15,16] has given the expression

$$D = \frac{3\,k\,T}{16\pi ab^2 z_o}\left[\frac{(2-p^2)\,p^2\,(1-p^2)^{\frac{1}{2}}\ln\left((1+(1-p^2)^{\frac{1}{2}})p^{-1}\right) - p^2}{(1-p^4)}\right] \qquad (12)$$

where $p = b/a < 1$.

Comparison of rise and decay

Watanabe has shown by integration of equ. 9 and equ. 10 that

$$\frac{A1}{A2} = \frac{4r+1}{r+1} \qquad (13)$$

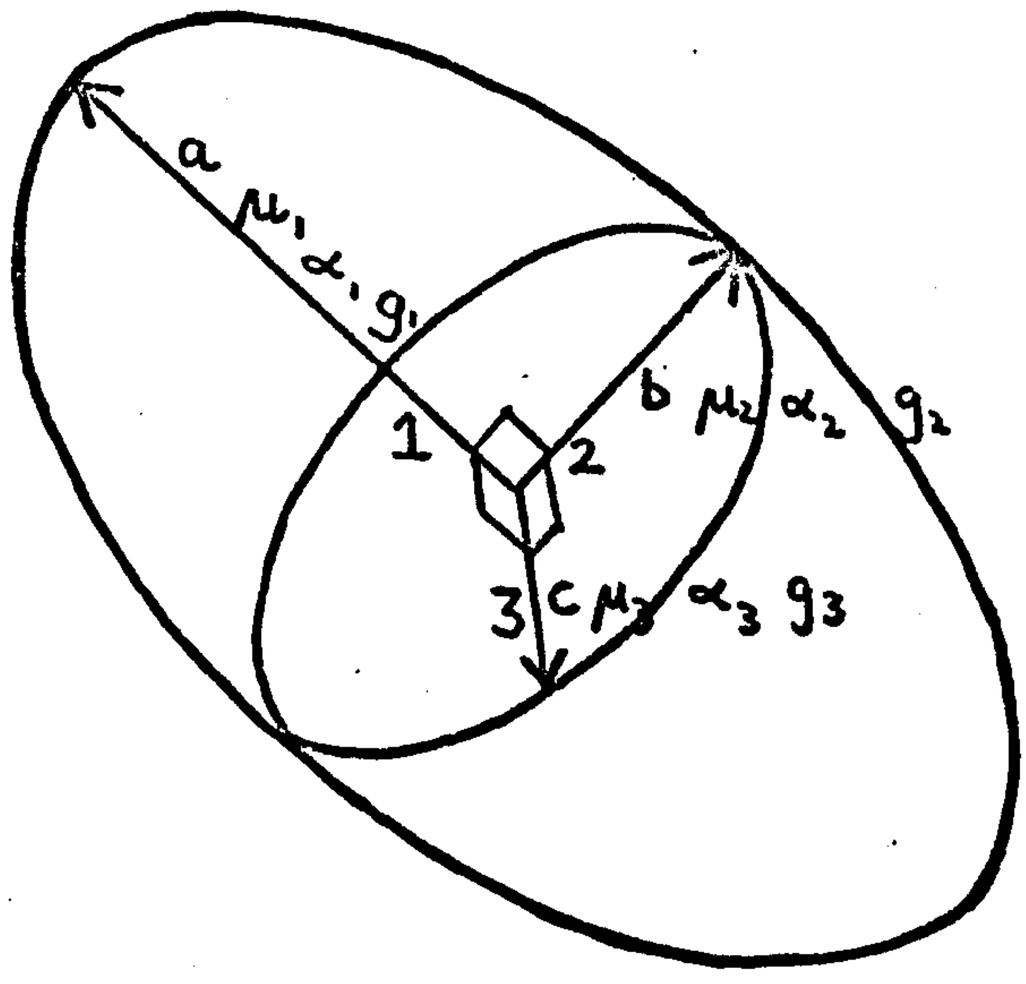

Figure 1

The model to which Benoit's theory applies requires:

$$a \neq b = c,$$
$$\mu_2 = \mu_3 = 0,$$
$$\alpha_2 = \alpha_3,$$
$$g_2 = g_3.$$

a/. 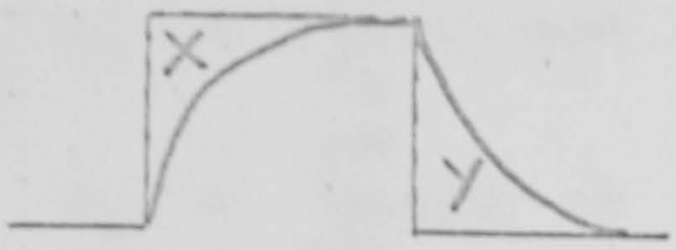

$r \geq 0$

$A_1/A_2 = X/Y$

b/. 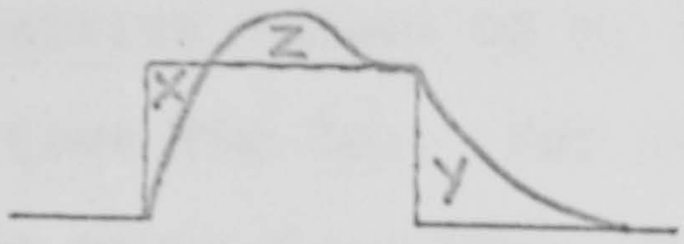

$-1 < r < 0$

$A_1/A_2 = (X-Z)/Y$

c/. 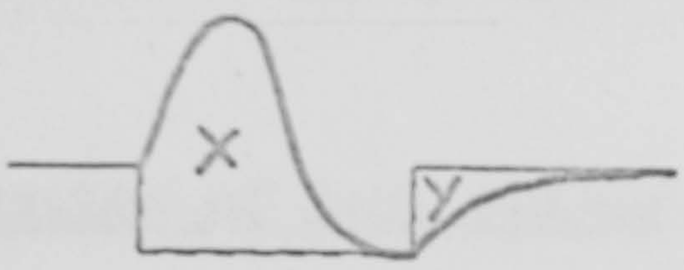

$r < -1$

$A_1/A_2 = -X/-Y$

Figure 2

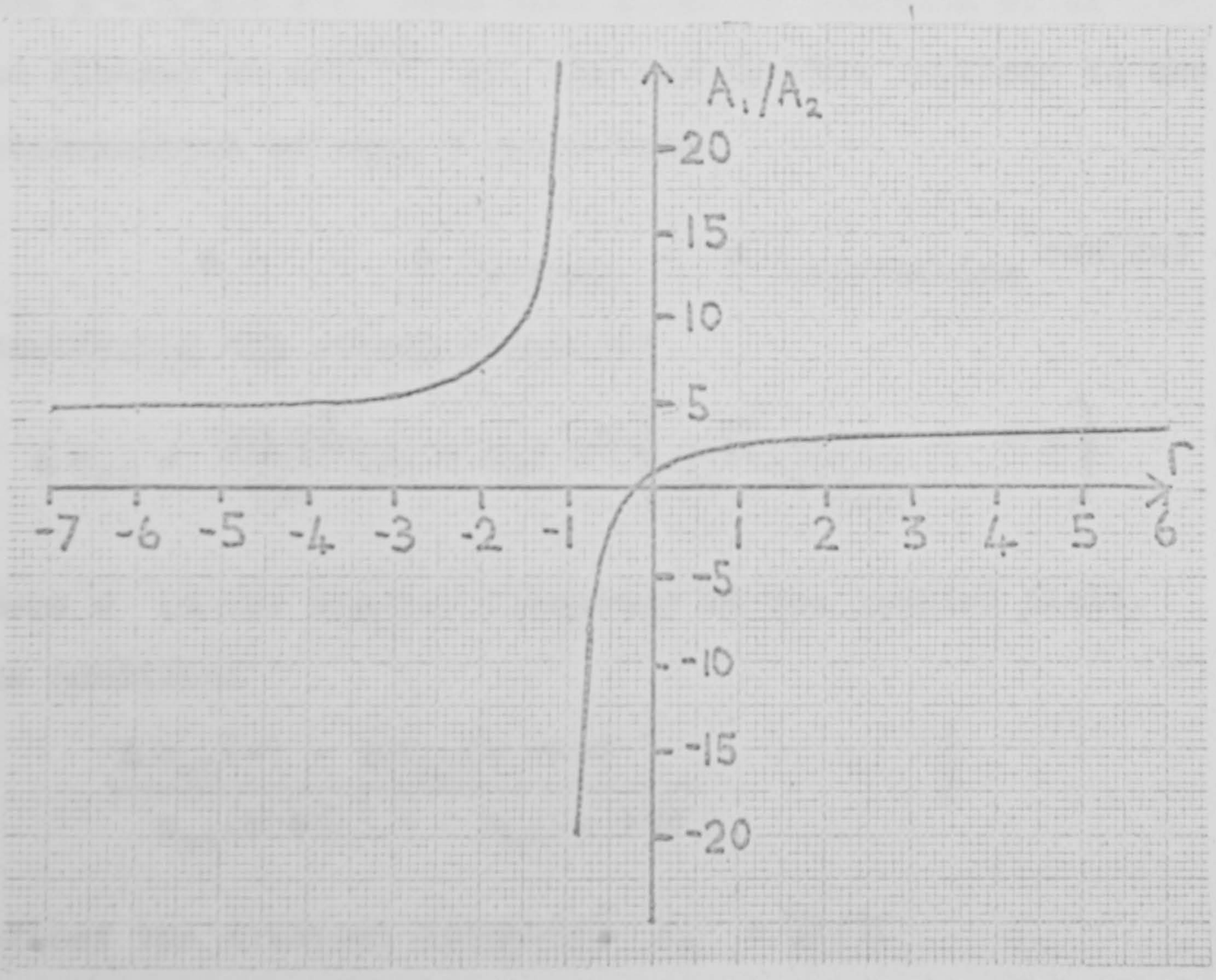

GRAPH 1 A_1/A_2 VERSUS r

where $A_1 = \int_0^{\infty} \Delta n(t \to \infty) - \Delta n(t)\ dt$ for the rise curve

and $A_2 = \int_0^{\infty} \Delta n(t)\ dt$ for the decay curve.

For positive values of r, the areas A_1 and A_2 can easily be found (see Fig 2a). For negative values of r greater care must be taken (see Figs. 2b and 2c). Values of A_1/A_2 as a function of r can be seen in Graph 1.

Application of A.C. pulses.

The equations governing the form of the birefringence when steady state conditions are reached in a field of the form $E = E_o \sin w t$ have been given by Thurston et Al[17] and Plummer et Al.[18] All the assumptions implicit in the determination of equ. 9 apply here.

$$\Delta n = \Delta n_{steady} + \Delta n_{alternating} \cos(2wt - \phi)$$

Considering the steady component

$$\Delta n_{st} = \frac{2\pi C \bar{\nu}}{15n} (g_1 - g_2) E^2 \left\{ \frac{b^2}{(1 + w^2/_{4D})} + 2c \right\} \qquad (14)$$

where w is the angular frequency of the applied field.

The condition

$$\frac{\Delta n_{st}(w) - \Delta n_{st}(w \to \infty)}{n_{st}(w \to 0) - n_{st}(w \to \infty)} = \frac{1}{2}$$

defines the critical frequency $f_c = D/\pi$. (15)

The alternating component is

$$\Delta n_{alt} = \frac{2\pi C \bar{\rho}}{15n} (g_1 - g_2) E^2 \left[\frac{b^4 + 2b^2c}{(1+\frac{w^2}{4D^2})(1+\frac{w^2}{9D^2})} + \frac{4c^2}{(1+\frac{w^2}{9D^2})} \right]^{\frac{1}{2}} \qquad (16)$$

Thurston and Bowling have presented graphs of $\Delta n_{st}/\Delta n_{st}(w\to 0)$ and $\Delta n_{alt}/\Delta n_{st}(w\to 0)$ as a function of $w/6D$ for various values of $b^2/2c$. The curve fitting technique of O'Konski[6] allows values of D and $b^2/2c$ to be determined (see Chapter 5).

Extension of the theory for the case of a non-axial dipole moment has not been made.

The variation of Δn_{st} and Δn_{alt} before steady state conditions are attained has not been determined (see reference 19). The decay of birefringence is given by equation 10.

Consider now the effects of polydispersity and flexibility of the particles.

<u>Polydispersity</u> in particle size and hence in the magnitudes of μ, $\alpha_1 - \alpha_2$ and D results in distortions in the rise, the electric field dependence,[5,20] the decay and the frequency dispersion[17] of birefringence. It is the decay region which has been of greatest interest. The decay curves can no longer be simulated by the single exponential function indicated in equation 10.

Characterisation of the decay in terms of the particle size distribution have been made using a peeling curve fitting[21] and a Laplace transform[22] method. Both methods have been reviewed and criticised by Schweitzer and Jennings.[23] These authors suggested that the initial slope of the graph $\log \Delta n(t)/\Delta n_{t=0}$ v time should be used. A further average relaxation time has been suggested by Yoshioka and Watanabe.[24]

Schweitzer and Jennings highlighted the dependence of the

initial slope and hence the decay curves on the electric field and the actual electrical properties of the molecules.

It is apparent that transient Kerr effect measurements are at present not capable of determining the complete distribution function of particle size. For this reason experimental relaxation times presented in this thesis are defined as the time, t, at which the following condition holds.

$$\frac{\Delta n(t)}{\Delta n_{t=0}} = e^{-1}$$

Flexibility in the molecular structure has been included in a number of theories. Kerr's law has been predicted[25,26] to occur at low fields, but the value of the Kerr constant itself was in error. Further theories are required which take excluded volume effects into account. Suitable equations to describe the rise of the birefringence in an electric field do not exist. The possible description of such experimentally observed changes using existing theories applicable to rigid particles is apparently not possible.[27]

The decay of the birefringence has been more widely studied. It is dependent not only on the rotation of the whole chain but also on the motion of chain segments.

Zimm[28] analysed the motion of a random chain in terms of normal modes of motion, of which the first mode corresponds to whole chain rotation. Stockmayer and Bauer[29] extended his work to electric birefringence to show that the relaxation time of the first mode is

$$\tau = k\ M\ [z]\ z_o/RT$$

where k is a constant equal to 0·61 and 0·43, for a free draining and non free draining coil respectively,

$[z]$ is the intrinsic viscosity of the solution

and M is the molecular weight of the chain.

The rotation of the whole chain is relatively slow compared with the motion of individual sections of the chain. Analysis of the decay transient at long times thus yields the value of τ required.

The higher modes of motion predicted by Zimm's model however have little relevance to the real behaviour of the segments.

The rotation of flexible molecules has been determined for the case of weakly bending rods and worm-like coils by Hearst.[30] Jennings and Brown[31] have applied these equations with success to a birefringence study of the flexible helical molecules of polyisocyanates. No method has yet been devised by which one can separate the effects of polydispersity and flexibility when they both occur.

Consider now the methods employed to interpret a large body of results[32] obtained for

<u>Conducting systems</u>

The mechanisms resulting in orientation of polyelectrolyte macromolecules have been reviewed elsewhere.[33,34] For instance,

1) Mobile charges in the bulk of the molecule may become polarised according to Maxwell-Wagner theory.

2) The movement of counterions which surround the highly charged molecule will also result in the molecule having an

induced moment. It would seem apparent that only those ions highly bound to the molecule will result in its physical orientation.(35)

Practically all the measurements made on conducting systems have been interpreted using equations specifically derived for insulating systems. The validity of this approach has been implied due to the reasonable agreement between results obtained for the various electro-optic methods.(32A) Recently Hornick and Weill(36) have applied their experimental results to the critical survey of the current theories of bound counterion polarisation for rigid particles. Despite its apparent crude nature reasonable agreement was found with the theory of Takashima.(39)

Prior to this study O'Konski and Krause(37) had presented a theory of the Kerr constant of rigid conducting particles. In addition to bulk conductivities they introduced surface conductivity terms to take into account the properties of the counter-ion cloud. The resulting expressions were of an extremely complex form.

For the case of Tobacco Mosaic Virus simplifications resulted in the derivation of a theoretical value of twice the magnitude of the experimental Kerr constant.

Relaxation effects of the polarising processes must also be taken into account in a.c. frequency dispersions(37) and the rise characteristics in d.c. pulsed fields.(37)

A further complication due to the electrophoretic orientation of highly charged assymmetric molecules has been suggested by Heller.(38) No experimental results have however been interpreted using such a mechanism.

Concluding remarks

The present state of the theory of the Kerr effect has been partially reviewed. It is apparent that the interpretation of the effect in terms of the intrinsic electrical and optical properties of macromolecules can best be made with insulating systems. Quantities derived from conducting systems using theories applicable to insulators can only be classed as empirical. When, as is the usual case, measurements are made on polydisperse samples, the unequivocal, accurate interpretation of the electrical and geometrical properties of the sample is not possible. Furthermore the poor rate of advancement of theories related to flexible molecules at present restricts the Kerr effect to almost only empirical observations.

References

1) Peterlin (A.), Stuart (H.A), Hand- und Jahrbuch der chemischen Physik, v.8, pt. 1B. Ed. A. Eucken, K.L. Wolf. Akademische Verlaggesellschaft, Leipzig.

2) Wiener (O.), Abh. sächs Akad. Wiss. 33, 507, 1912.

3) Cassim (J.Y.), Taylor (E.W.) Biophys J. 5, 531, 1965.

4) Taylor (E.W.), Cramer (W.) Biophys J. 3, 127-154, 1963.

5) O'Konski (C.T.) et Al, J. Phys. Chem. 63, 1558, 1959.

6) Yoshioka (K), O'Konski (C.T.) Biopolymers 4, 499, 1966.
'Gives details of curve-fitting method!

7) Matsumoto (M.) et Al Sci Papers of Coll. Gen. Educ. Univ. Tokyo 17, 173, 1967.

8) Shah (M.J.) J. Phys. Chem. 67, 2215, 1963.

9) Holcomb (D.N.), Tinoco (I.), J. Phys. Chem. 67, 2691-98, 1963.

10) Benoit (H.) Ann. de Phys. (Paris) 6, 561, 1951.

11) Tinoco (I.) J. Am. Chem. Soc. 77, 4485, 1955.

12) Nishinari (K.), Yoshioka (K.) Koll.-Zeit. und Zeit. für Polymere, 235, 1189, 1969.

13) Ridgeway (D.) J. Am. Chem. Soc. 88, 1104, 1966.

14) Burgers (J.M.) Verhandel. Koninkl. Ned. Akad. Wetenschap Afdel Natuurk Sect. 1, 16, 113, 1938.

15) Perrin (F.) J. de Phys. et le Radium, 5, 33, 1934.

16) Westley (F), Cohen (I.) Biopolymers 4, 201, 1966.
(Tabulates values obtained using Perrin's equations for various p).

17) Thurston (G.B.), Bowling (D.I.) J. Colloid Int. Sci. 30, 34, 1969.

18) Plummer (H.), Jennings (B.R.) J. Chem. Phys. 50, 1033, 1969.

19) Schweitzer (J.), Jennings (B.R.), J. Phys. D. Appl. Phys. 5, 297, 1972.

20) Matsumoto (M.), Watanabe (H.), Yoshioka (K.) Biopolymers 9, 1307, 1970.

21) Ingram (P.), Jerrard (H.G.) Brit. J. Appl. Phys. 14, 572, 1963.

22) Matsumoto (M.), Watanabe (H.), Yoshioka (K.) Koll. Z. u. Z. Polymere, 250, 298, 1972.

23) Schweitzer (J.), Jennings (B.R.) Biopolymers 11, 1077, 1972.

24) Yoshioka (K.), Watanabe (H.) ch. 7, 'Physical Principles and Techniques of Protein Chemistry' Ed. S. Leach, 1969.

25) Dows (D.A.) J. Chem. Phys. 41, 2656, 1964.

26) Nagai (K.), Ishikawa (T.) J. Chem. Phys. 43, 4508, 1965.

27) Yoshioka (K.), O'Konski (C.T.) J. Poly. Sci. 6, 421, 1968.

28) Zimm (B.H.) J. Chem. Phys. 24, 269, 1956.

29) Stockmayer (W.H.), Baur (M.E.) J. Am. Chem. Soc. 86, 3485, 1964.

30) Hearst (J.E.) J. Chem. Phys. 38, 1062, 1963.

31) Jennings (B.R.), Brown (B.L.) European Poly. J. 7, 805, 1971.

32) Stoylov (S.P.) Adv. Coll. Int. Sci. 3, 45, 1971.

32a) Page 105 of this review article.

33) Block (H.), North (A.M.) Adv. Mol. Relax Processes 1, 309, 1970.

34) Ingram (P.), Jerrard (H.G.), Sci. Prog. XLIX, 651, 1961.

35) Eigen (M.), Schwartz (G.), J. Coll. Sci. 12, 181, 1957.

36) Hornick (C.), Weill (G.) Biopolymers 10, 2345, 1971.

37) O'Konski (C.T.), Krause (S.) J. Phys. Chem. 74, 3243, 1970.

38) Heller (W.) Rev. Mod. Phys. 14, 390, 1942.

39) Takashima (S.) Adv. Chem Ser. 63, 232, 1967.

CHAPTER 3

The measurement of birefringence produced by transient electric fields.

Introduction

In Chapter 1 we saw that linearly polarised light incident on a birefringent solution may be resolved into two perpendicular linear vibrations, which on passing through the solution become out of phase. It is this phase difference, δ, which is actually measured by the detecting apparatus.

In the case where multiple reflections in the Kerr cell may be disregarded the actual birefringence of the solution may be determined from the expression

$$\delta = \frac{2\pi l}{\lambda}(n_{\parallel} - n_{\perp}) \qquad (3.1)$$

where l is the effective path length

λ is the wavelength of the light in vacuo

$n_{\parallel}$ and $n_{\perp}$ are the refractive indices of the solution parallel and perpendicular to the field direction.

Prior to the use of transient electric fields visual methods using manual adjustment of optical components to compensate for the phase difference were employed.[1] With the need however to observe rapid changes in phase difference two systems have been most widely used.

The first of these, depicted in Fig. 1A and commonly referred to as the quadratic system consists of a lens system producing a parallel beam of monochromatic light which

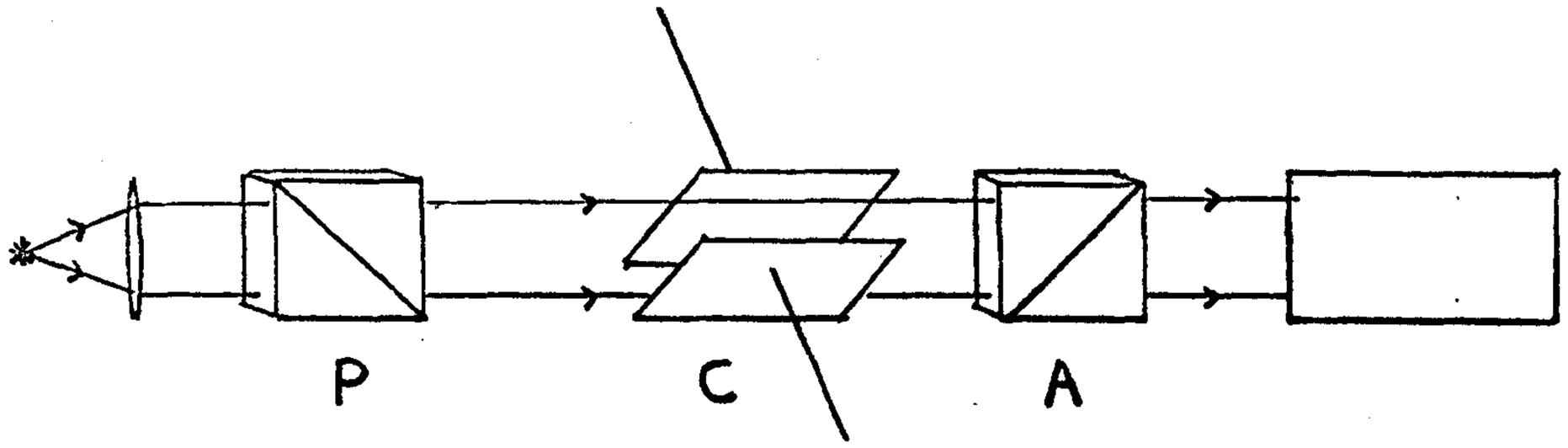

1a. THE QUADRATIC SYSTEM

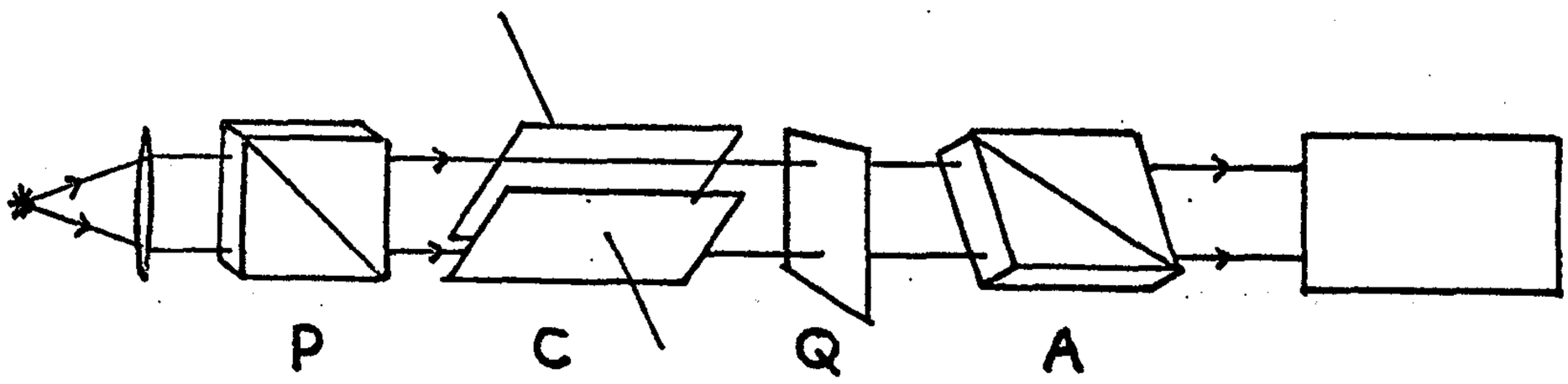

1b. THE LINEAR SYSTEM

Figure 1

traverses a polariser, P, a cell, C, positioned such that the electric field makes an angle of 45° with the incident plane of polarisation, and an analyser, A, crossed with respect to the polariser. The light emerging from the polariser falls on a photomultiplier tube which produces a voltage signal which is displayed on an oscilloscope trace. Light intensity changes which occur on application of the field pulse are approximately dependent on the square of the phase difference produced.(2)

An alternative arrangement, the linear system, is shown in Fig. 1B. It differs from the quadratic arrangement only in that a quarter-wave plate, Q, is inserted between the cell and analyser, with its fast or slow axis parallel to the initial plane of polarisation. The analyser is now offset from the crossed position such that light constantly reaches the photomultiplier. The magnitude of an intensity pulse is approximately linearly related to the phase difference produced.(2) This arrangement is therefore sensitive to changes in sign of $n_{\parallel} - n_{\perp}$.

The choice of system to be used is dependent on the relative importance of three major factors:

a) the distortion of the light pulse by incorrect settings of the optical components or the existence of stray phase differences, etc.

b) distortions introduced by the finite bandwidth of the detecting system, and

c) the sensitivity of the detection system to small changes in light intensity.

The two last mentioned effects have been reviewed in two papers.[2,3] The optical systems, however, do not appear to have been reviewed critically. For instance, various papers give some indication of the tolerances required for some of the component settings.[4,5,6] In continuous field work much effort was used to reduce the effects of stray phase differences.[1] In transient work however the magnitude of the effects has often been said to be small, and has then been simply neglected. For typical Kerr cells employed this is not the case, but only a few authors attempt to take into account this distorting influence, by theoretical[5] and practical means.[7,12] In fact a general poor understanding of the systems has led to unnecessary degrees of accuracy in setting up the components, in the use of white light and less than efficient use of calibration procedures.

It is the purpose of this chapter therefore to provide the necessary theory for determining the behaviour of both quadratic and linear systems. The relative importance of individual errors will be discussed so that each arrangement can be aligned and accurately calibrated. A review of the detection system characteristics will then be given so that the factors governing the choice of system will be complete.

Theory

The optical behaviour of the linear and quadratic systems can be determined in terms of the quantities defined in the legend of Fig. 2.

The method employed by the author to determine the

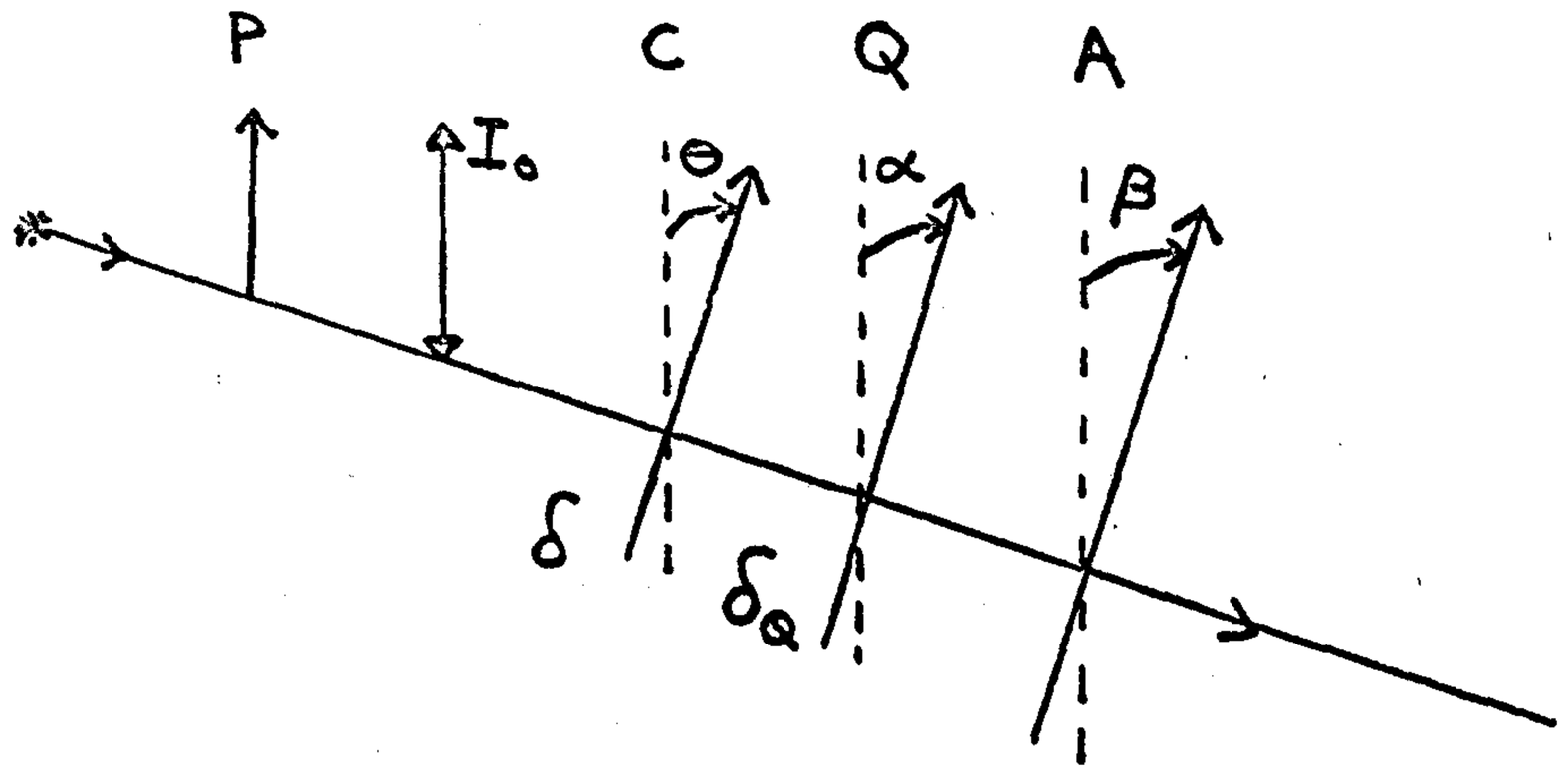

Figure 2.

The orientation of each component is measured in a clockwise direction from the vibration axis of the polariser. The angles are

θ for the field direction
α for the slow axis of the quarter-waveplate
β for the vibration axis of the analyser.

The phase differences introduced are

δ in the cell
δ_Q in the quarter waveplate

The intensity of the polarised light incident on the cell is I_o.

intensity of light reaching the photomultiplier is analogous to that derived by Jones.[8,9]

Several assumptions are made which are of practical importance:

(1) The light beam is monochromatic and parallel.

(2) Both analyser and polariser behave perfectly.

(3) The phase plates, i.e. the cell and quarter wave plate, are free from effects due to multiple reflections and are positioned such that their optical axes are vertical to the light beam.

(4) Dichroism and Optical Activity are not present in the system.

Light leaving the polariser can be resolved into two perpendicular vibrations:

$$\begin{bmatrix} E \\ O \end{bmatrix} = \begin{bmatrix} A \sin(wt) \\ O \end{bmatrix}$$

where E is in the plane of vibration of the polariser and A^2 is the intensity of light incident on the Kerr cell.

The Kerr cell when containing a birefringent medium acts as a uniaxial crystal with its optic axis parallel to the field direction. A transformation of coordinates allows one to describe the light leaving the polariser in terms of components E' and O' parallel and perpendicular to the electric field. In matrix notation therefore

$$\begin{bmatrix} E' \\ O' \end{bmatrix} = \begin{bmatrix} \cos\theta & -\sin\theta \\ \sin\theta & \cos\theta \end{bmatrix} \begin{bmatrix} A \sin wt \\ O \end{bmatrix}$$

$$\begin{bmatrix} E' \\ O' \end{bmatrix} = \begin{bmatrix} A \cos\theta & \sin(wt) \\ A \sin\theta & \sin(wt) \end{bmatrix}$$

The effect of the birefringent sample is to produce a phase difference between the two components. This is designated as δ which is equal to $\delta_{\parallel} - \delta_{\perp}$ or $\delta_{\varepsilon'} - \delta_{o'}$. The state of polarisation of the light leaving the cell has the description

$$\begin{bmatrix} E' \\ O' \end{bmatrix} = \begin{bmatrix} A \cos\theta & \sin(wt - \delta) \\ A \sin\theta & \sin(wt) \end{bmatrix}$$

This is now incident on the quarter-wave plate, and a further transformation into the fast and slow axes of the plate is required.

$$\begin{bmatrix} E'' \\ O'' \end{bmatrix} = \begin{bmatrix} \cos(\theta - \alpha) & \sin(\theta - \alpha) \\ -\sin(\theta - \alpha) & \cos(\theta - \alpha) \end{bmatrix} \begin{bmatrix} A \cos\theta & \sin(wt - \delta) \\ A \sin\theta & \sin(wt) \end{bmatrix}$$

Using the principle of superposition of waves

$$\begin{bmatrix} E'' \\ O'' \end{bmatrix} = \begin{bmatrix} B & \sin(wt - W) \\ C & \sin(wt - Z) \end{bmatrix}$$

where

$$B = (b_1^2 + b_2^2 + 2b_1b_2 \cos\delta)^{\frac{1}{2}}$$

$$C = (c_1^2 + c_2^2 + 2c_1c_2 \cos\delta)^{\frac{1}{2}}$$

$$W = \tan^{-1}\left(\frac{-b_2 \sin\delta}{b_1 + b_2 \cos\delta}\right)$$

$$Z = \tan^{-1}\left(\frac{-c_2 \sin\delta}{c_1 + c_2 \cos\delta}\right)$$

$b_1 = A \cos\theta \cos(\theta - \alpha)$ $\quad$ $b_2 = A \sin\theta \sin(\theta - \alpha)$

$c_1 = -A \cos\theta \sin(\theta - \alpha)$ $\quad$ $c_2 = A \sin\theta \cos(\theta - \alpha)$

The quarter-wave plate introduces a phase difference of δ_Q between the two components and is of positive magnitude if the slow axis corresponds to the axis shown in Fig. 2.

The transformation of the resulting state of polarisation into the axes of the analyser allows one to determine the component in the plane of vibration of the analyser E'''.

$$\begin{bmatrix} E''' \\ O''' \end{bmatrix} = \begin{bmatrix} \cos(\alpha - \beta) & \sin(\alpha - \beta) \\ -\sin(\alpha - \beta) & \cos(\alpha - \beta) \end{bmatrix} \begin{bmatrix} B \sin(wt - W - \delta_Q + Z) \\ C \sin(wt) \end{bmatrix}$$

$$\begin{bmatrix} E''' \\ O''' \end{bmatrix} = \begin{bmatrix} D \sin(wt - \chi) \\ E \sin(wt) \end{bmatrix}$$

The light intensity reaching the photomultiplier, I, is therefore

$$I = D^2 = B^2 \cos^2(\alpha - \beta) + C^2 \sin^2(\alpha - \beta) + 2BC \cos(\alpha - \beta) \sin(\alpha - \beta) \cos(-W - \delta_Q + Z) \quad (1)$$

Equation (1) can be reduced to very simple forms commonly used in

The linear system characterised by the values

$$\theta = 45^\circ, \qquad \alpha = 0^\circ, \qquad \beta = 90 - \chi^\circ,$$

$$I = I_o(\cos^2\chi \sin^2(\delta/2) + \sin^2\chi \cos^2(\delta/2) + 0{\cdot}5 \sin 2\chi \sin\delta_Q \sin\delta) \quad (2)$$

for $\delta_Q = +\pi/2$

$$I = I_o \sin^2(\chi + \delta/2) \quad (3)$$

The change in light intensity, ΔI, on production of a phase difference in the Kerr cell is therefore

$$\Delta I = I_o \left[\sin^2(\chi + \delta/2) - \sin^2(\chi) \right] \qquad (4)$$

By suitable choice of χ such that $\chi + \delta/2$ and χ are both small, and $\chi \gg \delta$ equation (4) takes the form of a simple linear relationship.

$$\Delta I \simeq I_o \chi \delta \qquad (5)$$

The sign of ΔI depends on that of χ and δ.

The quadratic system

requires the removal of the quarter-wave plate such that $\delta_a = 0$ and $\alpha = 0$.

Setting $\theta = 45°$ $\beta = 90°$

$$I = I_o \sin^2(\delta/2) \qquad (6)$$

which is also equal to the change in intensity which occurs. For small values of δ equation (6) is approximately a simple quadratic relationship

$$\Delta I = I_o \delta^2/4 \qquad (7)$$

The calibration procedure

is performed so that I_o may be determined.

For both systems the analyser is rotated from the crossed position.

Provided that

$$\delta = 0, \quad \alpha = 0$$

the intensity of light reaching the photomultiplier is

$$I = I_o \sin^2 \chi \qquad (8)$$

The slope of a graph of I v $\sin^2\chi$ yields the value of I_o.

Error Analysis

The procedure outlined in the section above has been simulated in a computer program written by the author. Any number of components, introducing any desired phase difference and at any arbitrary orientation, may be tested.

The program determines the change in intensity of the light reaching the photomultiplier when a known phase difference is introduced into a system which is incorrectly aligned.

The value of δ then determined using the exact expressions (4) and (6) or the approximations (5) and (7) will be in error. The magnitude of this error, Δ %, given by

$$\Delta = \left[\frac{\delta(\text{ACTUAL}) - \delta(\text{CALCULATED})}{\delta(\text{ACTUAL})} \right] \times 100$$

and the distortion introduced in the alignment form the output of the program. A similar procedure enables the errors in the value of I_o to be determined. The importance of any distorting influence can then be ascertained.

Results of Error Analysis

Errors resulting from the misalignment of the optical systems will be additional to errors introduced by the display system and measurement methods. Consideration of the magnitude of the latter's errors allows one to ascertain when the former errors can be neglected.

A typical transient display system[3] allows the measurement of the phase difference at the maximum height of

a noiseless pulse to be ascertained within an error of 3% and 7% for quadratic and linear detection respectively.

The accuracy in determining the shape of a light pulse is however to a large extent a function of the error involved in measuring the height along the pulse relative to that at its maximum height. This is primarily dependent on the amount of noise present on the pulse. For a noiseless pulse, relaxation times can be measured to within 4% accuracy.(3)

Errors in the absolute magnitude of phase difference and distortions in the pulse shape may both occur if the systems are incorrectly adjusted.

It is the purpose of this discussion to indicate the errors involved in the absolute measurement of phase difference. Factors which introduce errors dependent on the magnitude of δ will distort the pulse shape. Due to the complexity in determining the errors which will result in the measurement of relaxation times only occasional examples will be given.

In a practical context, the range of values of δ observed is typically 4×10^{-5} to 0·5 Radians, and an additional error in δ of the order of 1% due to errors in aligning the system is negligible.

Consider therefore the errors evaluated for <u>the quadratic system</u>.

(A) <u>The validity of the quadratic approximation</u> is illustrated in Graph 1. For values of δ as high as 0·5 radians, less than 1% error is introduced. Above 0·5 the error increases

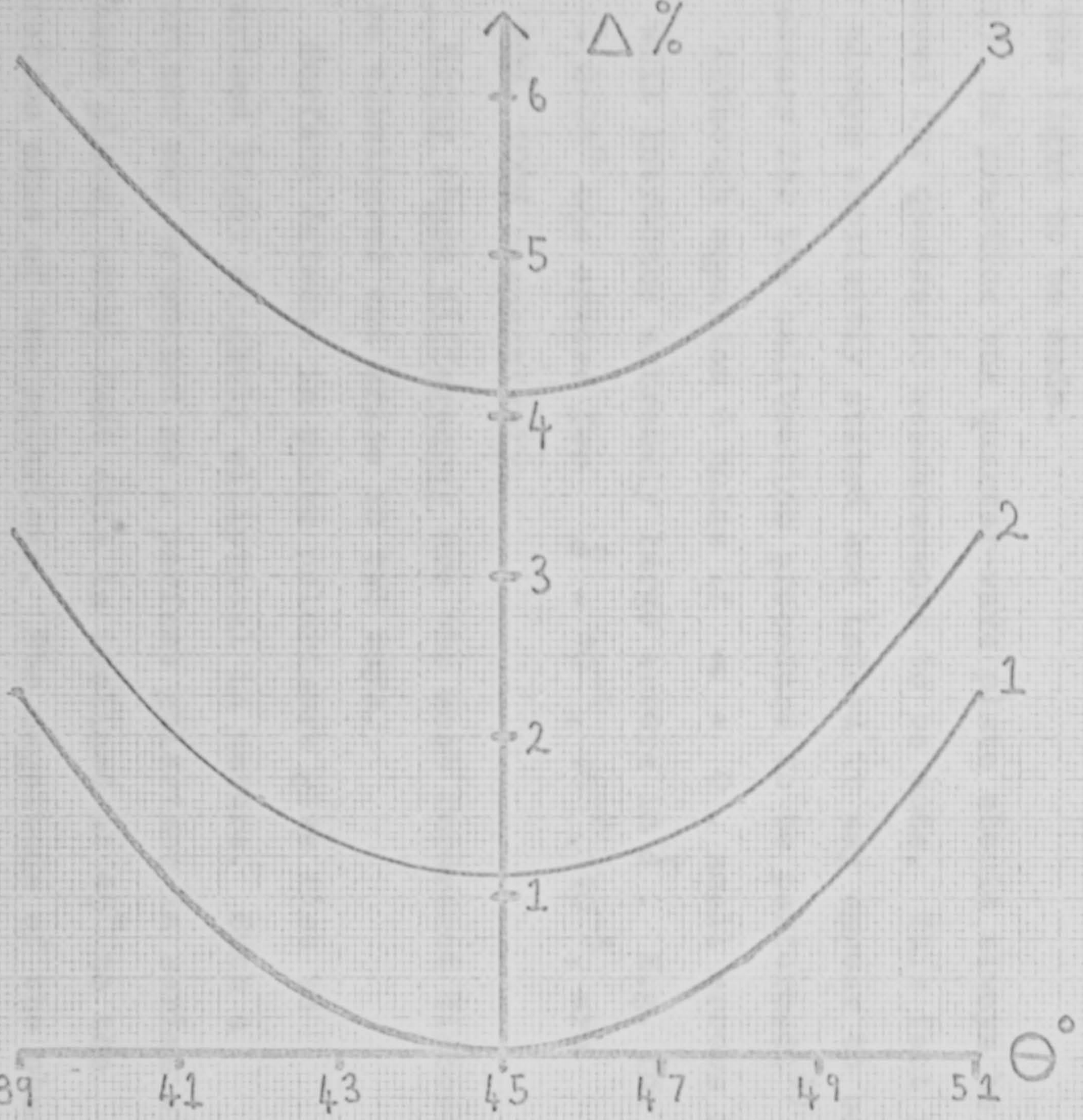

GRAPH 1

Δ VERSUS Θ

USING THE QUADRATIC APPROXIMATION

Curves 1, 2, 3 are for values of δ actual equal to ≤0·1, 0·5, and 1·0 respectively.

rapidly and in such circumstances the exact expression

$$\dot{\delta} = 2 \times \sin^{-1}\left(\left(\Delta I / I_o\right)^{\frac{1}{2}}\right) \qquad (9)$$

should be employed.

(B) Component misalignment and misuse.

(i) The Kerr cell offset from its 45° orientation by $\pm 4^{\circ}$ introduces an additional error of 1% (see Graph 1).

(ii) The analyser offset from the crossed position by less than 3° introduces less than 1% error. Signal to noise considerations (see page 59) however require good extinction of the light to be made.

(iii) In practice the quarter-wave plate should always be removed for quadratic measurements to be made. This fact is not always explicitly stated and indeed it may appear to be necessary for the calibration procedure to be performed.(3)

Although equation 6 holds if $\alpha = 0$, small errors in α will introduce extremely large errors in δ. E.g. for $\alpha = 0{\cdot}05^{\circ}$ the errors for $\delta = 10^{-1}, 10^{-2}, 10^{-3}$, are 2%. 20%, 100% respectively.

(C) Stray phase differences are the most important distortion to be eliminated and arise in two ways.

Surface defects in prism polarisers give rise to polarised light slightly elliptical in nature. Such a polariser may be treated as a perfect polariser in series with a phase plate, whose fast axis is inclined at 45° to the vibration axis of the polariser. The magnitude of the phase difference so introduced at a wavelength of 546 nm varies from 2×10^{-4} to as high as 2×10^{-3} for typical

Glan-Thompson polarisers.

The Kerr cell end windows also introduce stray phase differences owing to the residual strain in the optical material itself, and to a greater degree in the method of construction of the cell. This phase difference has a magnitude of the order of 3×10^{-3} for a good cell[11] but may easily be 3×10^{-2} for a poorer one.[12]

In order to determine the effect of a single phase plate in series with the Kerr cell, Graph 2 was constructed. It can be deduced that to reduce the level of error to less than 1% two courses of action are possible.

(i) The magnitude of the stray phase difference, δ_{STRAY}, must be reduced to less than 1% of that being measured, δ.

(ii) The optic axis of the phase plate is rotated so that it lies parallel or perpendicular to the vibration direction of the polariser.

In practice one is dealing with a series of phase plates representing the polariser, both windows of the cell and the sample itself.[13] Graph 2 however gives a very good indication of the required practical procedure to eliminate the effect of stray phase differences.

The magnitude of δ_{STRAY} in an experimental arrangement must be less than 1×10^{-4} for it to be classed as negligible, in most practical circumstances. As shown above, this value is much smaller than that normally encountered, where recourse must be made to the second approach.

Graph 2 shows that rotation of a phase plate of 5×10^{-3} to an angle within 2^{o} of the parallel position would reduce

GRAPH 2

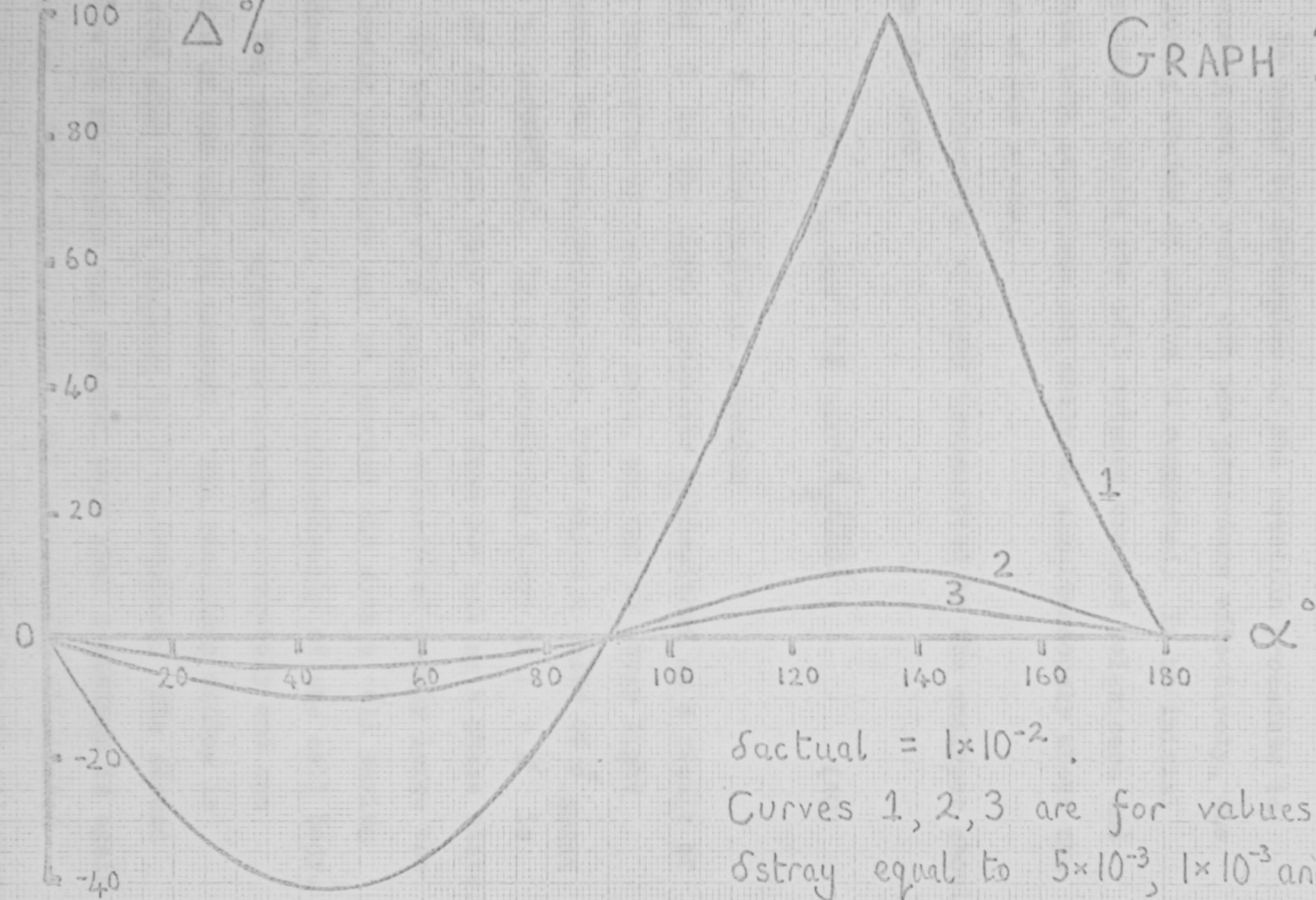

δactual = 1×10^{-2}.

Curves 1, 2, 3 are for values of δstray equal to 5×10^{-3}, 1×10^{-3} and 5×10^{-4}.

its effect to that of a phase plate of 5×10^{-4} in series with the cell.

In order to determine if the rotation procedure is necessary, and to carry out the procedure effectively, the following course of action is suggested. In an initial experiment, place the cell between crossed polarisers and rotate both polariser and analyser simultaneously about the axis of the system.

The intensity of light transmitted by the analyser should take the form

$$I = I_o \sin^2 2\gamma \sin^2\left(\frac{\delta_{STRAY}}{2}\right) \qquad (10)$$

where γ is the angle of rotation

and I is the light intensity transmitted as a result of the inclusion of the Kerr cell, and not to stray light reaching the photomultiplier, from which a value of δ_{STRAY} can be determined. If the resulting Graph of I v γ is not of this form then the cell does not act as a phase plate.

If the value of δ_{STRAY} is considered unduly large the following procedure can be carried out with a cell having windows which may be rotated independently of the cell body.

The quadratic system is aligned accurately and one window of the cell is removed. The remaining window is rotated such that a minimum in I is obtained. The second window is now added and rotated such that a minimum is again obtained. This situation has not necessarily eliminated δ_{STRAY}. If the value of δ_{STRAY} introduced by the polariser is larger than the sum of the magnitudes of δ_{STRAY} of each

window, a minimum can be obtained but a large value of δ_{STRAY} may still exist.

It should be noted that due to the very small changes in intensity which have to be measured the bandwidth of the detecting system should be adjusted to a low value as shown later in this chapter.

If the value and effect of δ_{STRAY} cannot still be neglected the following allowance should be made once the Kerr cell has been ascertained to act as a phase plate. The value of the stray phase difference which should be allowed for is not that given by equation (10), but as follows

$$\delta_{\substack{stray \\ effective}} = 2 \sin^{-1}\left(\frac{I}{I_o}\right)^{\frac{1}{2}} \qquad (10A)$$

where I is the value of light intensity transmitted when the system is aligned correctly and an allowance has been made for stray light reaching the photomultiplier.

A simple extension of equation (9),

$$\delta = 2 \sin^{-1}\left\{\left[\left(\frac{\Delta I}{I_o}\right) + \sin^2 \delta_{\substack{stray \\ effective}}\right]^{\frac{1}{2}}\right\} - \delta_{\substack{stray \\ effective}} \qquad (10B)$$

will yield the correct value of δ if the sign of $\delta_{\substack{stray \\ effective}}$ has been determined correctly (see Chapter 4).

An allowance for the effect of δ_{STRAY} by a further theoretical means was attempted by Orrtung and Meyers.[5] The iterative procedure suggested was simulated in a program written by the author. Their own work, however, shows the relevance of the approach. From measurements of δ in the range 1 to 4 x 10^{-2} they were able to determine a value of

δ_{STRAY} of 3×10^{-3} within an error of $\pm$ 30%. The effect of δ_{STRAY} was therefor reduced by a factor of three.

The method is however not universally applicable, as it relies on an a priori knowledge of the dependence of δ on the electric field. This approach also does nothing to reduce the level of the stray light reaching the photomultiplier.

Distortion in the shape of the decay transient will occur due to the presence of δ_{STRAY}. Consider a system which is stray free and in which the phase difference produced in the cell decays according to the equation

$$\delta(t) = \delta_{t=0}\, e^{-t/\tau}$$

Assuming the quadratic approximation holds, it follows that the corresponding changes in intensity are governed by the equation

$$\triangle I(t) = \triangle I(t=0)\, e^{-2t/\tau} \qquad (11)$$

A plot of $\ln\left(\frac{\triangle I(t)}{\triangle I(t=0)}\right)$ v t therefore has a slope of $\frac{-2}{\tau}$.

However in the presence of strays

$$\frac{\triangle I(t)}{\triangle I(t=0)} = \left(e^{\frac{-2t}{\tau}} + W\, e^{-t/\tau} \right) / \left(1 + W \right)$$

$$\text{where} \quad W = \frac{2\,\delta_{STRAY}}{\delta(t=0)}$$

and for $W \gg 1$

$$\frac{\triangle I(t)}{\triangle I(t=0)} = e^{-t/\tau}$$

The value of Υ determined from the log plot will be in error by 100%. For intermediate values of N the observed behaviour of the particles in the cell will be described by two relaxation times. In such cases therefore it is important to make the proposed correction for δ_{STRAY} when analysing the decay transient.

(D) The quadratic calibration procedure has the primary objective of determining I_o but it is also employed to test the linear behaviour of the photomultiplier tube. However, non-linearity of the slope of the graph of I v $\sin^2\chi$ might also be indicative of distortions in the optical arrangement. In order to detect this type of distortion a plot of I v $\sin^2\chi$ must be made for positive and negative values of χ.

The only optical distortion we need consider is that due to stray phase differences.

It can be shown that

$$\frac{I_+ - I_-}{\sin^2(|\chi|)} = \frac{\sin 4\alpha \sin 2|\chi| \sin^2\frac{\delta_{STRAY}}{2}}{\sin^2(|\chi|)} \qquad (12)$$

where I_+ (I_-) is the value of intensity for χ positive (negative) and α is that previously defined.

For α = 0 and 45^o no difference in the two plots can occur.

For α = $22\frac{1}{2}$ the plots are at their greatest separation.

Only values of δ_{stray} greater than 5×10^{-2} introduce significant differentiation of the two slopes. Such values of δ_{stray} are not normally encountered.

Observation of the difference in slopes and the accuracy with which I_o can be measured is dependent on the accuracy with which χ can be determined. I_o must be determined to within ± 2%, i.e. for values of χ up to 5^o the analyser must be adjustable to better than $0{\cdot}05^o$.

Such an error in I_o will introduce a 1% error for values of δ in the quadratic region, but a 10% uncertainty will occur for values of δ equal to π .

The Quadratic Alignment Procedure suggested by the error analysis above is therefore as follows:

1) Adjust the sensitivity of the detection system to a high value.

2) In a separate experiment determine the magnitude and orientation of the stray phase difference of the cell.

3) Now cross the polariser and analyser as accurately as possible.

4) Include the Kerr cell such that the field direction is at $45^o \pm 2^o$ to the vibration direction of the polariser.

5) If it is necessary, rotate the cell windows.

6) Adjust the detection system so that transient light pulses can be observed without distortion.

7) Carry out the calibration procedure, determining I_o to ± 2% accuracy.

For phase differences below 0·5, the quadratic approximation may be used.

For noiseless transients, values of δ greater than

100 times the remaining effective stray phase difference can now be measured to ±1% accuracy if $\delta < 0{\cdot}5$.

It should be noted that the system has been aligned such that the error in $\Delta I/I_o$ is of the order of 2%. The corresponding error for values of δ approaching π is however 10%.

Consider now the results of the error analysis for

The Linear System

(A) The validity of the approximation to linear behaviour is illustrated in Graph 3.

Typical values of α from 0 to $\pm$ 12° and phase differences of 1×10^{-4} to 1×10^{-2} have been chosen.

The complex nature of the curves is due to the inapplicability of the approximations $\sin^2(\alpha + \delta/2) = (\alpha + \delta/2)^2$ at high, and $\alpha \gg \delta$ at low values of α.

The correct choice of α can be made from this graph.

Primarily, for positive values of δ, the resulting error can only be zero for positive values of α and vice versa for negative values of δ. In either case this corresponds to a system in which a positive change in intensity occurs on production of the phase difference.

Therefore for values of δ up to $+ 1 \times 10^{-2}$, $\alpha = + 7°$ may be employed. Above 1×10^{-2} the magnitude of the required angle increases rapidly.

The exact relationship used to determine δ is given in the calibration procedure.

It can be shown in a manner equivalent to that primarily

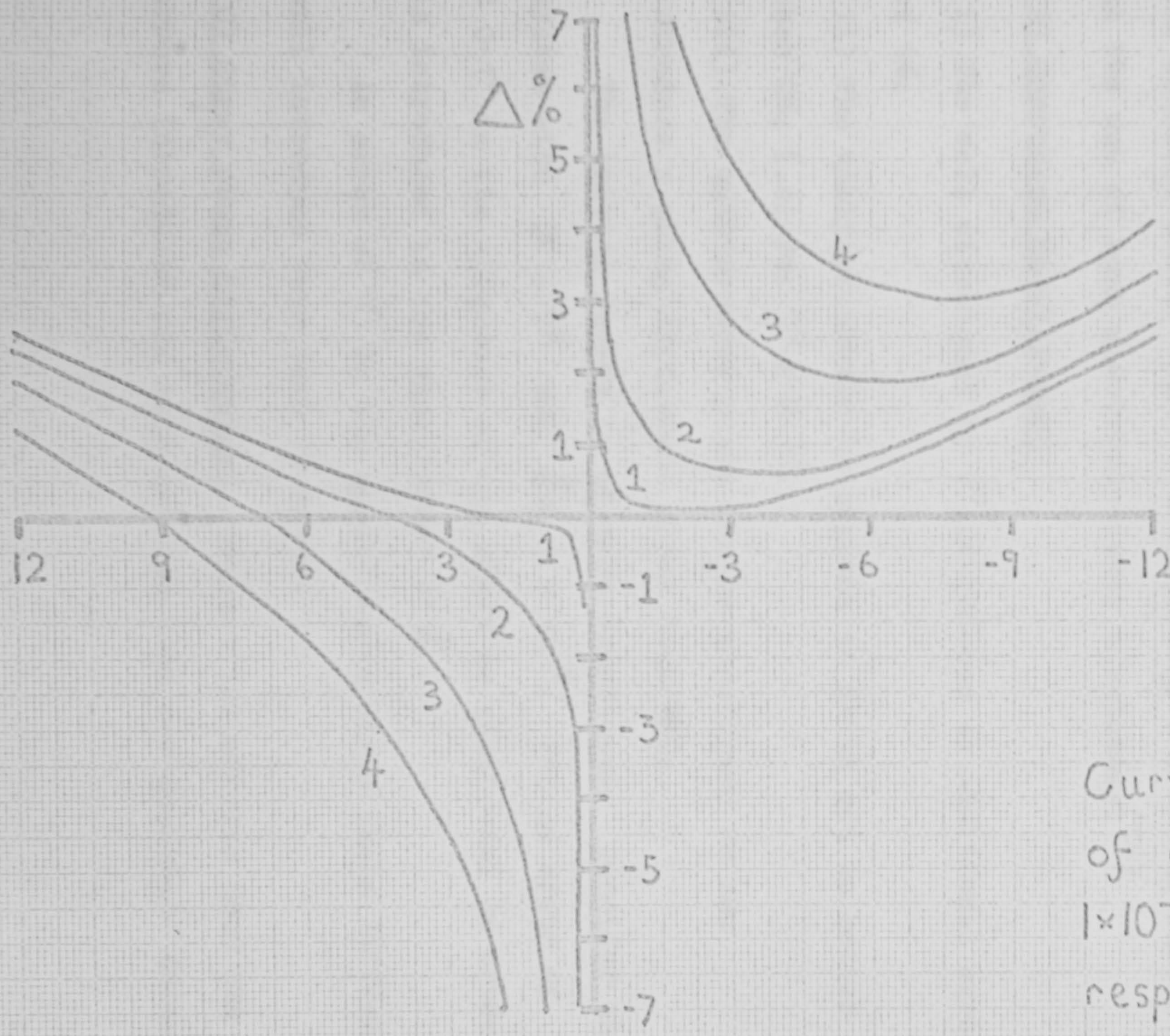

GRAPH 3

Δ VERSUS X

DUE TO USE OF THE LINEAR APPROXIMATION

Curves 1, 2, 3, 4 are for values of δactual equal to 1×10^{-4}, 1×10^{-3}, 5×10^{-3} and 1×10^{-2} respectively.

given that if the linear approximation holds, the slope of the logarithmic decay plot is given by

$$\frac{d}{dt}\left(\ln \frac{\Delta I(t)}{\Delta I(t=0)}\right) = -\tau^{-1}$$

If, however, the approximation is used in situations where it is not valid, then at worst the slope will be $-2\tau^{-1}$ and for intermediary cases two relaxation times will simulate the observed trace. This observation is a limiting factor in the use of some electronic decay simulators.(14)

(B) Component Misalignment

(i) The cell misaligned by 4^{o} introduces an additional error of 1%.

(ii) The analyser should be capable of being set to better than 2%, i.e. for $7^{o} \pm 0{\cdot}1^{o}$.

(iii) The quarter-wave plate can be misaligned or can introduce a phase difference other than $\pi/2$.

The initial factor is of more importance. Consider the system with $\chi = 7^{o}$ and $\delta < 1 \times 10^{-2}$. For an error of $\pm 0{\cdot}1^{o}$ in the alignment of the plate an additional 2% error is introduced in the measurement of δ.

An error of 5^{o} in the quarter-wave plate phase difference will introduce less than 1% error.

(C) Stray phase differences. Table 1 illustrates that the errors introduced are much smaller than for quadratic detection.

δ STRAY / δ	10^{-3}	5×10^{-3}	1×10^{-2}	-1×10^{-2}	-5×10^{-3}	-1×10^{-3}
1×10^{-3}	0·5	2·4	4·6	-0·5	-2·5	-5·1
1×10^{-2}	0·5	2·4	4·6	-0·5	-2·5	-5·1

TABLE *1 % Error in δ due to δ stray in linear system.

To construct the table the exact expression, equation 13, and a value of χ equal to 5° have been used. No correction was applied to the value of I_χ.

For 1% error to occur, δ_{STRAY} must be reduced to $2 \times 10^{-2}\chi$ radians. For example for $\chi = 7°$, δ_{STRAY} must be reduced (by rotation of the cell windows, if necessary) to 2×10^{-3}.

(D) The linear calibration procedure is not generally used to determine I_o, since a sample of this, I_χ, is constantly transmitted by the uncrossed analyser. The phase difference is then determined from the exact expression

$$\delta = 2.\sin^{-1}\left[\left(\frac{\Delta I}{I_\chi} + 1\right)^{\frac{1}{2}} \sin\chi\right] - \chi \qquad (13)$$

This procedure can however be of considerable use in aligning the system, again requiring a plot of I v $\sin^2\chi$ to be made for either side of the crossed position.

Graph 4 illustrates typical plots obtained when the quarter-wave plate is misaligned. If a stray phase difference

GRAPH 4

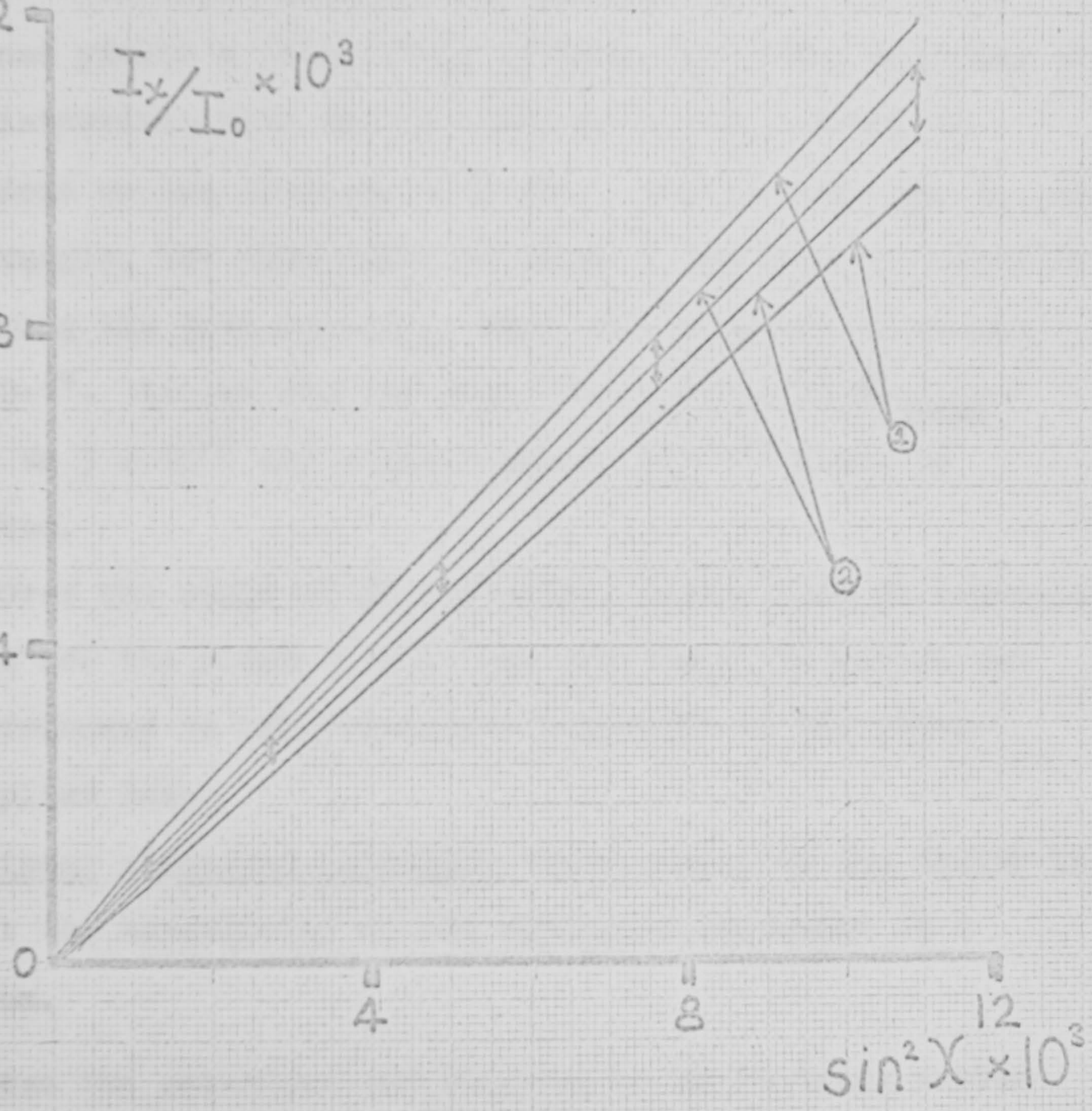

CALIBRATION PLOT OVER 6° RANGE

Curves 1 and 2 are the plots obtained for the quarter waveplate misaligned by 0·2° and 0·1° respectively

was the only distortion present, curves 1 and 2 of Graph 4 would be indicative of strays of magnitude 5×10^{-3} and 1×10^{-2} radians respectively. The average of the plots obtained yields a value of I_o if required. The magnitude of the distortion which may be observed by this method is dependent on the accuracy with which the analyser can be set. For example, the bars shown on Graph 4 indicate the error in measuring the true intensity when the analyser can be set to $\pm 0{\cdot}1^{o}$. It can then be seen that a value of δ_{STRAY} equal to 3×10^{-3} and a misalignment of $0{\cdot}1^{o}$ could be detected.

Over the range of χ indicated, little loss of linearity occurs for the plots so that any additional curvature can be attributed to the non-linear behaviour of the photo-multiplier tube.

The linear alignment procedure recommended by the author is:

1) Set the sensitivity of the detection equipment to a maximum.

2) Cross the polariser and analyser to an accuracy better than $0{\cdot}05^{o}$.

3) Include the quarter-wave plate and rotate for a minimum in the transmitted light intensity. Accuracy is required to better than $\pm 0{\cdot}05^{o}$.

4) Check alignment using calibration procedure.

5) Include the cell and adjust to 45^{o} position, to within $\pm 2^{o}$.

6) Carry out calibration procedure and rotate windows of cell if necessary.

7) If the linear approximation is to be used:-

For values of cell phase difference up to 1×10^{-2} the analyser should be uncrossed by 7° to an accuracy of $\pm 0.05^{\circ}$.

The error in δ will be $\pm$ 2% from all sources. For values of δ greater than 1×10^{-2} the value of χ should be carefully chosen.

8) If the exact expression is used:-

A value of χ not less than 6° should still be employed.

9) Adjust the detection equipment so that transient light pulses can be observed without further distortion.

It should be noted that the above error analysis has been confined to reducing the error in $\Delta I/I_o$ to the order of $\pm$ 2%. As for quadratic detection this uncertainty will give large errors for values of δ approaching $(\pi/2 - \chi)^{\circ}$.

Validity of assumptions under experimental conditions

(1) White light has often[15,16,17,18] been used in transient work to increase the sensitivity of the apparatus (see Chapters 5 & 6).

O'Konski's and Haltner's treatment[15] of white light used in conjunction with a monochromatic system at an effective wavelength, λ_ε, appears to have been universally applied to both quadratic and linear systems employing continuous or line light sources. The validity of the O'Konski approach, and the magnitude of the errors introduced have never been critically examined.

Consider therefore the following analysis:-

Assuming that birefringence is independent of wavelength

$$\delta(\lambda) = \frac{\lambda_\varepsilon \delta_\varepsilon}{\lambda} \qquad \delta_Q(\lambda) = \frac{\lambda_Q}{\lambda}(\pi/2)$$

where

$\delta(\lambda)$ and $\delta_Q(\lambda)$ are the phase differences of the sample and quarter-wave plate at a wavelength λ

δ_ε is the phase difference occurring at the assumed equivalent wavelength λ_ε,

λ_Q is the wavelength at which the quarter-wave plate has a $\pi/2$ phase difference.

On application of an electric field to the sample the changes in transmitted light intensity $\blacktriangle I_Q$ and $\blacktriangle I_L$ for the quadratic and linear systems respectively are

$$\blacktriangle I_Q = \int_{\lambda_1}^{\lambda_2} I(\lambda) \sin^2\left(\frac{\lambda_\varepsilon \delta_\varepsilon}{2\lambda}\right) d\lambda \qquad (14)$$

$$\Delta I_L = \int_{\lambda_1}^{\lambda_2} I(\lambda)\left[\cos(2\chi)\,\sin^2\left(\frac{\lambda_c d_c}{2\lambda}\right) + \tfrac{1}{2}\sin(2\chi)\sin\left(\frac{\lambda_c d_c}{\lambda}\right)\sin\left(\frac{\lambda_a d_a}{\lambda}\right)\right] d\lambda \qquad (15)$$

where $I(\lambda)$ is the product of the spectral response of the detection system and the spectral emission of the light source.

To simulate the use of a continuous source

$$I(\lambda) = \exp\left[-(\lambda - \lambda')^2/(2\sigma^2)\right] \qquad (16)$$

where λ' is the wavelength at the maximum height and σ is the halfwidth of the gaussian distribution.

For a line source

$$I(\lambda) = \sum_{i=1}^{N} A_i(2\pi S_i^2)^{-1}\exp\left[-(\lambda - \lambda_i)^2/(2S_i^2)\right] \qquad (17)$$

where the i^{th} spectral line has an amplitude, A_i, wavelength at maximum height, λ_i and halfwidth S_i.

Computer programs have been written by the author to evaluate the integrals (14) and (15). The phase difference corresponding to the relevant change in intensity has then been determined using the exact expressions (9) and (13) and graphs produced comparing the calculated phase difference with that occurring at the assumed equivalent wavelength.

Graph 5 indicates the relevance of O'Konski's procedure to the use of a tungsten lamp with a linear or quadratic system. For its construction, equation (16) was adjusted to

$$I(\lambda) = \lambda\exp\left[-(\lambda - \lambda')^2/(2\sigma^2)\right]$$

so that λ' corresponds to the effective wavelength chosen by O'Konski.

GRAPH 5

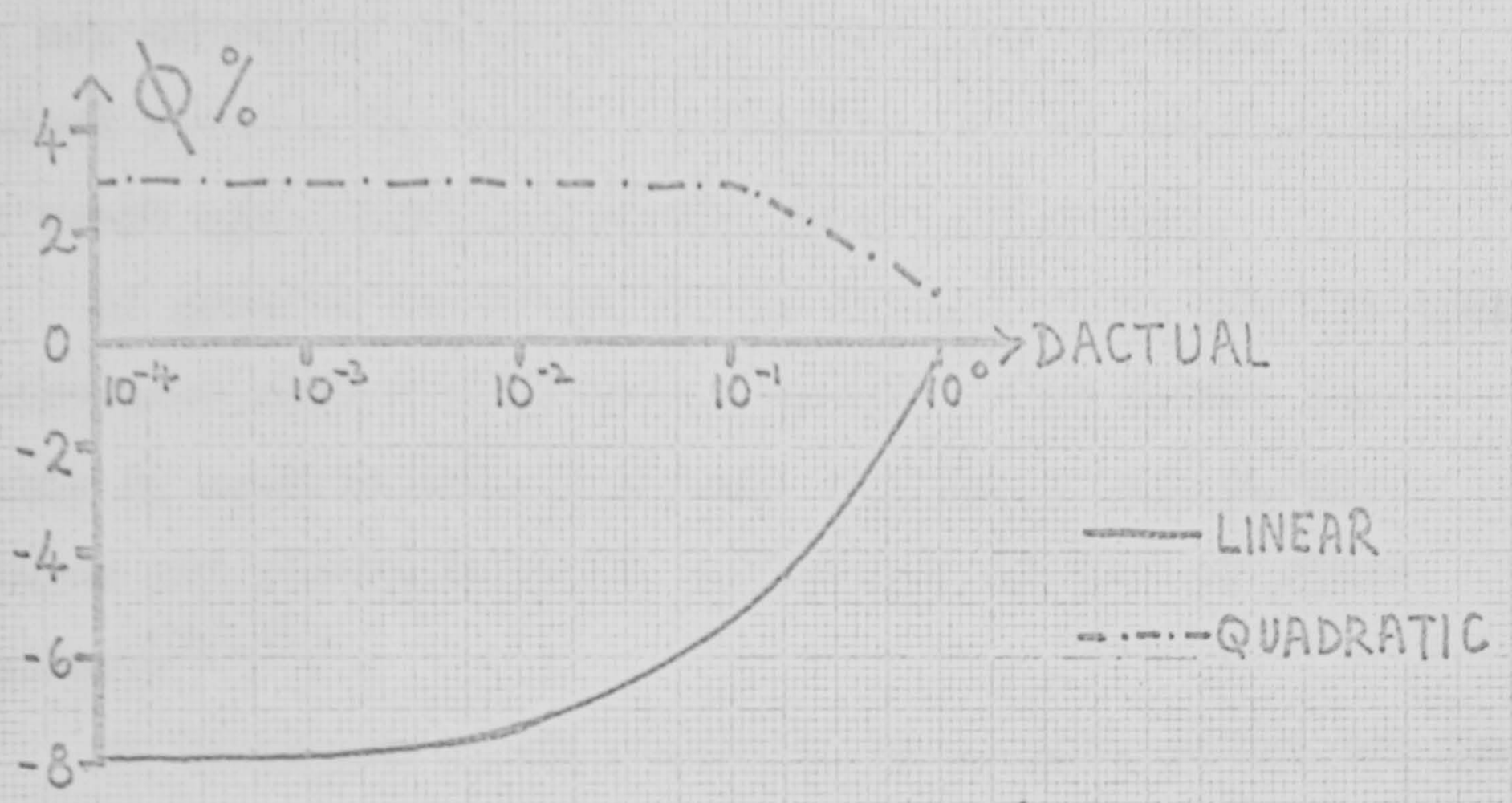

Φ VERSUS δACTUAL (O'KONSKI'S METHOD)

Where $\Phi\% = \left(\frac{\delta calculated - \delta actual}{\delta actual}\right) \times 100$

and δactual is the phase difference occuring at the assumed equivalent wavelength

Errors apply to the case

$\lambda' = 5,500$ $\sigma = 1,250$ $\lambda_1 = 3,500$ $\lambda_2 = 8,000$

and for linear detection $\chi = 6°$ and $\lambda_0 = \lambda'$

It is sufficient to say that the equivalent wavelength is not correctly identified by O'Konski's approach and indeed because the error involved is not of constant value an exact equivalent wavelength cannot be found.

Of greater relevance to the author's work are the errors introduced when a line source is used. The values (see Table 2) used to form $I(\lambda)$ are typical of the mercury source and photomultiplier used by the author and other workers.[17,19]

To determine if an effective wavelength exists for the linear system, Graph 6 was constructed. Each curve represents the use of a different quarter-wave plate and a value of λ_ε equal to the particular λ_Q. The average discrepancy between $\delta_{observed}$ and δ_ε is a minimum for λ_Q equal to 4,150 $\mathring{A}$ and the maximum error introduced is only 1%. However, when only one quarter-wave plate is available, for instance one calibrated at 5461 $\mathring{A}$, Graph 6 can still be used to find a value of λ_ε. The horizontal portion of curve 1 indicates that an effective wavelength 10% lower than 5461, i.e. 4900, can be chosen for phase differences up to 1×10^{-2}. For larger values the error increases rapidly so that distortion of the true pulse shape occurs but this corresponds to an error of the order of only 4% in the measurement of a single relaxation time.

Consider now a mercury lamp with a quadratic system. Complications involving the choice of χ and λ_Q are no longer present in the analysis. An effective wavelength of 4100 $\mathring{A}$

GRAPH 6

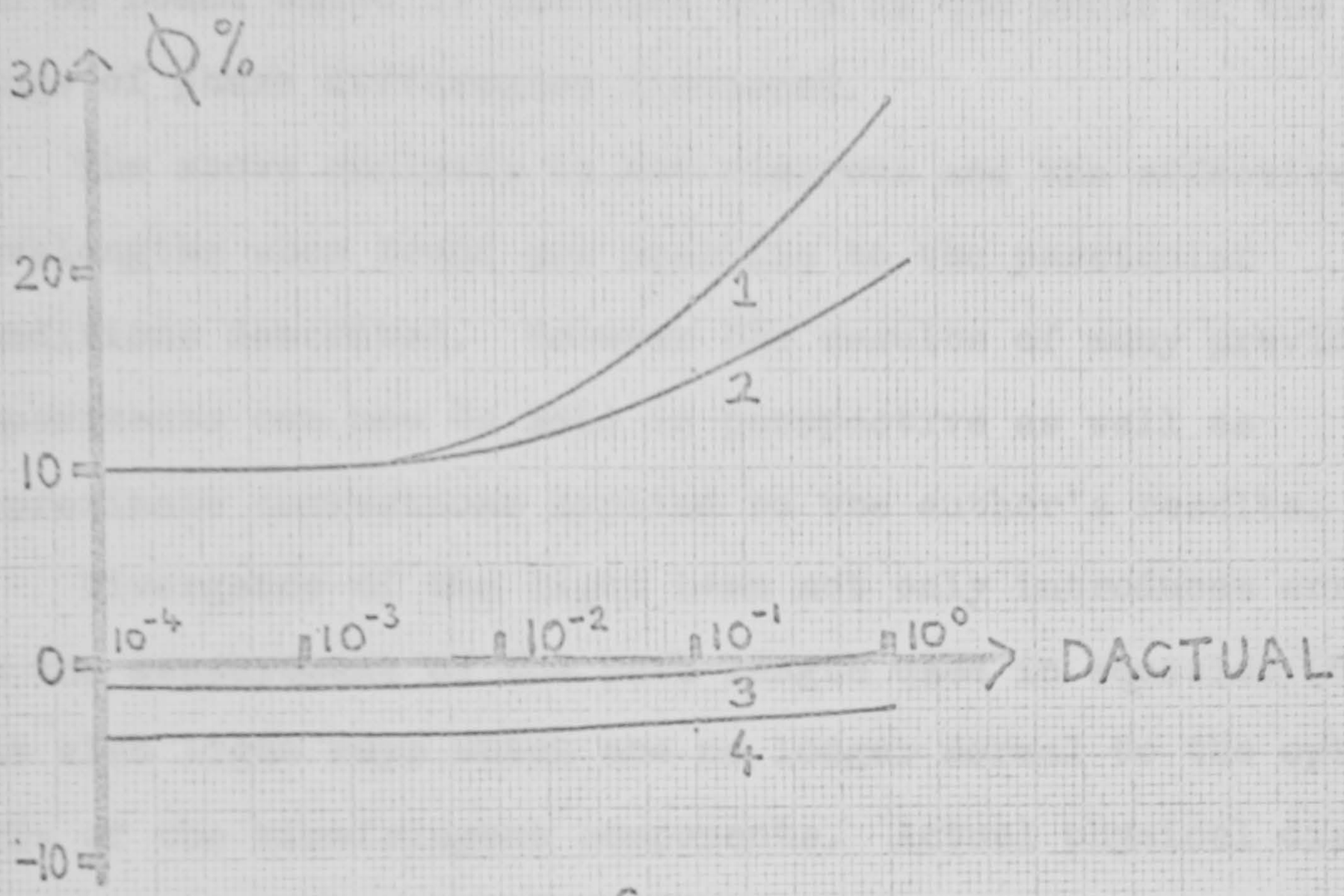

Q VERSUS δ ACTUAL FOR A LINE SOURCE AND LINEAR DETECTION

Curves 1,2,3,4 are for values of λ_0 equal to 5,461, 5,000, 4,150, and 4,050, respectively.

$X = 6°$ and equation 17 was used to represent the line spectrum with the following values

i	λ_i	S_i	A_i
1	3650	30	256
2	4050	30	180
3	4350	30	240
4	5461	30	72
5	5780	30	28

$\lambda_1 = 3,500$

$\lambda_2 = 6,000$

TABLE 2

can be found which is accurate to 1% in the whole of the range of phase differences discussed.

The above analysis is not rigorous and the effective wavelengths when found are specific to the particular conditions described. However the results of many previous experiments can now be held in perspective as well as approximate corrections applied to the author's results.

Divergence of the light beam not only introduces errors in the measurement of the path length used in equation (1) but also light rays which are no longer normal to the optic axis of the birefringent components. Actual physical displacement of the two resolved components of the beam will then occur.

(2) The errors introduced because of imperfect behaviour of the polariser and analyser can be deduced from the work of King and Talim.[10] Variations in the orientation of the polarised beam across the face of the polariser can be neglected, ellipticity of the beam may be considerable but contributes only a small fraction of the light transmitted by crossed polarisers. The effect of transmitted unpolarised light, generally referred to as stray light, on the equations, is simply that of an additive constant when the total intensity reaching the photomultiplier is measured and is not present when changes in intensity are determined.

(3) The effect of multiple reflections in a phase plate is to make it introduce a phase difference not simply related to its thickness and to render it dichroic (see Ref.9).

Multiple reflections in the quarter-wave plate can be reduced by methods described by Jerrard.[20] Their effect however in the Kerr cell does not appear to have been discussed, even for the design of a multiple reflection Kerr cell.[21]

(4) Of particular interest is the presence of dichroic and optically active behaviour in the solution.

Dichroic behaviour can readily be taken account of using the Jones calculus.[8,9] The experimental separation of linear absorptive dichroism and linear birefringence is treated in a recent paper.[22] Dichroism might also be present as a result of the manner in which the sample scatters light (see Chapter 7).

The Jones calculus can again be used for the interpretation of birefringence measurements on optically active molecules,[23] but with difficulty.

Limitations in the measurement of phase difference due to noise considerations.

The above analysis deals with systematic errors in the measurement of phase differences and the relaxation times of the transient effects. Additional accidental errors occur due to noise present on the transients. Such noise originates from random fluctuations in the light source output, the particulate nature of light, i.e. shot noise, statistical variations in the secondary emission coefficient of the photomultiplier dynodes and finally, Johnson noise developed in the photomultiplier load resistance. Badoz[3] considered the minimum phase differences which could be measured by the quadratic and linear systems.

Considering only shot noise and a system employing single shot methods,

For $K_i > (\delta_{Qmin})^2$

$$\delta_{Q\ min} = 2\left[\frac{2 K_i \Delta f}{\phi_0 q}\right]^{\frac{1}{4}} \qquad (18)$$

For $K_i = 0$

$$\delta_{Q\ min} = 2\left[\frac{2 \Delta f}{\phi_0 q}\right]^{\frac{1}{2}} \qquad (19)$$

and for $\chi \gg K_i^{\frac{1}{2}}$

$$\delta_{L\ min} = \left(\frac{2\Delta f}{\phi_0 q}\right)^{\frac{1}{2}} \qquad (20)$$

where Δf is the noise bandwidth of the detecting equipment

ϕ_0 is the light flux incident on the analysing prism

in terms of photons per second

$K_i \phi_o$ is the stray light flux incident on the photomultiplier

q is the quantum efficiency of the photomultiplier cathode.

Equations (19) and (20) illustrate that the linear system is the more sensitive. Equations (18) and (20) illustrate the important practical variables which can be minimised K_i, Δf or maximised ϕ_o, q to produce low noise transients. Due to the power relationships, very large variations in these values are required to increase satisfactorily the sensitivity of either arrangement.

It is to be noted that the equations are independent of the gain of the photomultiplier tube. In reality this is not so, the third factor in the list above was not taken into account by Badoz. The actual dependence can be[24] included in the equations above by multiplying Δf by a factor a^2, this being a minimum for photomultiplier tubes with a high first stage gain.

The final factor involving the photomultiplier tube is Johnson noise and for all practical circumstances this can be neglected.[24]

Badoz also considered noise due to variations in the output of the light source. Although long time variations will effect absolute measurements it is rapid fluctuations during the pulse which determine if the corresponding phase difference will be observed. Consider the variation in I_o to be dI_o then

$$\delta_{Q\ min} = 2\left(K_i\left(\frac{dI_o}{I_o}\right)\right)^{\frac{1}{2}} \qquad (21)$$

$$\delta_{L\ min} = \left(\chi\frac{dI_o}{I_o}\right) \qquad (22)$$

These values of δ_{min} might under certain circumstances be greater than those of equations (18) and (19). The limiting phase difference could also be smaller for the quadratic system unless χ is adjusted accordingly.

Limitations due to non-linear behaviour of the photomultiplier

Distortions in the size and shape of a transient will occur if the photomultiplier operates in a non-linear region. This may well occur if the light flux incident on the tube is high, a necessary requirement for maximum sensitivity. For linear behaviour a typical photomultiplier[24] must produce an anode current of less than 10μAmp and 1 mA for continuous and pulsed light levels respectively. The low value of 10μAmps may limit the use of linear detection in circumstances where a small value for the anode load resistance is required.

Distortion of pulse shape caused by a finite bandwidth

The reduction of the bandwidth of the detecting system improves the signal to noise ratio of both the quadratic and linear systems. However, distortion of the recorded pulse shape also occurs.

Consider the sample to be composed of molecules having one relaxation time, τ , then the decay of the light pulse on removal of the field is, for quadratic detection

$$\Delta I(t) = \Delta I(t=0) \exp (-2t/\tau)$$

and for linear detection

$$\Delta I(t) = \Delta I(t=0) \exp (- {}^{t}/\tau)$$

if the relevant approximations hold.

If the input impedance of the detection system following the photomultiplier anode can be specified by a resistance, R, in parallel with a capacitance, C, then the recorded decay pulse has the form[3]

$$\Delta V(t) = \Delta V(t=0) \left[(\tau \exp(-2t/\tau) - 2 A \exp(^{-t}/_{A}))/(\tau - 2A) \right]$$

$$\Delta V(t) = \Delta V(t=0) \left[(\tau \exp(^{-t}/\tau) - A * \exp(^{-t}/_{A}))/(\tau - A) \right] ;$$

for quadratic and linear detection respectively,

where A is the time constant of the detection system which is equal to (RC),

V is the voltage produced across R,

and the noise bandwidth of the system is equal to $(4 A)^{-1}$.

Graphs 7 and 8 indicate the extent of the distortion introduced in the logarithmic plot of the decay.

Riddiford and Jerrard also present equations for the case of molecules represented by two relaxation times. It is sufficient to say that such transients can only be analysed

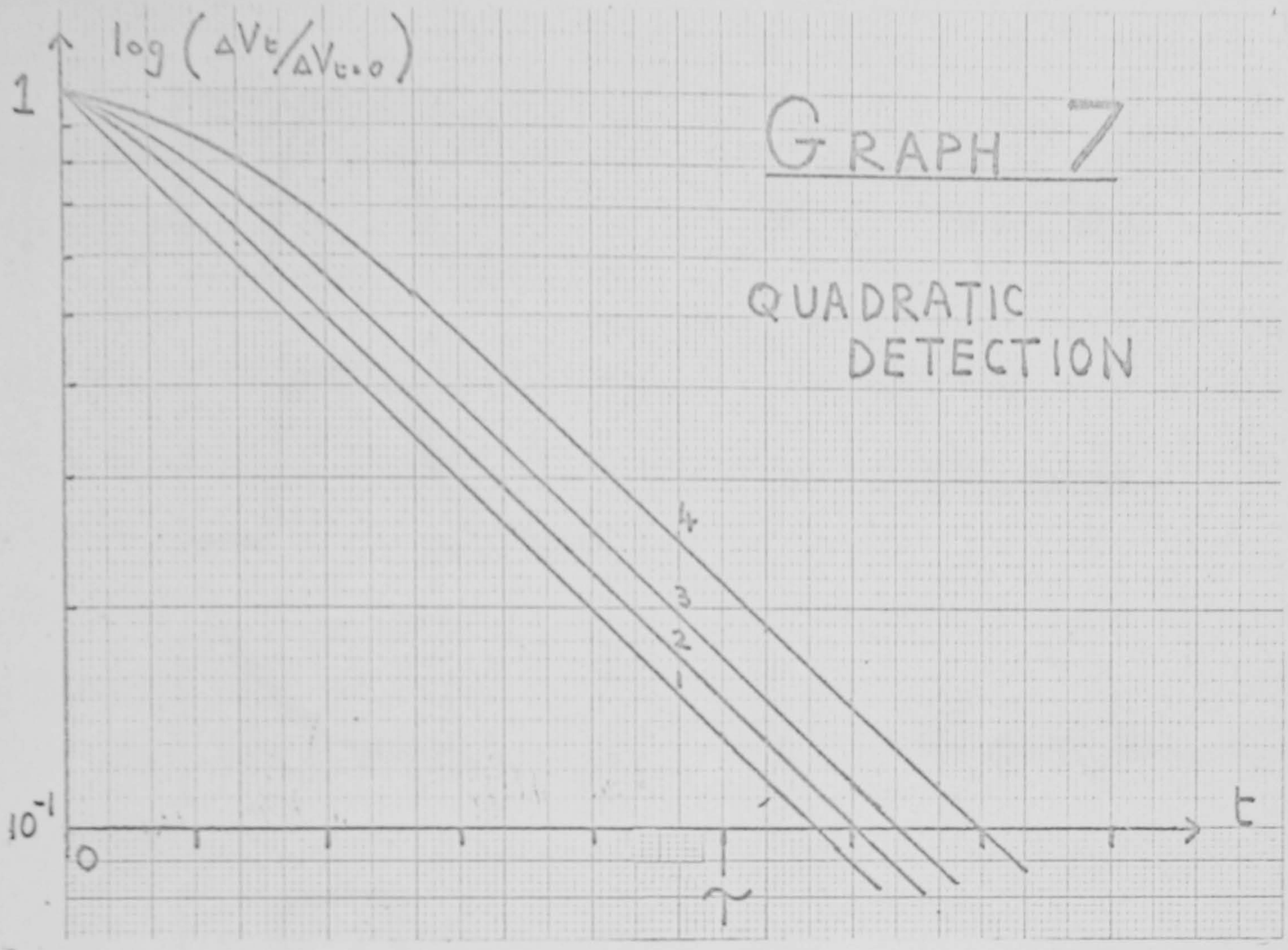

GRAPH 7

QUADRATIC DETECTION

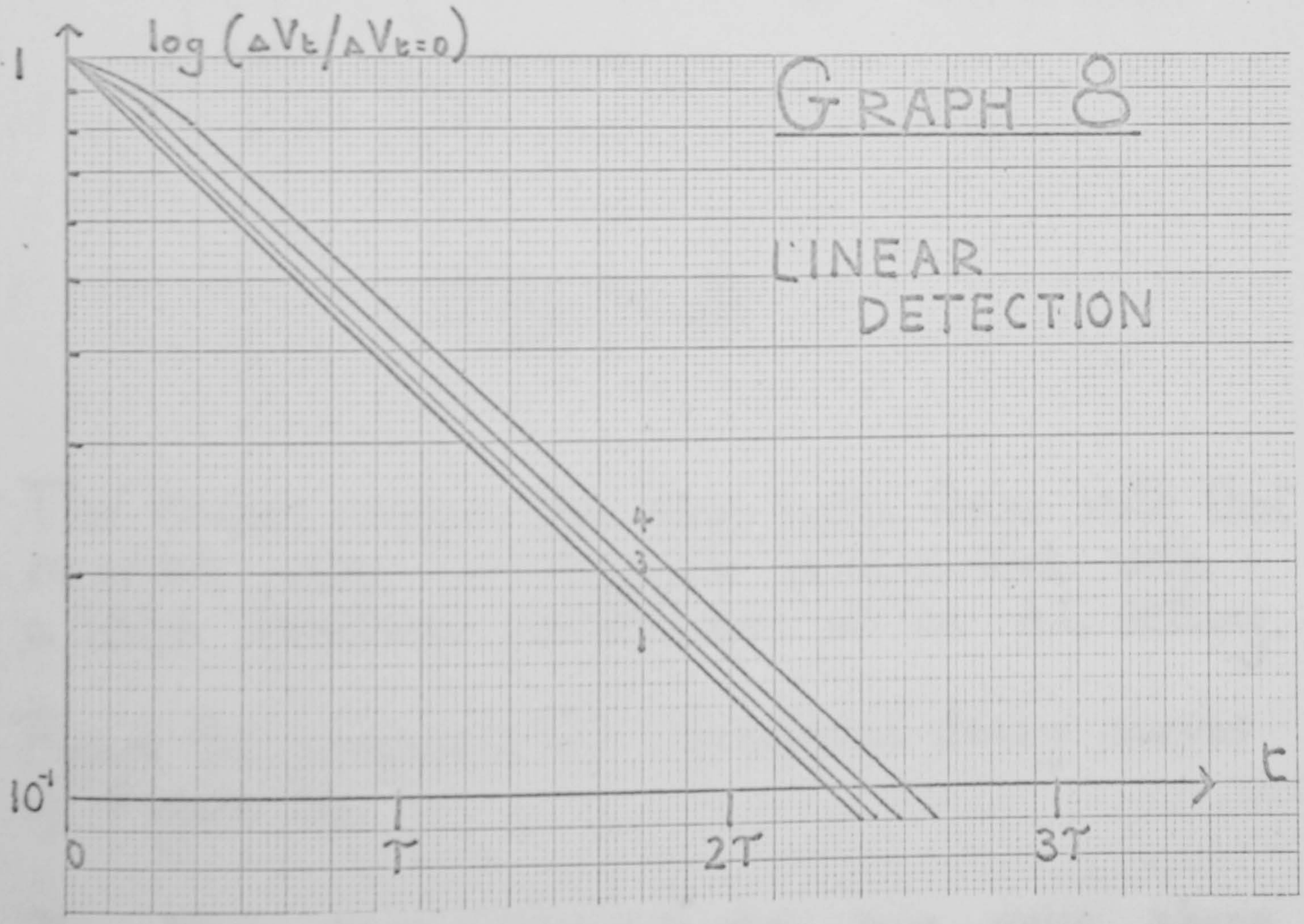

GRAPH 8

LINEAR DETECTION

Curves 1, 2, 3 and 4 are for values of T/A equal to ∞, 20, 10 and 5 respectively.

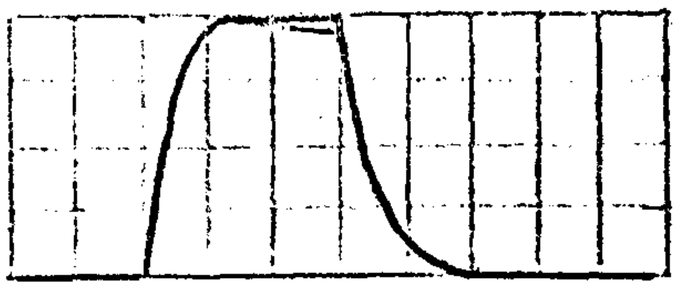

a. 1msec/div.

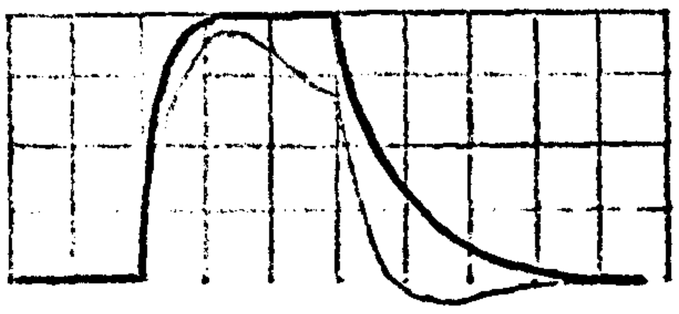

b. 50 msec/div.

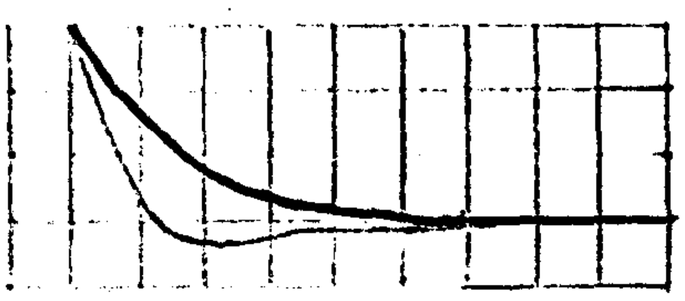

c. 50 msec/div.

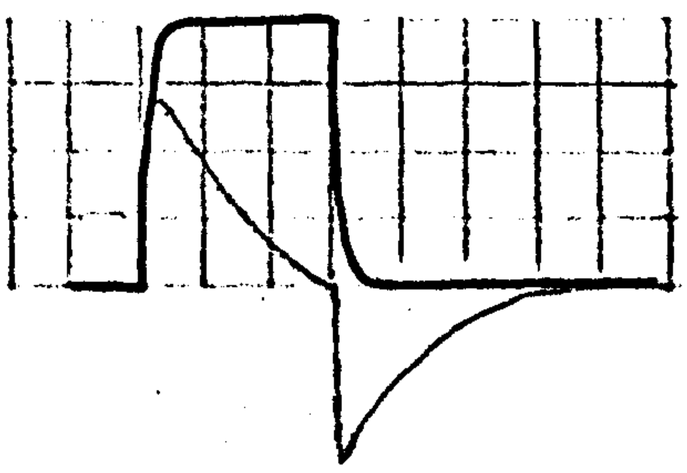

d. 0·5 sec/div.

Figure 3.

The traces compare the true pulse shape with that recorded using a Type 80 plug in unit with a 585A Tektronix oscilloscope on an A.C. setting.

Figure 3c compares the normalised decay curves of Figure 3b.

The dark trace represents the true pulse shape

when the detection time constant is less than one fiftieth of the smallest molecular relaxation time.

A second type of distortion, particularly relevant when the linear system is used, may be present. The observation of a small change in a high steady light level requires the resulting steady voltage to be adjusted to a small value. This can be done with a blocking capacitor: however, low frequency Fourier components of the transient will be removed.

The resulting distortions which may occur are illustrated in Figure 3.

Summary

The measurement of transient birefringence changes using the quadratic and linear systems has been reviewed. It is shown that accurate measurements of phase difference can only be made when the absence of dichroism and optical activity has been established, and when the alignment procedures suggested are performed. Although systematic errors may be reduced in this way, random fluctuations in light intensity and shot noise ultimately limit the accuracy of measurement.

There are no distinctive theoretical advantages in the use of either system. However it is the author's contention that the linear system with the advantages of:- greater sensitivity, allowing constant monitoring of the light intensity, the ability to discern the sign of the birefringence, and its insensitivity to the effects of stray phase differences,

is the better choice. The approximation to linear behaviour has such limited application, however, that exact expressions should be employed.

This work also suggests that whenever birefringence transients are published some indication of the magnitude of the phase differences observed should be given.

References

1) Le Fevre (C.G.) & (R.J.), 'Techniques of Organic Chemistry', vol. I part 3 3rd edn. Ed. A. Weissberger, 1960.

2) Badoz (J.), J. Phys. et le Radium 17, 143A, 1956.

3) Riddiford (C.L.), Jerrard (H.G.) J. Phys. D. 3, 1317, 1970.

4) Jerrard (H.G.), J. Opt. Soc. Am. 44, 289, 1954.

5) Orrtung (W.) & Meyers (J.), J. Phys. Chem. 67, 1905, 1963.

6) Houssier (C.) & Frederiq (E.), Biochim. Biophys. Acta, 120, 113, 1966.

7) Jerrard, (H.G.) et al, J. Phys. E. 2, 761, 1969.

8) Jones (R.C.), J. Opt. Soc. Am. 31, 488, 1941.

9) Clarke and Grainger, 'Polarised Light and Optical Measurement', Pergamon Press 1971.

10) King (R.J.) & Talim (S.P.) J. Phys. E. 4, 93, 1971.

11) King (R.J.), J. Sci. Instrum. 43, 924, 1966.

12) Matsumoto (M.) et al, Biopolymers 6, 929, 1968.

13) Hurwitz (H.) & Jones (R.C.), J. Opt. Soc. Am. 31, 493, 1941.

14) Brown (B.L.), Jennings (B.R.), J. Phys. E. 3, 195, 1970.

15) O'Konski (C.T.), Haltner (A.J.), J. Am. Chem. Soc. 79, 5634, 1957.

16) Kahn (L.D.), Witnauer, Biochimica et Biophysica Acta, 243, 388, 1971.

17) Riddiford (C.L.), Jennings (B.R.), Biopolymers 5, 757, 1967.

18) Golub (E.I.), Nazarenko (V.G.), Biophys. J. 7, 13, 1967.

19) Jennings (B.R.), Browm (B.L.), European polymer journal, 7, 805, 1971.

20) Jerrard (H.G.), J. Opt. Soc. Am. 42, 159, 1952.

21) Marroney (R.) et al, CR. Acad. Sc. Paris, b, 275, 341, 1972.

22) Houssier (C.), Kubalc (H.G.), Biopolymers 10, 2421, 1971.

23) Champion (J.V.) et al, J. Phys. D. 5, 510, 1972.

24) E.M.I. Handbook.

CHAPTER 4

Apparatus and Data Handling Procedures

Introduction

The author's apparatus was established on apparatus inherited from a previous worker. It is thus of essentially the same principle as that described elsewhere.[1] A number of improvements have been incorporated, however, based on housing the optical equipment in a light tight box, and the development of the Kerr cells. In particular a novel method of data handling has been employed and incorporated directly into the apparatus, which allowed transients to be recorded in digital form and then analysed using a computer.

Incomplete work has also been carried out on improving the past author's microsecond pulse system.

Details of the performance of individual components and the calibration of the equipment using nitrobenzene will be given.

The Apparatus

The equipment can be seen in Photograph 1 and in Fig. 1. It consisted of three sections, an optical, a pulse generating and a transient display system. The optical system can be closely observed in Photographs 2.

The optical system employed a 500 watt d.c. high pressure mercury arc lamp as the light source (1). A highly stabilised voltage source, 70 V ± 0·01% at 7 amp, built by the author,

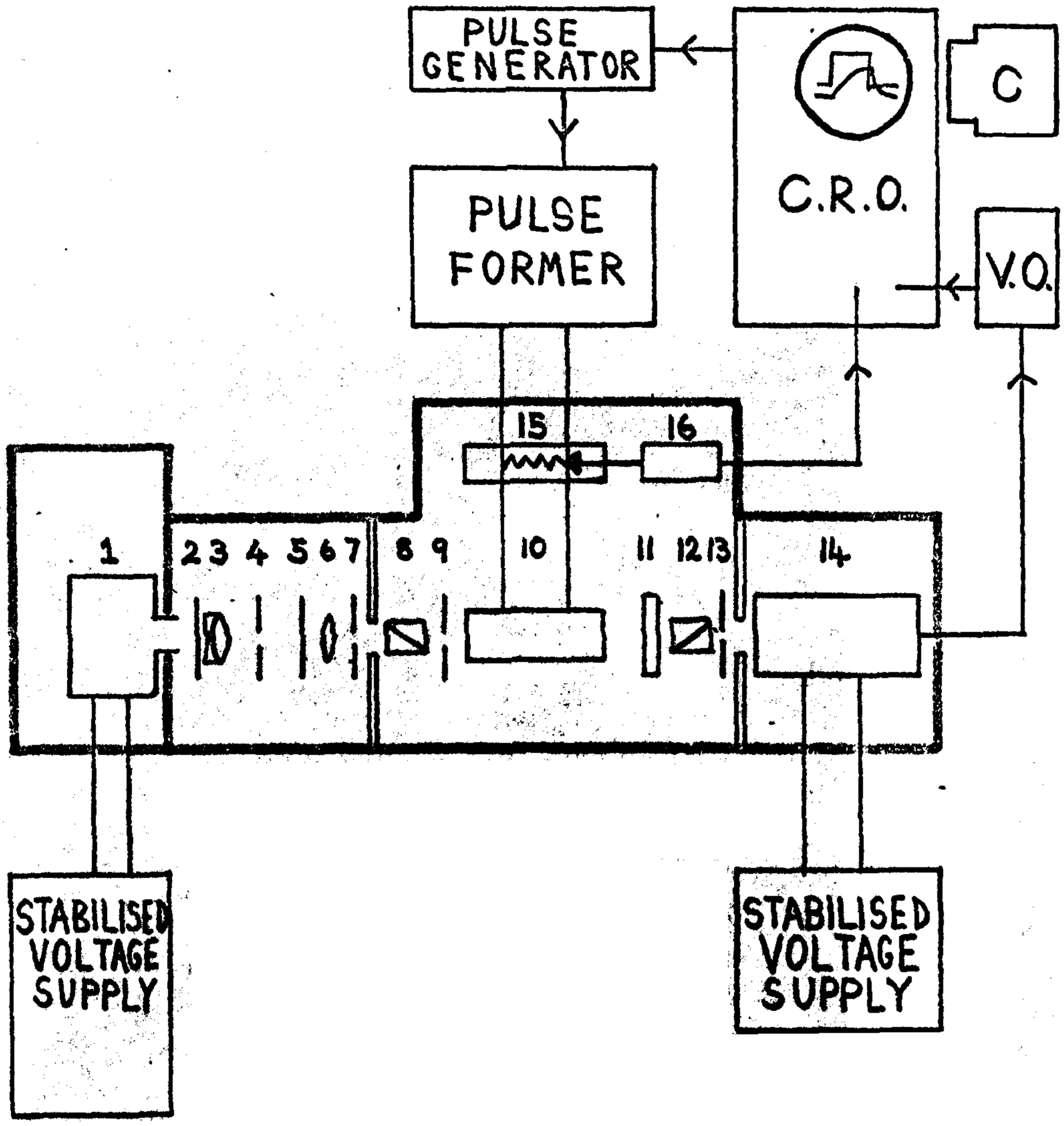

See text for description of numbered components in light tight box and additional lettered components.

THE APPARATUS
AS USED WITH THE LINEAR SYSTEM

FIGURE 1

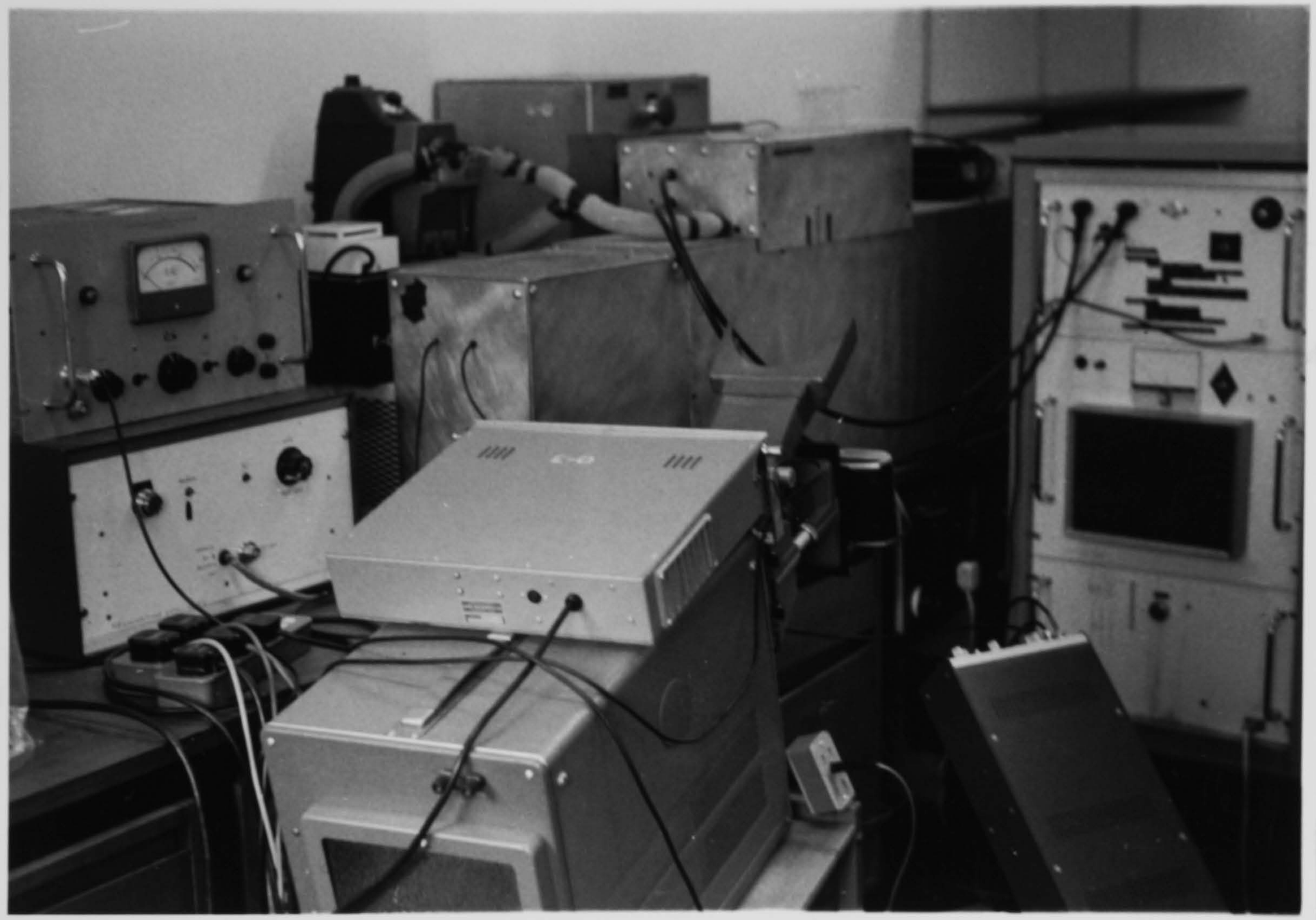

PHOTOGRAPH 1 THE APPARATUS

PHOTOGRAPH 2 THE OPTICAL SYSTEM

powered the arc; however, the light output had a noise level of 1% and short term stability of ± 3%. The lamp was positioned in a sheet-iron case which was mounted on a steel platform. Adjustment of the lamp in all three dimensions was possible. The whole assembly was contained in a box which could be detached from the main optical compartment. The location of the equipment was such that only crude anti-vibration mountings, rubber stoppers attached to the base of the box, were required.

A filter (2) made of HA3 heat absorbing glass, obtained from Optical Works Ltd., Ealing, protected an achromatic lens (3) from the heat generated by the arc. This lens was of focal length 8 cms and focused the arc onto a pinhole, (4), placed at the focal point of a second lens (6) which had a focal length of 10 cms. An interference filter (5) isolated and transmitted the required wavelength of the mercury spectrum. The divergence of the light beam incident on the polariser after passage through the diaphragm (7) was 1×10^{-2} radians at best. The power of the collimated beam at 5461 Å was of the order of 10 μwatt, which was considerably lower than that of 0·6 watt radiated by the arc. The polariser (8) was of the Glan Thompson type and was held in a rotatable mount. The mount and the position of the polariser in the mount were adjusted such that the light beam was at all times normal to the polariser face. The orientation of the plane of vibration of the polariser was ascertained by the pile of plates method. The polariser was rotated so that it would not transmit light reflected at Brewster's angle

from a pile of glass microscope slides. The front face of the glass slides was set to be normal to the horizontal plane, defined using a small spirit level. The polariser was then rotated through 45°. Repeated measurements indicated that the plane of vibration could be set to ± 1°. The polariser mount itself could be accurately set at 0·1° intervals by means of a Vernier scale.

A slit (9) reduced the width of the polarised beam so that reflections off the electrodes of the Kerr cell (10) did not occur. The design of the Kerr cells employed will be described in detail later. The flat base of each cell could be accurately located in troughs milled in a steel platform. The platform itself was adjusted to lie in a horizontal plane. This plane was definable to ± 12 minutes using the small spirit level. The polariser was rotated so that its plane of vibration was at 45° to the platform and hence to the cell electrodes. The overall accuracy of this procedure was ascertained when the quadratic calibration measurements were performed on nitrobenzene. A constant voltage was applied to the cell and the amplitude of the optical trace was recorded as a function of the orientation of the polariser and analyser. Graph 1 indicates that an error of ± 3° could be incurred. This figure indicates the accuracy with which the cells could be machined and positioned.

The quarter-wave plate (11) (a thin sheet of mica) previously calibrated at 5461 Å, was held in position on a rotatable mount and accurately aligned perpendicular to the light beam. The analyser (12) was of exactly the same construction as the polariser, and similarly aligned. Finally

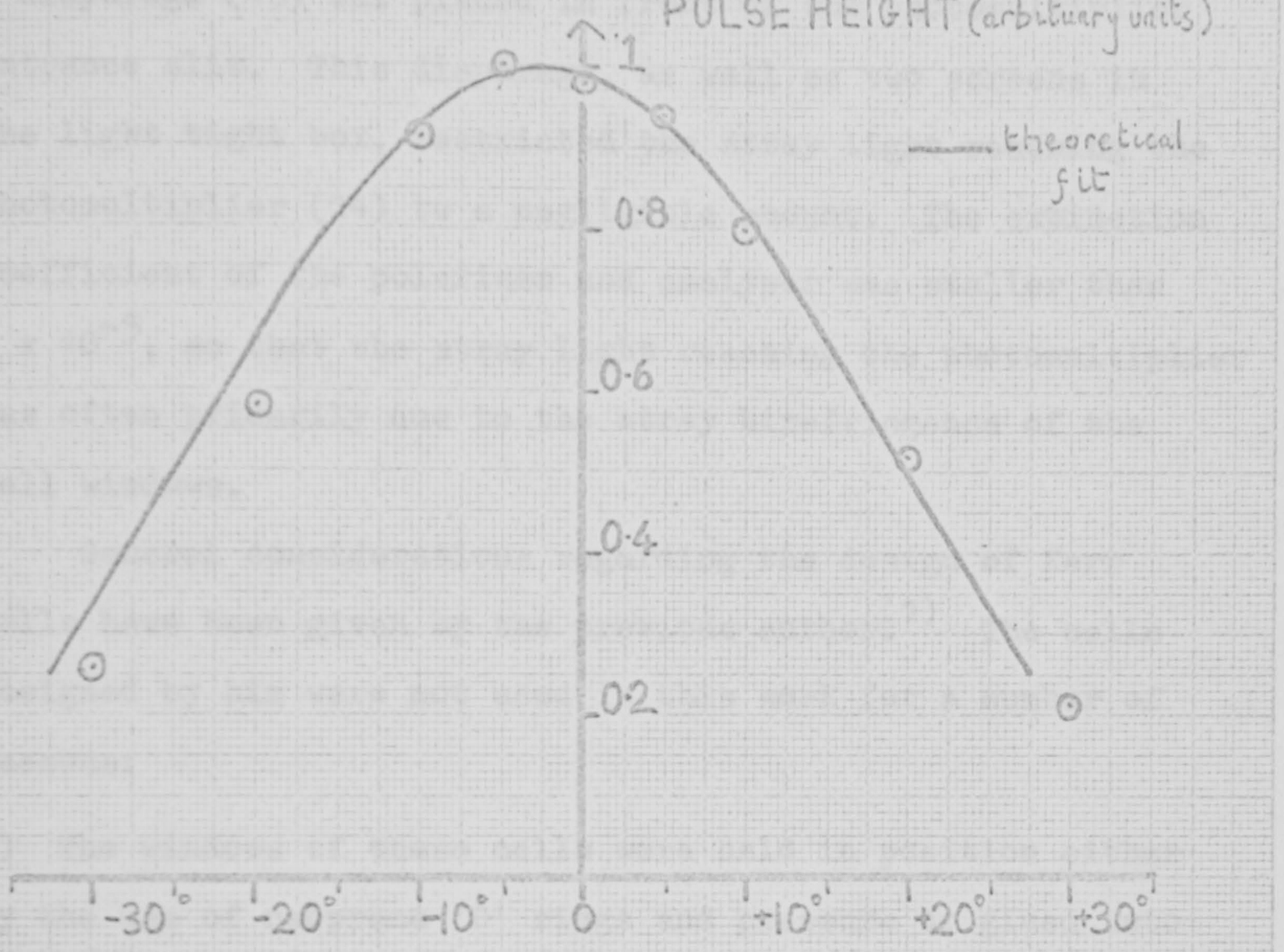
PULSE HEIGHT (arbitrary units)
1
0·8
0·6
0·4
0·2
theoretical fit
-30°
-20°
-10°
0
+10°
+20°
+30°
ELECTRODE ORIENTATION
with respect to initial aligned position

GRAPH 1

a diaphragm (13) was placed in front of the photomultiplier entrance slit. This diaphragm, as well as two screens in the light tight box, restricted the stray light reaching the photomultiplier (14) to a negligible amount. The extinction coefficient of the polariser and analyser was smaller than 1×10^{-5}, so that the stray light reaching the photomultiplier was often primarily due to the stray birefringence of the cell windows.

General considerations regarding the design of Kerr cells have been given by the previous author.[1] The cells designed by him were not used in this work for a number of reasons:

1) The windows of those cells were held in position either by the use of neoprene 'O' rings and pressure or glued into place using Araldite. Both 'O' rings and Araldite were attacked by common organic solvents such as chloroform and metacresol used in this work.

2) The windows were strain free microscope cover slips but both methods of clamping introduced relatively high stray phase differences. Graph 2 was plotted in accordance with the procedure described in Chapter 3 and has the form predicted by equation 10 of that chapter. The phase difference introduced was therefore typically 3×10^{-2} radians at 5461 Å for the windows held with Araldite.

3) The effective phase difference had to be determined each time the cells were used.

To overcome problem 1 above, cell 1 was constructed (see

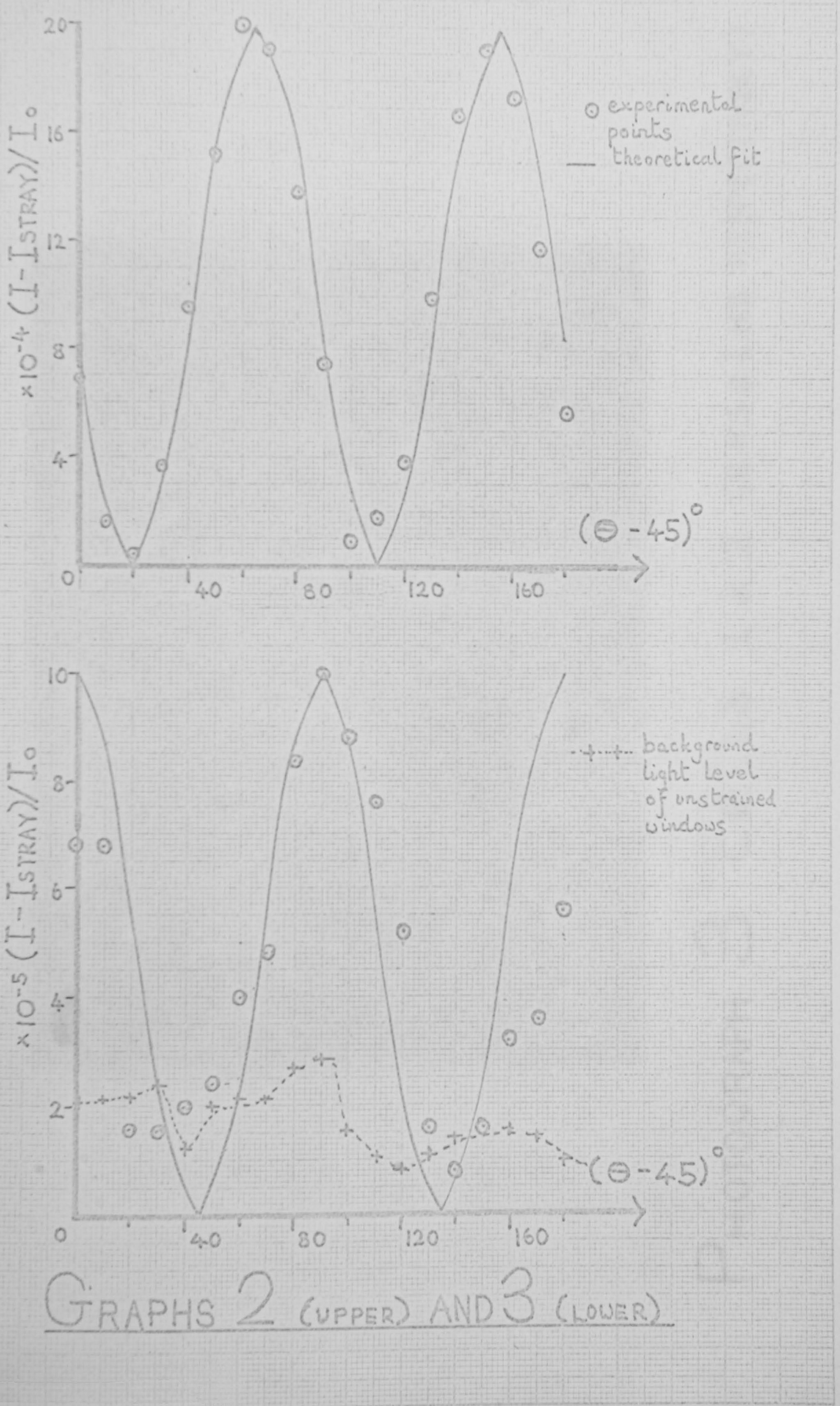

GRAPHS 2 (UPPER) AND 3 (LOWER)

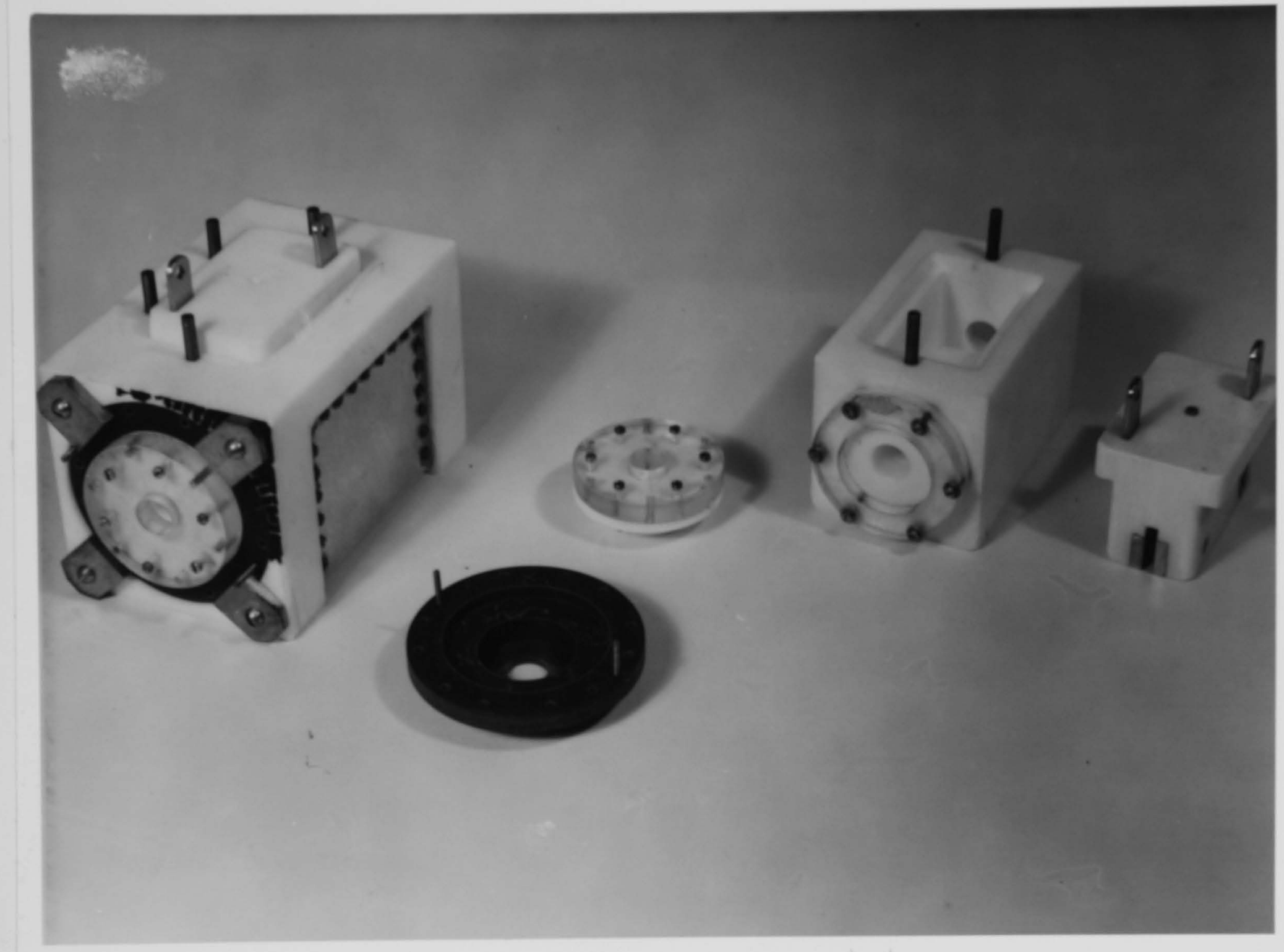

PHOTOGRAPH 3 CELLS 1 & 2 (R.H.S & L.H.S RESPECTIVELY)

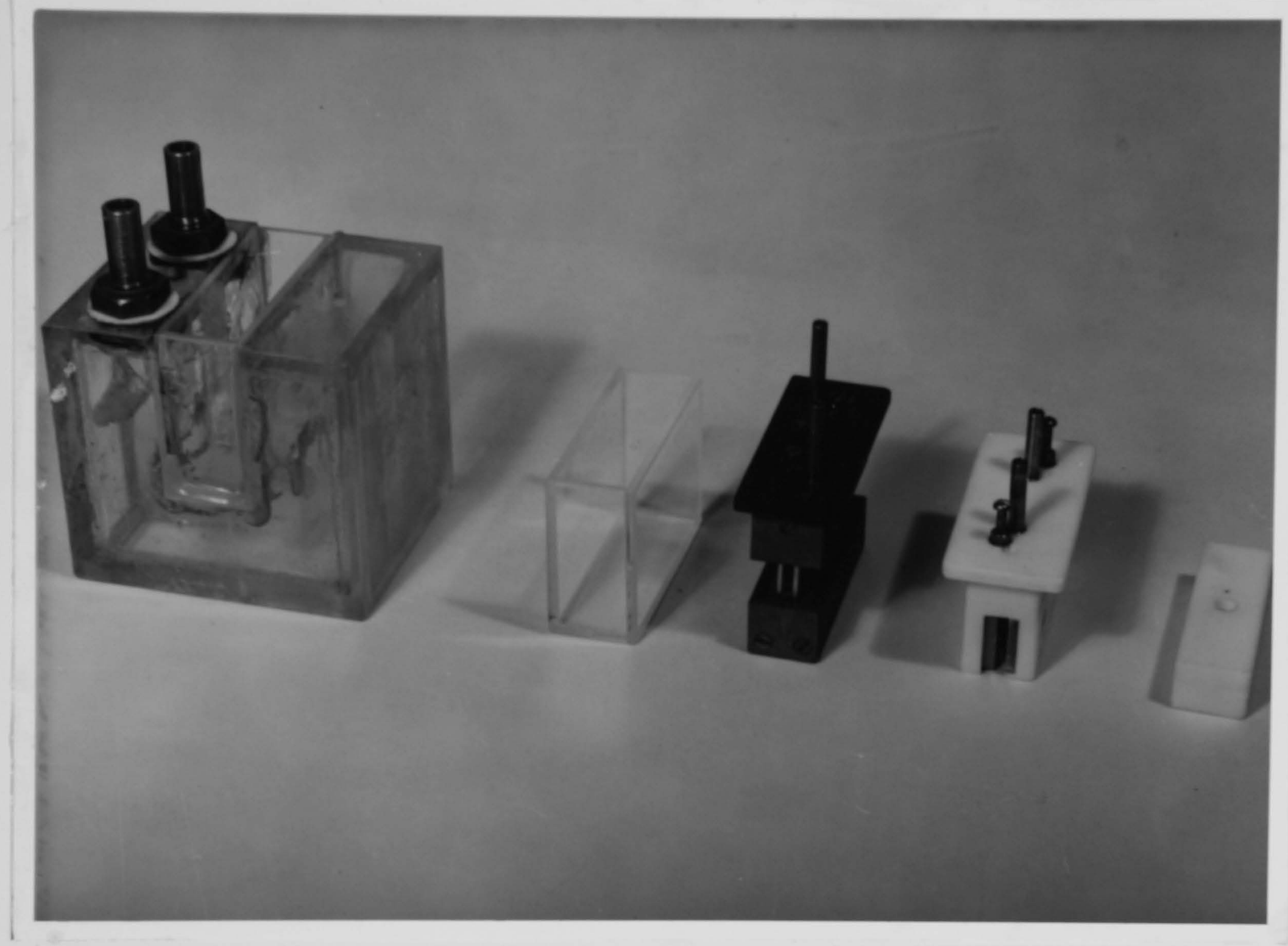

PHOTOGRAPH 4 CELLS 3 & 4 WITH ELECTRODE MOUNTINGS 1 & 2

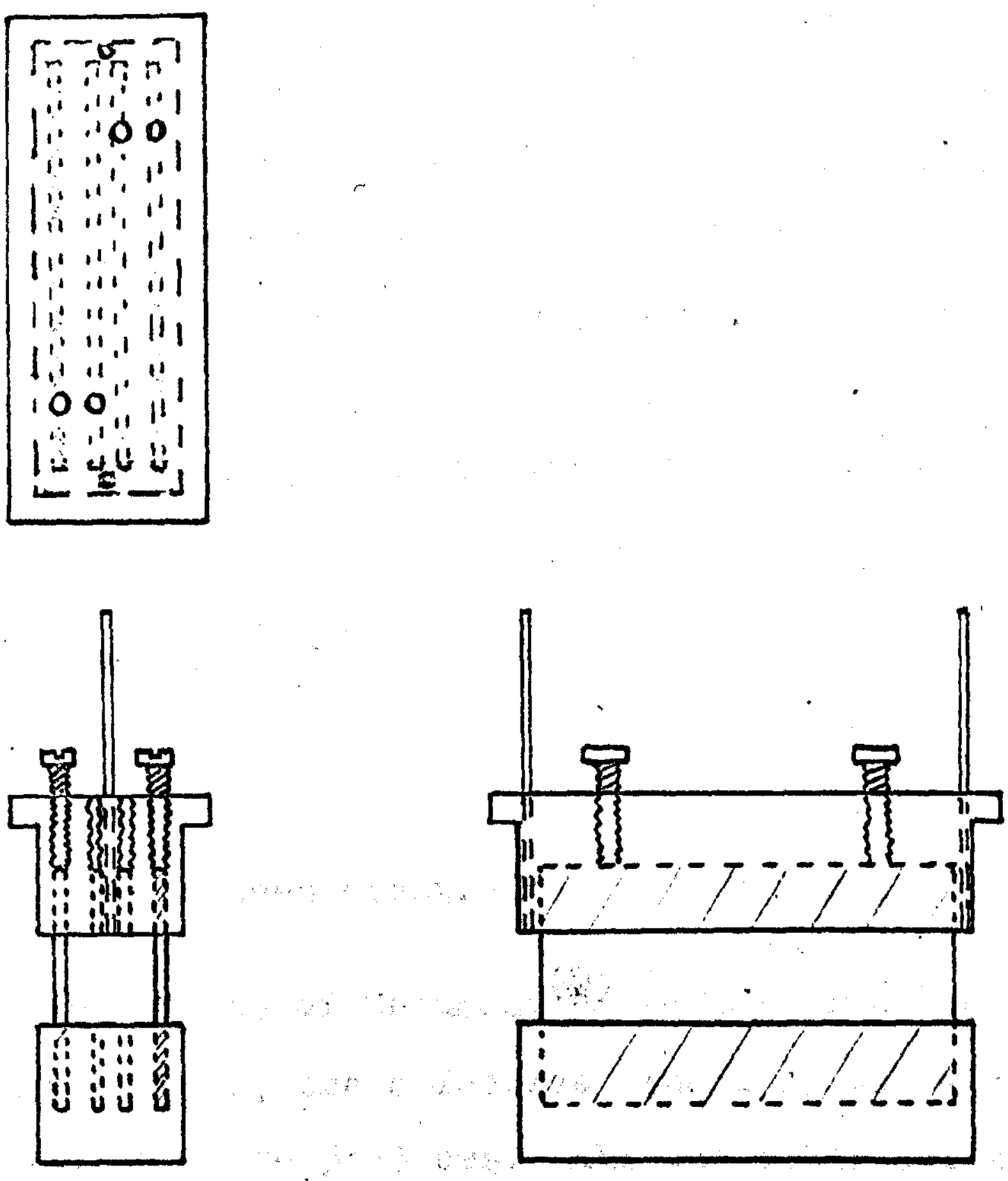

SCALE, LIFE SIZE

DIMENSIONS OF STAINLESS STEEL ELECTRODES,

LENGTH 4·5cms, HEIGHT IN SOLUTION 1cm, THICKNESS 1mm,

SEPARATION 2·16mm, 6·00mm OR AS SHOWN 1·00 cm.

MOUNTING MATERIAL, TUFNOL (KITE BRAND)

FIGURE 2 ELECTRODE MOUNTING No.1

Photograph 3). The cell windows were held against the PTFE body with PTFE end caps screwed onto the body. The windows acted reasonably well as a single phase plate as shown in Graph 3. The phase difference introduced was of the order of 6×10^{-3}. The electrodes were of stainless steel and mounted on a PTFE block which was push fitted into the cell body.

The dimensions in centimetres of the electrodes were as follows:-

length	5·00
height	0·95
thickness	0·30
gap between electrodes	0·258 ± 0·002

Using the equations of Chaumont[2] to take into account field edge effects, the effective length of the electrodes was determined to be 5·13 cms. All the other cells employed had electrodes of similar length and dimension. However the construction of the cells was not in exact accordance with the theoretical situation envisaged by Chaumont, so that the correspondingly small corrections were not used.

Cell 2 was constructed in order to eliminate the effects of the stray phase difference (see Photograph 3). In accordance with the suggestions of Chapter 3 the cell windows were held in PTFE end pieces which could be rotated. Unfortunately clamping the end pieces to the cell body to prevent leaks always reintroduced additional strains. Because of this the PTFE end pieces were replaced by Kite brand

Tufnol, kindly supplied by Tufnol Ltd., Peckham. This was a sturdier material but did not prevent strains being transmitted to the windows. This cell design was therefore abandoned.

Eventually the body of Cell 1 warped. Consequently the cell leaked and the distorted windows focused the light beam when the cell was filled with solution. After due consideration a spectrophotometer cell was used. Cells of a completely fused type were specially built by Hellma (England) Ltd., Westcliff-on-sea, see cell 3, Photo 4. They introduced a stray phase difference constant in direction and of magnitude 2×10^{-3} radians at 5461 Å. The cells did not leak and therefore admirably satisfied the three requirements above. However, the cells were susceptible to fracture and required gentle treatment.

One of the cells was mounted in a perspex water jacket using Araldite (see cell 4, photograph 4). Consequently the stray phase difference rose to 1×10^{-2} radians.

Two electrode assemblies were made to fit loosely into the spectrophotometer cells (see photograph 4.) The first, El 1, was made of Kite brand Tufnol. The stainless steel electrodes were push fitted into slots accurately machined in the upper and lower pieces of Tufnol. Stainless steeel screws made the electrical connection to each electrode. The assembly could be easily dismantled for cleaning and used with electrode separations of 0·20, 0·60 and 1·00 cm.

The second electrode assembly, El 2, was made out of PTFE. It could not be machined as accurately as Kite brand Tufnol but had a greater resistance to organic solvents.

The volume of solution required was 7 ccs. and 2 ccs. when El 1 and El 2 respectively were used. Inlets through which the cell could be filled were provided on each electrode assembly.

A scale diagram of the Tufnol electrode assembly is given in Fig. 2.

The electric field pulse system

The first stage in the generation of the high voltage pulse was common to both the d.c. and a.c. pulse systems used. A pulse from the oscilloscope, type 585A Tektronix, triggered a Claude Lyons type PG 21 pulse generator, which produced a single low voltage pulse of variable magnitude and duration. This pulse was then amplified by the following pulse forming networks.

P.G. 1 (see Fig. 3) delivered a d.c. pulse of magnitude 0 to 600 V at 1 Amp and duration greater than 5 m.sec. A Wareham power amplifier type C 646 amplified a 0 to 1 Volt d.c. level obtained from a battery and potentiometer arrangement.

A system of reed relays allowed the voltage to be developed across a 1 KΩ load resistance, $R_{\ }$, in parallel with the Kerr cell, KC, on arrival of the P.G. 21 pulse. The transistor pulse generator previously designed[1] was found to be unsatisfactory due to a constant voltage difference at its output.

P.G. 2 (see Fig. 4) provided a d.c. pulse of magnitude 400 to

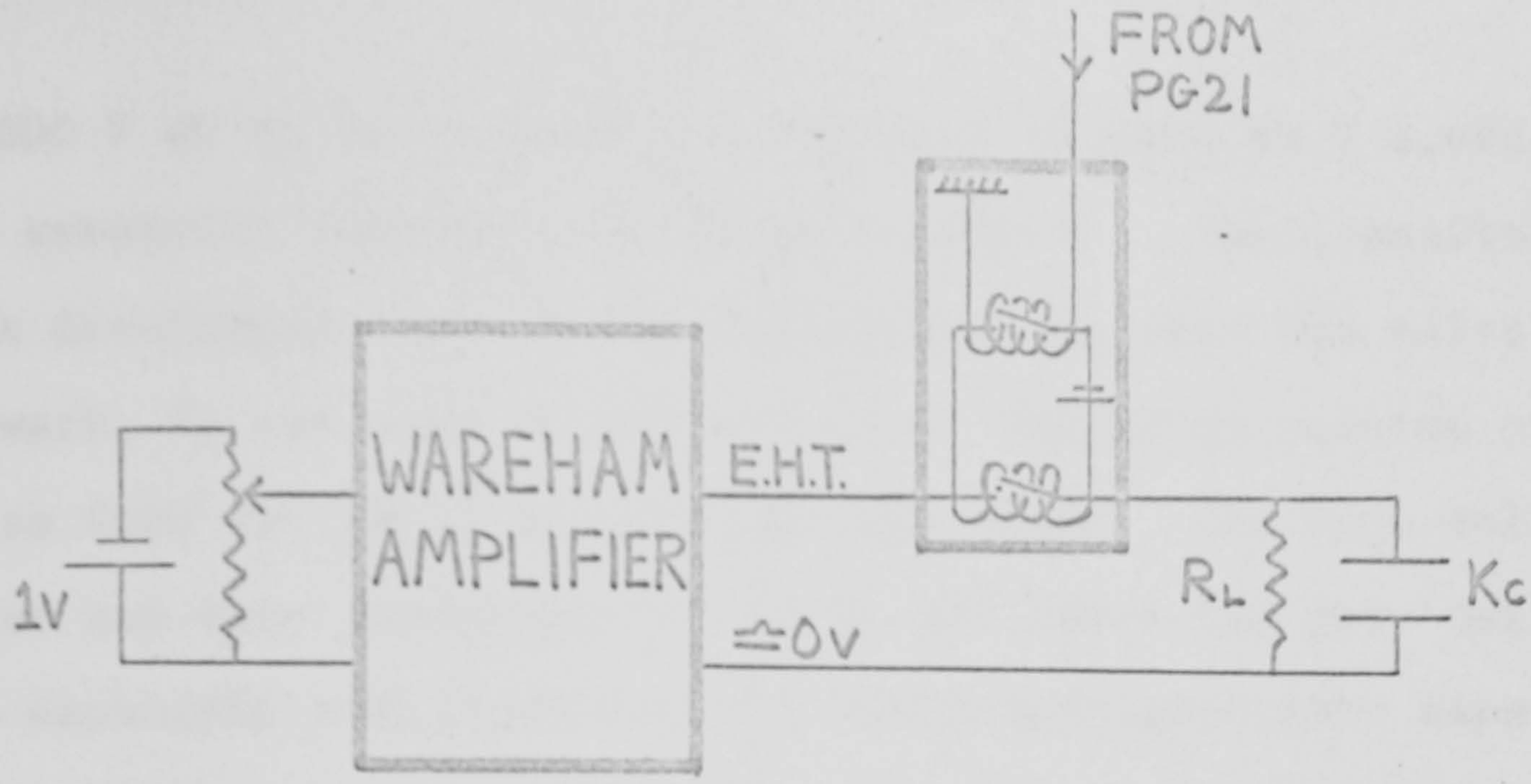

FIGURE 3.

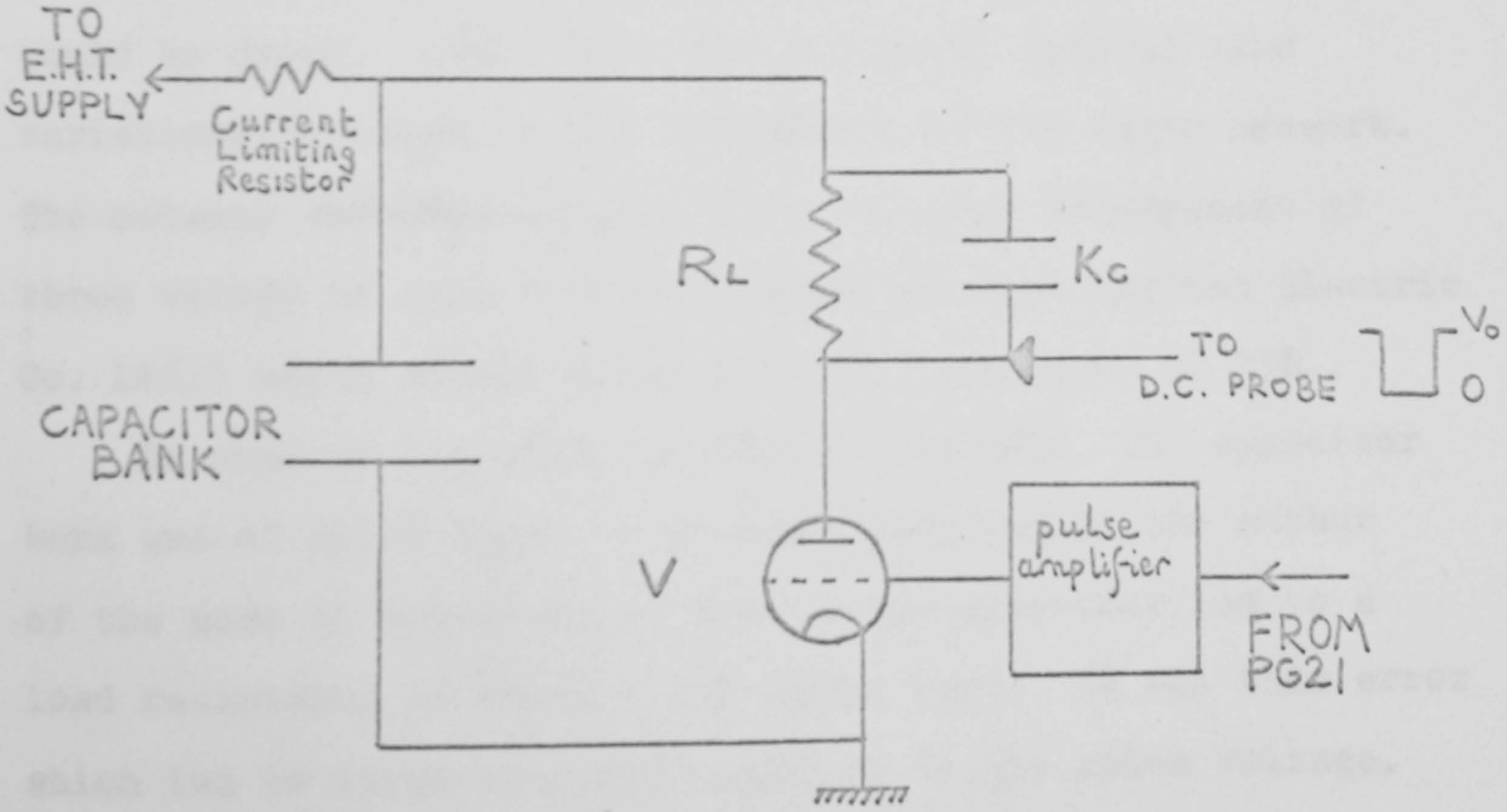

FIGURE 4

10,000 V at up to 10 Amps and duration 50 μsec to 1 m.sec. The essential elements are shown in Fig. 4. The capacitor bank discharged through the resistance, R, when the valve network, V, was made to conduct by an amplified version of the pulse from the P.G. 21 low voltage generator. The high voltage pulse was thus generated across R_L and hence the Kerr cell. The capacitor bank consisted of two 50 μF capacitors capable of working at 10 KV. They were supplied by British Insulated Callender Cables Ltd. of Helsby, Cheshire. Pulses could be applied to a total load of 2,000 Ω with only a 1% change in the voltage across the capacitor bank. If greater changes in pulse shape could be tolerated , currents up to 10 Amp could be drawn. Above this current level drastic time variations occurred in the resistance of the valve network. The network actually consisted of a parallel arrangement of three valves of type C 1150/1 (obtained from English Electric Co. Ltd.) which normally had a total resistance of 25Ω.

In some of the work carried out in PBLA the capacitor bank was of value 3 μF. A misunderstanding by the author of the mode of operation of this pulse generator led to a load resistance of value 1 KΩ being used. It was this error which led to large changes occurring in the pulse voltage. The resistance of the cell containing the PBLA solution was considerably greater than 1 KΩ so that the value of R_L should have been correspondingly increased.

P.G. 3 was used to deliver voltage pulses up to 5,000 V and duration greater than 5 m.sec. It was constructed by replacing the valve network of P.G. 2 with the relay arrangement

used in P.G 1. The reed relay employed (Type GB 129 B obtained from Astralux Limited, Brightlingsea, Essex) limited the currents which could be drawn to 3 Amps. Above 800 volts relay bounce occurred, which seriously distorted the decay of the optical pulse.

P.G 4 produced a.c. field pulses in a manner analogous to P.G. 1. A low voltage R.C. oscillator, supplied by Levell Electronics Ltd., High Barnet, Herts., provided a signal of variable frequency 1·5 Hz to 150 kHz. The Wareham amplifier amplified this signal over the frequency range 0 to 3 kHz. An amplifier type 254 obtained from Airmec Ltd. amplified signals of frequency 15 Hz to 30 kHz with a maximum output of 800 Volts R.M.S. at 0·2 Amps.

The relay was positioned on the output side of the amplifier. This had two advantages; any d.c. component could be easily monitored before being removed, and little distortion occurred in the pulse shape.

The load resistance (15) in parallel with the cell and the attenuator (16) used to monitor the voltage pulse were both housed in the upper compartment of the light tight box. The lid of this compartment activated microswitches so that an alarm bell rang if the lid was accidentally removed.

The detection system

The applied electric field pulses were monitored using a Tektronix 6013 A d.c. voltage probe. This had an attenuating factor of approximately 1,000 to 1 and a response time of

14 n sec.

The optical signal was detected using a 56 AVP photomultiplier. This was housed to avoid interference from stray electric and magnetic fields in the manner previously described.(1) The dynode chain and stabilised voltage supply were also those previously used. In accordance with the considerations in Chapter 3, a simple battery and potentiometer arrangement (V.O.) was used to offset any large d.c. level at the photomultiplier output.

The dual channel input of the oscilloscope allowed the optical and field pulses to be simultaneously displayed and photographed. Polaroid film, type 46 L Land projection film was used. Both the electric field probe and the oscilloscope input attenuators were calibrated using the external calibration source of the oscilloscope. This procedure was accurate to ± 3%.

A photographic enlarger was used to project the recorded film negative onto a large sheet of graph paper. The graph paper was placed on a bench top and could be readily moved for ease of measurement. The maximum height of a transient could be measured to 1% accuracy. A slightly less accurate but much more versatile method of transient analysis was also employed and is described later.

Use and performance of equipment

The systematic manner in which measurements were made on an undocumented solution can be seen in flow diagram 1.

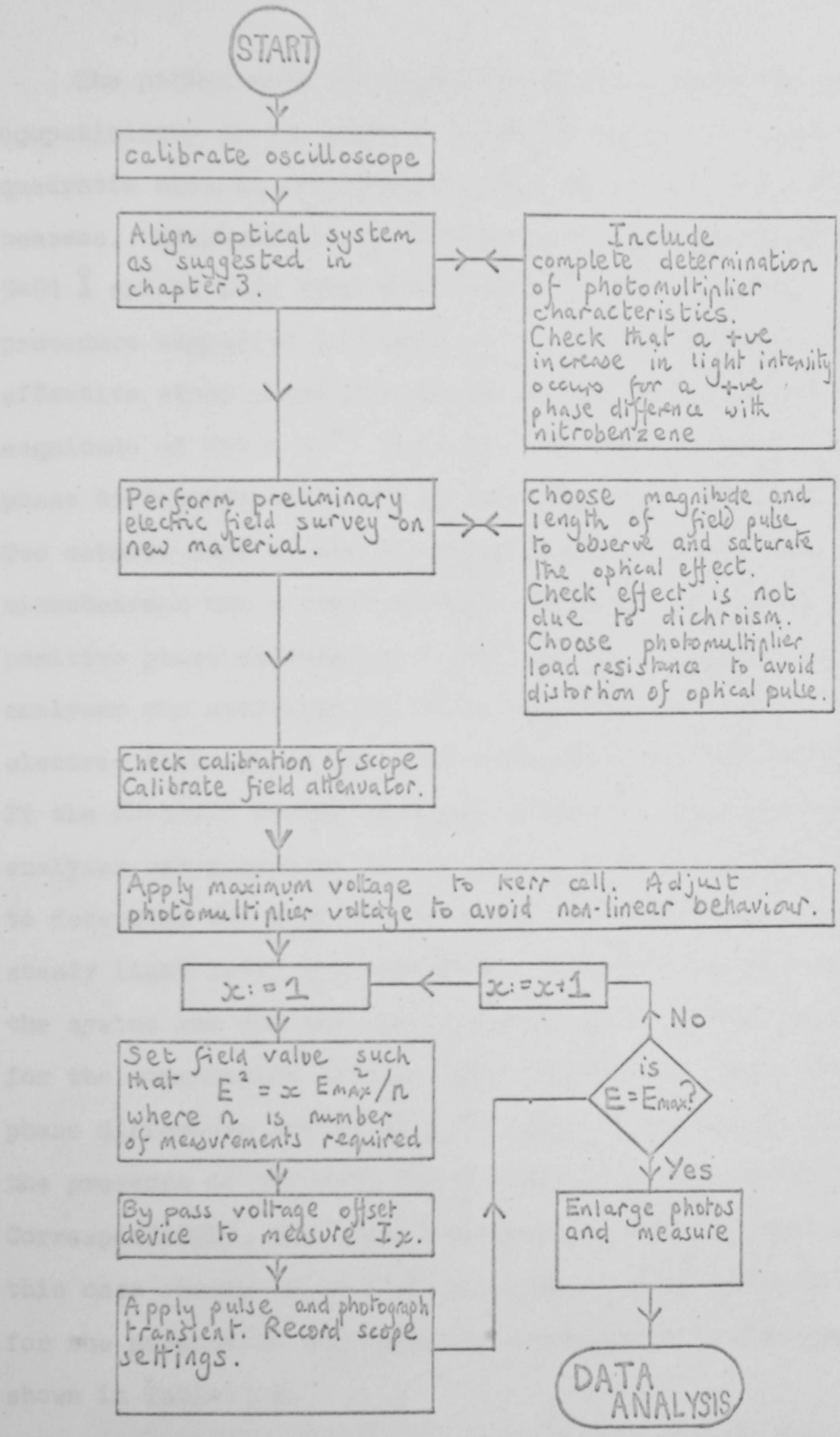

FLOW DIAGRAM 1

Method of taking linear measurements

The performance of the equipment as a whole and the compatibility of the results obtained using the linear and quadratic optical arrangements were determined using Nitrobenzene. Measurements were made using light of wavelength 5461 Å and at room temperature 25 ± 2° C. Using the procedure suggested in Chapter 3 it was ascertained that the effective stray phase difference of the cell used had a magnitude of $3{\cdot}4 \times 10^{-2}$ radians. The sign, however, of the phase difference could not be determined by that procedure. Two methods used by the author employed the fact that nitrobenzene has a positive Kerr constant and hence introduced positive phase differences. For the linear system the analyser was uncrossed by 6° as suggested in Chapter 3. An electric field pulse was then applied across the nitrobenzene. If the observed change in light intensity was negative the analyser was uncrossed in the opposite direction by 6°. Now to determine the sign of the stray phase difference the steady light level was measured. The cell was removed from the system and the new steady level was recorded. On allowance for the attenuation of the light beam by the cell, the stray phase difference was of positive sign if the light level in the presence of the cell was greater than that in its absence. Correspondingly, the angle uncrossed by the analyser was in this case chosen to be 7·0° (i.e. χ + δ stray/2) not 6·0° for the purpose of the computer calculation of the results shown in Table 1 a.

Immediately after these measurements the quarter-wave plate was removed and measurements using the quadratic system

To convert phase differences to birefringence values multiply by $1 \cdot 74 \times 10^{-6}$.

$\delta \times 10^1$	E KV/cm	B c.g.s. units $\times 10^5$
·385	1·90	3·07
1·10	3·23	3·01
2·07	4·64	2·75
3·48	5·85	2·91
3·73	7·57	2.86
9·99	9·89	2·93

1 a. Results obtained with the linear system and corrected for stray birefringence.

$\delta \times 10^1$		E KV/cm	B c.g.s. units	
uncorrected	corrected		uncorrected	corrected
·744	·478	2·25	4·23	2·72
1·22	·922	3·13	3·56	2·70
2·18	1·82	4·54	3·03	2·52
2·98	2·66	5·65	2·67	2·38
4·42	4·09	6·96	2·61	2·42
6·03	5·71	8·08	2·65	2·50

1 b. Results obtained with the quadratic system.

TABLE 1. Measurements performed on nitrobenzene.

were performed on the same sample of nitrobenzene. The results of that experiment can be seen in Table 1 b. It is evident that values of the Kerr constant decreased with increasing phase difference. This again showed that the stray phase difference had a positive sign. Table 1 b also includes the values obtained on correcting the results for the stray phase difference $+ 3{\cdot}4 \times 10^{-2}$ radians.

For linear detection the average value of the Kerr constant was $2{\cdot}92\ (\pm\ 0{\cdot}10) \times 10^{-5}$ cm statvolt^{-2}. The root mean square error was 3% and the greatest deviation from the average value was 6% of the average value.

For quadratic detection the Kerr constant was $2{\cdot}55\ (\pm\ 0{\cdot}13) \times 10^{-5}$ cm statvolt^{-2}. The error was 5% and the greatest deviation from the average value was 7% of the average value.

It should be noted that the errors determined here are not universally applicable to the use of the equipment. If large phase differences are observed such that $\sin(\delta/2)$ approaches 1 then the error will drastically increase.

The two Kerr constants were not consistent within the accuracies indicated. This may have been due to an unknown imperfection in the quarter-wave plate, the operation of the photomultiplier in steady light level conditions, or a greater variation in temperature than that suggested by the room temperature quoted above.

Both results were considerably lower than the most quoted value of $3{\cdot}8 \times 10^{-5}$ cm statvolt^{-2}. Tests with reserve components indicated that the discrepancy was not due to the

equipment. Indeed Benoit,[3] who obtained a value of 3·30 (± 0·1) x 10^{-5} cm statvolt^{-2} at 22° C remarked on the wide range of values quoted, i.e. 2·49 to 3·86 x 10^{-5} cm statvolt^{-2}. The result obtained here is likewise attributed to the purity of the nitrobenzene tested, which was micro-analytic standard nitrobenzene obtained from Hopkins and Williams Ltd., Chadwell Heath, Essex.

The response time of the photomultiplier and the associated display circuitry was ascertained without the need to apply an electric field pulse to the nitrobenzene. The stray light reaching the photomultiplier was reduced to such a low value that single photons could be observed. The decay of the single photon traces yielded the time constants T.C. shown in Table 2 directly below.

RkΩ	T.C. μsec
1	0·1
10^2	10
10^3	50
where R is the photomultiplier load resistance.	

TABLE 2

The individual pulse generators produced pulses which did not conform exactly to a rectangular shape. The additional response time introduced was measured by observing the corresponding optical pulse from nitrobenzene.

Extension of the display system to incorporate a transient recorder

The extended system included a Biomation 610 transient recorder interfaced to Facit type 4070 tape punch. Many details of the source and performance of this equipment are given in the paper[4] in Appendix 1, and only useful additional information is included here. The position of the data-logging equipment with respect to the whole system can be seen in Fig. 5. For functions other than actually recording the transient, such as the alignment of the optical equipment, the calibration of the field attenuator, and the measurement of the steady light level present, the oscilloscope was employed. This also simplified the program necessary to analyse the data.

The data fed to the ICL 1903 computing system consisted of paper tape and data cards.

The paper tape was of a complex character. In addition to the blocks of 128 six bit binary words depicting the observed applied electric field or optical response the tape consisted of spurious characters due to electrical noise and incorrectly recorded transients. Useful information was separated from the noise by a length of blank tape and an arbitrary number of words in which all eight characters were punched (see Fig. 6). The latter words were a standard feature of the tape punch used and only produced on the tape if the analogue replica of the recorded transient was deemed satisfactory by the author. Before forwarding the tape for computer analysis the length of each block of useful inform-

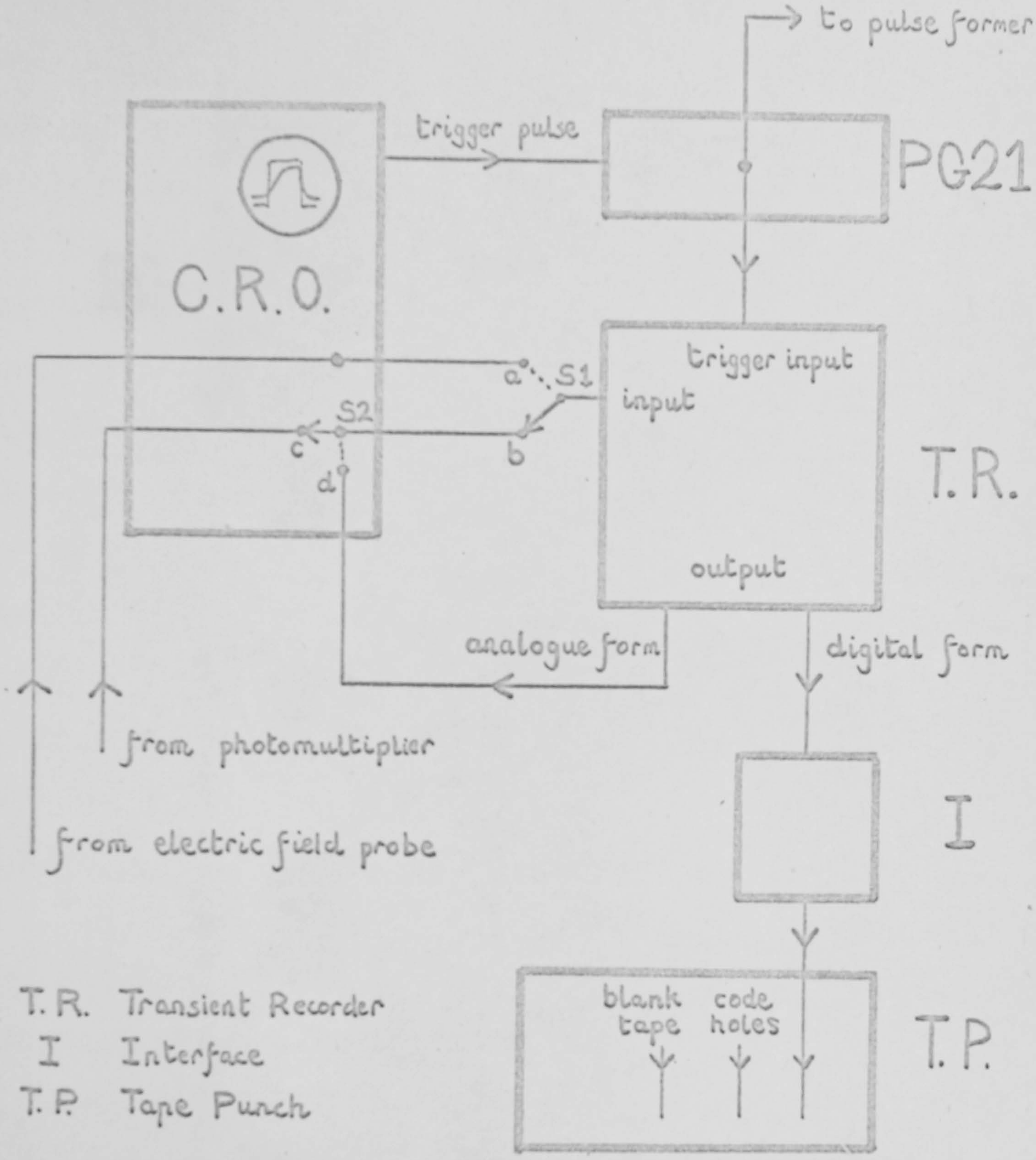

T.R. Transient Recorder
I Interface
T.P Tape Punch

FIGURE 5 DATA LOGGING ARRANGEMENT

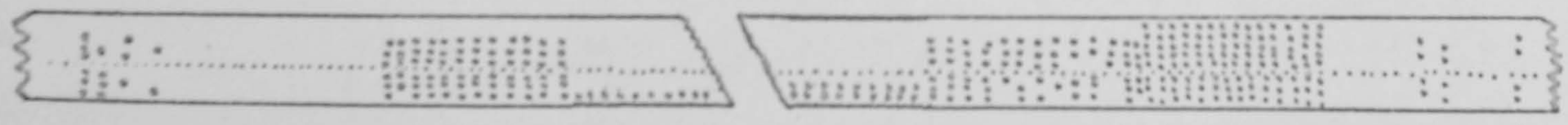

FIGURE 6 THE PUNCHED TAPE

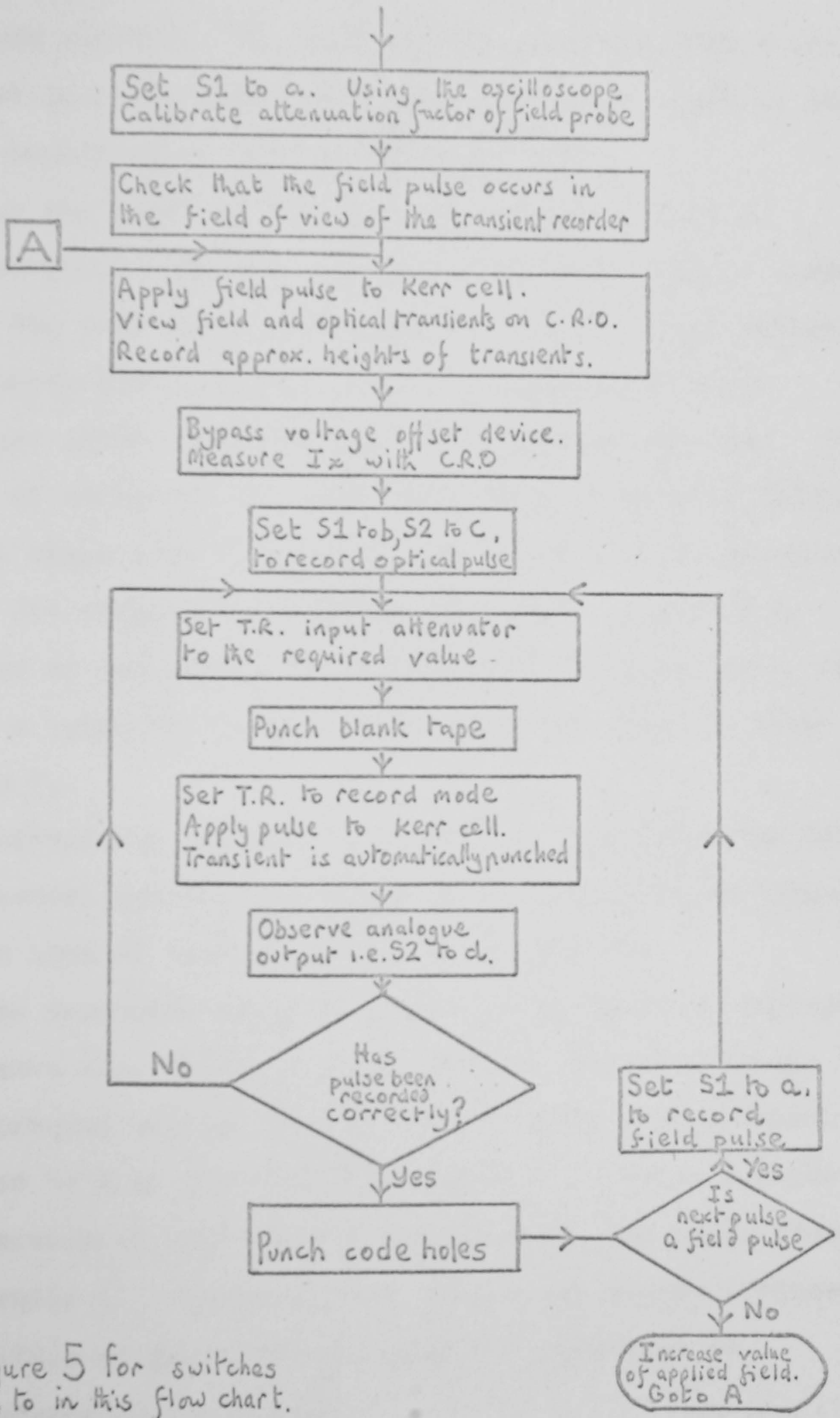

See Figure 5 for switches referred to in this flow chart.

FLOW DIAGRAM 2 — A recording cycle with the 610 transient recorder

ation was checked. If, as sometimes occurred, 128 words were not punched, then additional words were manually punched at the beginning of the recorded transient.

For the computer system used the tape was of an unconventional form and required translation into a standard form. The tape was input backwards into the tape reader. Only information occurring after a sequence of eight character words was converted into standard ICL code. This method of analysing the tape obviated the need for additional sets of characters to indicate the arrival of a transient and on its completion to indicate whether it should be analysed or rejected. The sequence of steps necessary to record a transient in the manner above is shown in flow diagram 2.

Information contained on the data cards depicted the experimental conditions, the transient recorder settings for, and the area of each transient to be analysed.

The transient recorder could not be usefully employed to observe a.c. electric field pulses. Correspondingly the algol program written by the author analysed only transients produced by d.c. electric field pulses. A brief outline of the function of that program was given in the paper found in Appendix 1. Samples of the tables and graphs produced on analysis of quadratic measurements performed on nitrobenzene are as follows.

The experimental conditions

S.I. units are used unless stated otherwise.

Wavelength of incident light = 6.30 &-7

Electrode length = 5.00 &-2

Electrode separation = 5.00 &-3

Kerr constant of solvent = 0.00 & 0

Angle uncrossed by analyser = 0.00 & 0

Concentration of solution = 1.00 & 0

Results of calibration procedure $V = V_0 \sin^2 \chi + c$

V_0 = 1·81 & 1 ± 1·54 & -1

c = 6·06 & -4 ± 2·27 & -2

Factor required to convert

phase difference to birefringence = 2.01 & -4

Symbols & X represents 10^{+X}

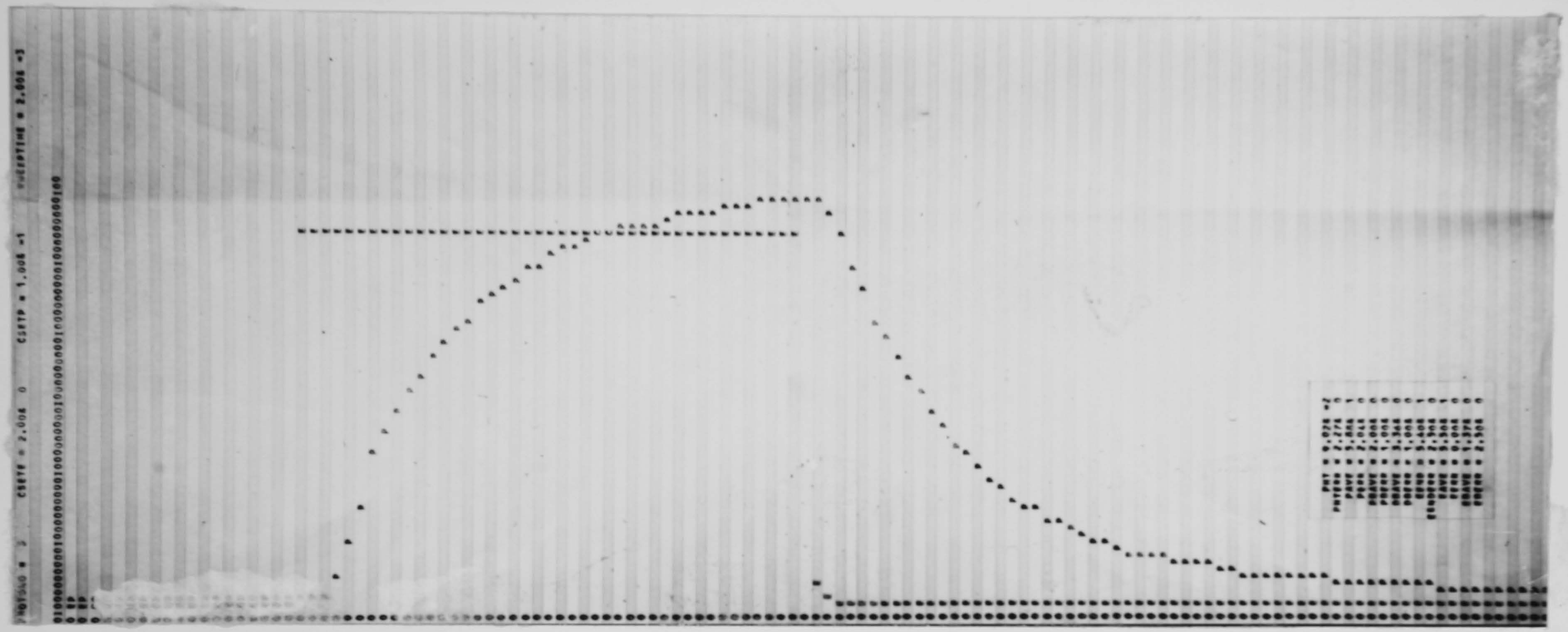

The optical and electric field transients superimposed on one graph.

the transient fall and decay of the nitrobenzene optical response was artificially introduced by using a capacitor in the photomultiplier output circuit.

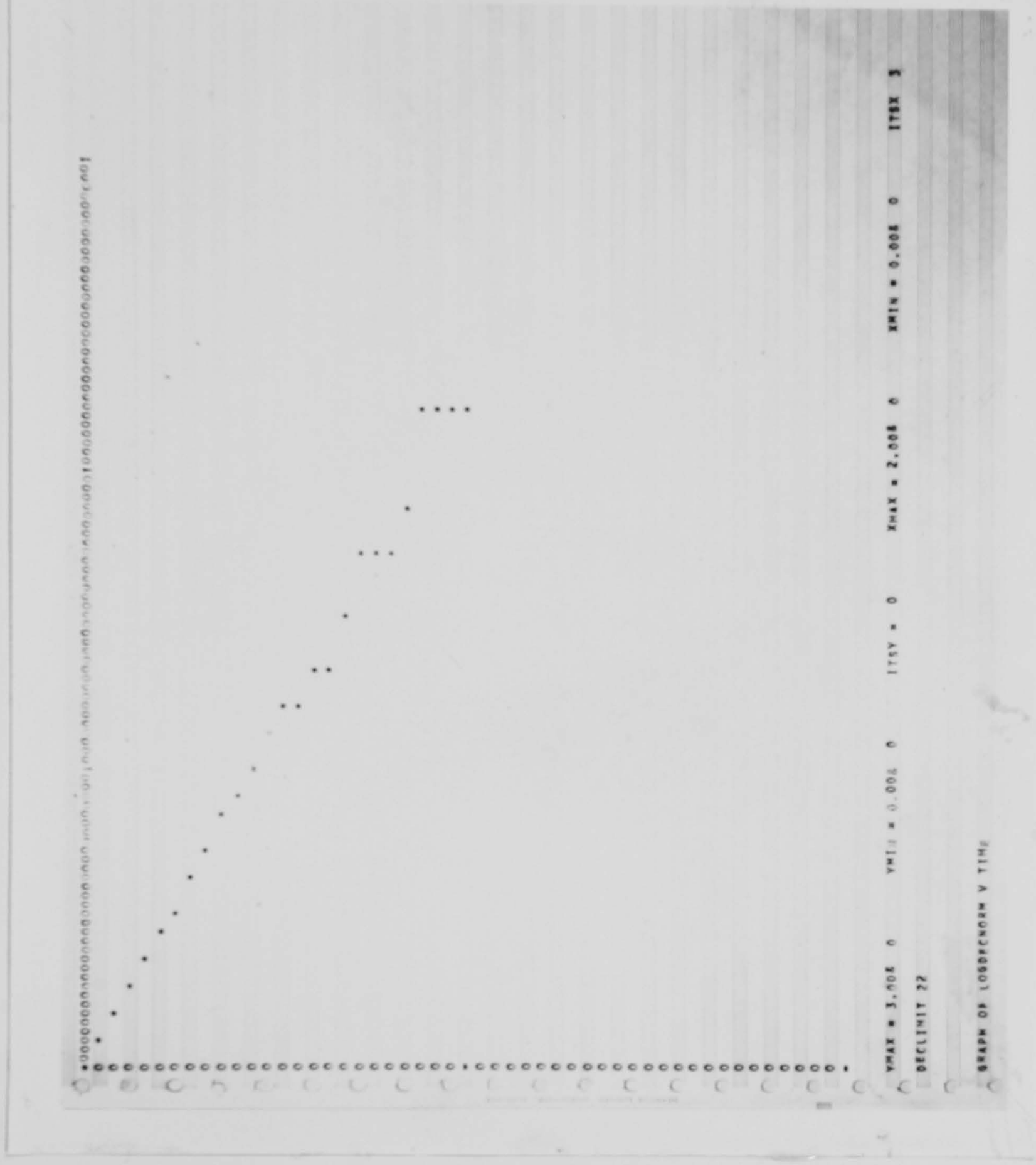

A decay plot : $-\ln \delta(t)/\delta(t=0)$ versus time

This plot was obtained for the transient previously shown.

Time axis	0 to 2 msec
$-\ln \delta(t)/\delta(t=0)$ axis	0 to 3

WATANABES B

PHOTONO	DSOLUTE	DSOLVENT	EHT-V/M	EHT↑2	BMKS	B/C	BCGS
1	4.528 -1	0.00& 0	7.938 5	6.298 11	2.298-12	2.298-12	2.068 -5
2	3.278 -1	0.00& 0	5.998 5	3.508 11	2.908-12	2.908-12	2.618 -5
3	1.418 -1	0.00& 0	3.818 5	1.458 11	3.108-12	3.108-12	2.798 -5
4	6.538 -2	0.00& 0	2.338 5	5.418 10	3.848-12	3.848-12	3.468 -5

Final Table of steady state values obtained from four transients

Columns 5 and 6 can be used for the curve fitting procedure of O'konski (see Chapter 2)
Column 7 includes values of the Specific Kerr constant.
Column 8 includes values of B in c.g.s. units.
Note: the wide discrepancy in values of B is due to the presence of an uncorrected stray phase difference.

PUT ON 1ST 10 POINTS OF LOGPLOT TO A+B*X+C*X↑2
DECAYTABLE
CAUTION 0 DBASE= 1 DBASE< 2 DBASE> DBASE

PHOTO

PHOTO	CHECK	A	B	C	COMPAR	EHT↑2
1	0	2.718 -2 +/- 1.488 -3	-1.168 3 +/- 5.968 0	2.358 5 +/- 5.008 3	-2.438 -1	6.298 11
2	0	-1.548 -2 +/- 4.998 -4	-1.998 3 +/- 5.508 0	-3.868 5 +/- 1.268 4	8.558 -2	3.598 11
3	0	2.618 -3 +/- 2.768 -4	-2.238 3 +/- 3.058 0	-1.138 5 +/- 7.018 3	2.238 -2	1.458 11
4	0	2.448 -2 +/- 1.718 -3	-2.608 3 +/- 1.588 1	1.008 6 +/- 3.058 4	-2.018 -1	5.418 10

Final Table of results obtained from curve fitting the decay transients.

Column 2 includes a check on the behaviour of the baseline of the optical transient.
Column 4 includes values of $B = -6 \times D$. Where D is the rotary diffusion constant.
Column 6 indicates the amount of curvature in each decay logarithmic plot.

Of interest is the manner in which the decay of the optical pulse was simulated. Values of intensity along the decay were converted into phase differences. Initially a simplex curve fitting procedure was employed to fit a function of the form $Ae^{-Bt} + Ce^{-Dt}$ to the converted decay. Initial estimates of the fitted parameters of a general nature were used:

$$A = C = 0{\cdot}5$$

$$B = 5D = \left(\frac{1}{5} \left(\frac{128 - K}{100} \right) L \right)^{-1}$$

where K was the position of the decay origin,

and L was the transient recorder timebase setting.

A good fit was always found but in too large a time. Similar but faster procedures are apparently available.[5] Even so the resolution of the transient recorder analogue to digital converter did not allow much significance to be attached to the long time exponential. For these reasons the initial slope of the decay plot was analysed in the manner of Schweitzer and Jennings using a matrix curve fitting procedure. A function of the form $y = a + bt + ct^2$ was fitted to the first ten points of the logarithmic plot of the decay. The constant b was therefore the value of the initial slope required. This procedure was exceptionally fast and also gave an estimate of the error in b. Extension of the program to evaluate the dimensions of the solute molecules was not performed as a large number of procedures for different particle shapes would have been required.

In conclusion, disadvantages of the system were that: it did not dispose of the oscilloscope display system, a greater time was required to record the transients, the accuracy of the measurements was limited by the resolution of the analogue to digital converter, and two pulses had to be applied to the solution to observe both the electric field and the optical transients. The advantages of the system were that: it was relatively inexpensive, it overcame the use of many rolls of polaroid film and it diminished strikingly the time required to analyse the results.

The observation of pulses of duration 1 to 5 μsec.

The hydrogen thyratron generator described by the previous author was redesigned as shown schematically in Fig. 8 by Mr. G. Ford of the Electronics Unit, Brunel University. The additional advantages of this system were that: three pulse widths could be readily chosen. Interlocking circuits disconnected the e.h.t. supply after the delay line was charged, and only then could a trigger pulse be applied to the thyratron grid. The output to the cell was also disconnected if the cover of the light tight box was removed. The three pulses which could be obtained are shown in Fig. 9, and had a maximum amplitude of 5 kV set by the 10 kV e.h.t. supply. The droop and relatively long fall time were both unsatisfactory characteristics, especially of the longer pulses. Moreover on applying the pulse to cause the thyratron to conduct, noise was generated which could be observed at the photomultiplier output. In addition repetitive pulses were not identical. This latter

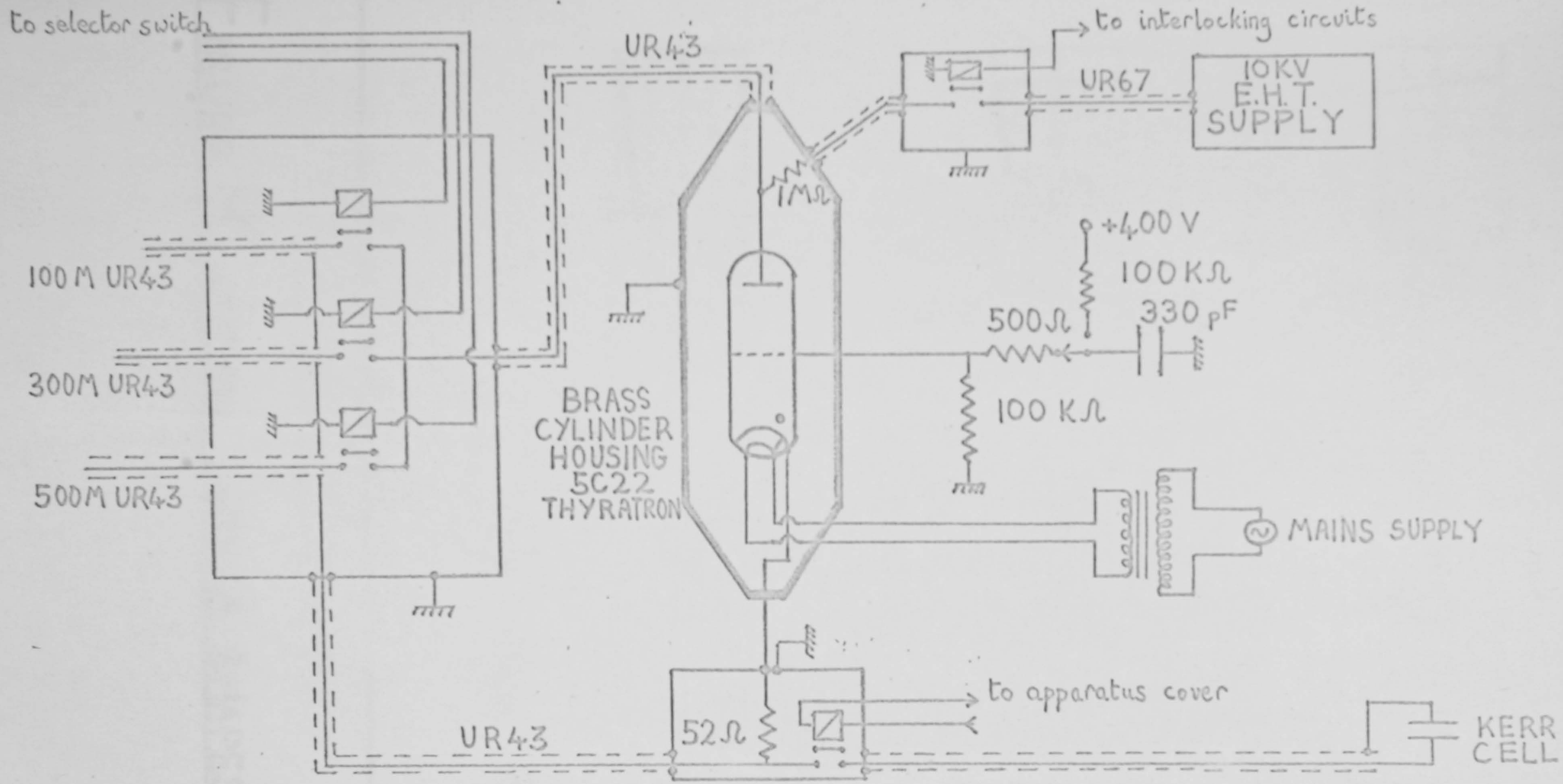

FIGURE 8 HYDROGEN THYRATRON/DELAY LINE PULSE SYSTEM

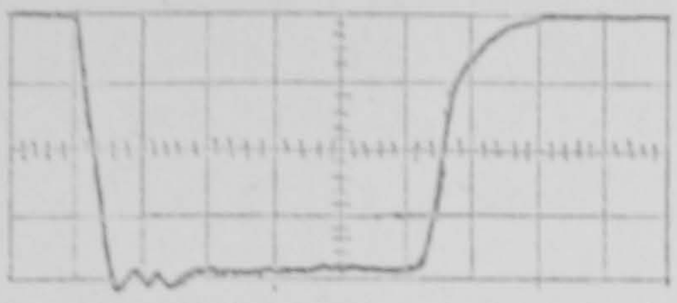

1 μsec.

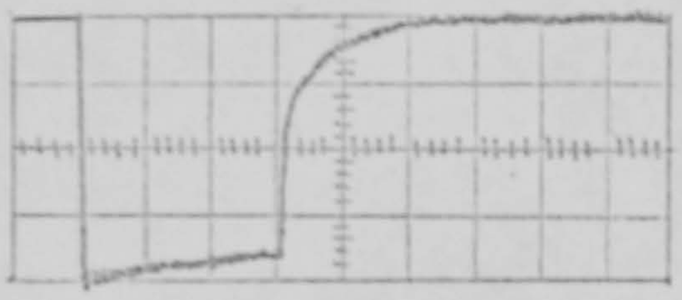

3 μsec.

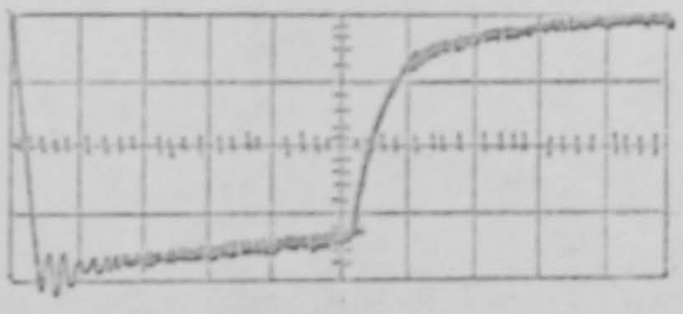

5 μsec.

pulse voltage 5Kv.

FIGURE 9 H.T./D.L. PULSE SHAPES.

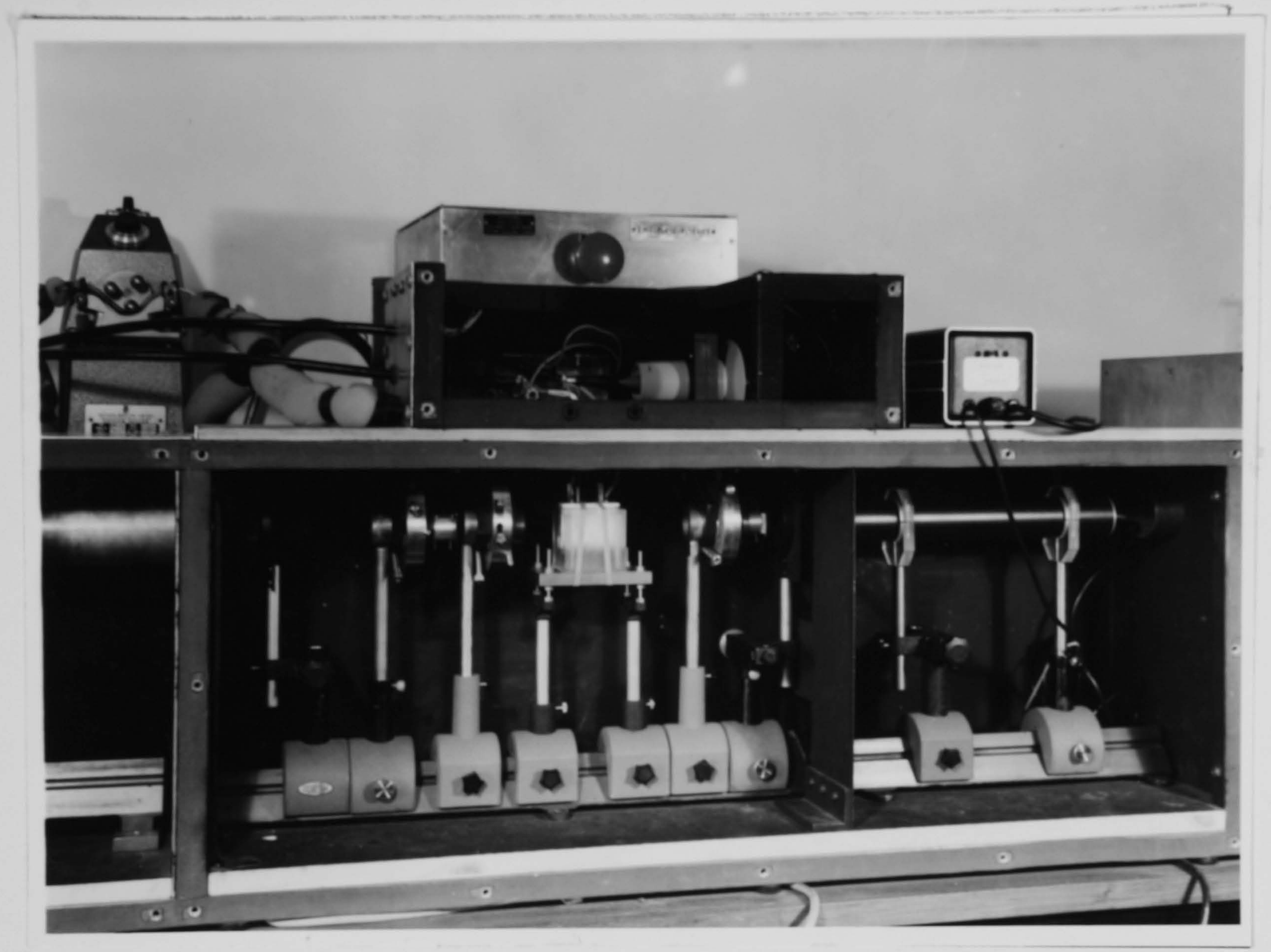

PHOTOGRAPH 5 OPTICAL SYSTEM WITH HE-NE LASER

fault was of importance because both the optical and electrical signals could not be simultaneously viewed with the 585 A oscilloscope. For these reasons the generator was not used by the author other than for the tests carried out.

The optical system was also updated so that 1 μsec optical pulses could be detected with little noise. A He-Ne laser was obtained from Coherent Radiation Ltd., Royston, Herts. It was easily included in the present equipment as shown in photo 5, and provided a beam of 0·8 mm diameter and 1·0 milliradians divergence at a power of 1·5 mW. The intensity of the beam had a noise level of 1% and long term stability of 5%. Unfortunately the state of polarisation of the light output varied with time. However the laser tube could be rotated so that the stability of the light intensity transmitted by the polariser was at a minimum of ± 2%.

The 56 AVP photomultiplier tube was replaced by a 9816 KB photomultiplier tube obtained from EMI Electronics Ltd., Hayes, Middlesex. The photomultiplier load resistance was reduced to 500 Ω so as to increase the bandwidth of the system. This also reduced to 5 mV the maximum steady optical signal which could be obtained. This signal was at the limit of the sensitivity of the oscilloscope and of the same order of magnitude as the noise generated by the thyratron circuit. These two considerations permitted only quadratic detection to be used.

The pulses were recorded photographically using a high speed polaroid film, type 410 Land roll film.

This system was capable of detecting phase differences

greater than 3×10^{-2} radians for 1 μsec pulses.

Suggested Improvements to Present Optical System

Especially for the case of quadratic detection an additional photomultiplier would be of use to monitor the output intensity of the lamp and laser continuously. Both were subject to short term as well as long term drift. Inclusion of the photomultiplier in the manner suggested by Orrtung and Meyers[7] would be most beneficial. It should be noted, however, that this method would not allow for additional light penetrating the analyser due to bubbles or thermal currents formed in the Kerr cell.

The analyser mounting should then be replaced by one which could be rotated accurately.

Even with these improvements the system is not satisfactory for measuring phase differences greater than 2 radians unless more accurate procedures are included for aligning the cell, calibrating the oscilloscope and determining I_o.

A working design for rotatable Kerr cell windows has been given elsewhere.[8]

References

1) Brown (B.L.), Ph.D. Thesis - University of London 1970.

2) Chaumont (L.), Annales de Physique 5, 18, 1966.

3) Benoit (H.), Ann. de Phys. (Paris) 6, 561, 1951.

4) Rudd (P.J.), Jennings (B.R.), Laboratory Practice
22, 535, 1973.

5) Colson (P.), Thesis - Universite de Liege 1972.

6) Schweitzer (J.F.), Jennings (B.R.) Biopolymers
11, 1077, 1972.

7) Orrtung (W.H.), Meyers (J.A.), J. Phys. Chem.
67, 1905, 1963.

8) Jerrard (H.G.), Riddiford (C.L.), Ingram (P.),
J. Phys. E. 2, 701, 1969.

CHAPTER 5

Kerr effect study on poly - β - benzyl - l - aspartate

Introduction

Poly - β - benzyl - l - aspartate (PBLA) is a polypeptide with the repeating unit

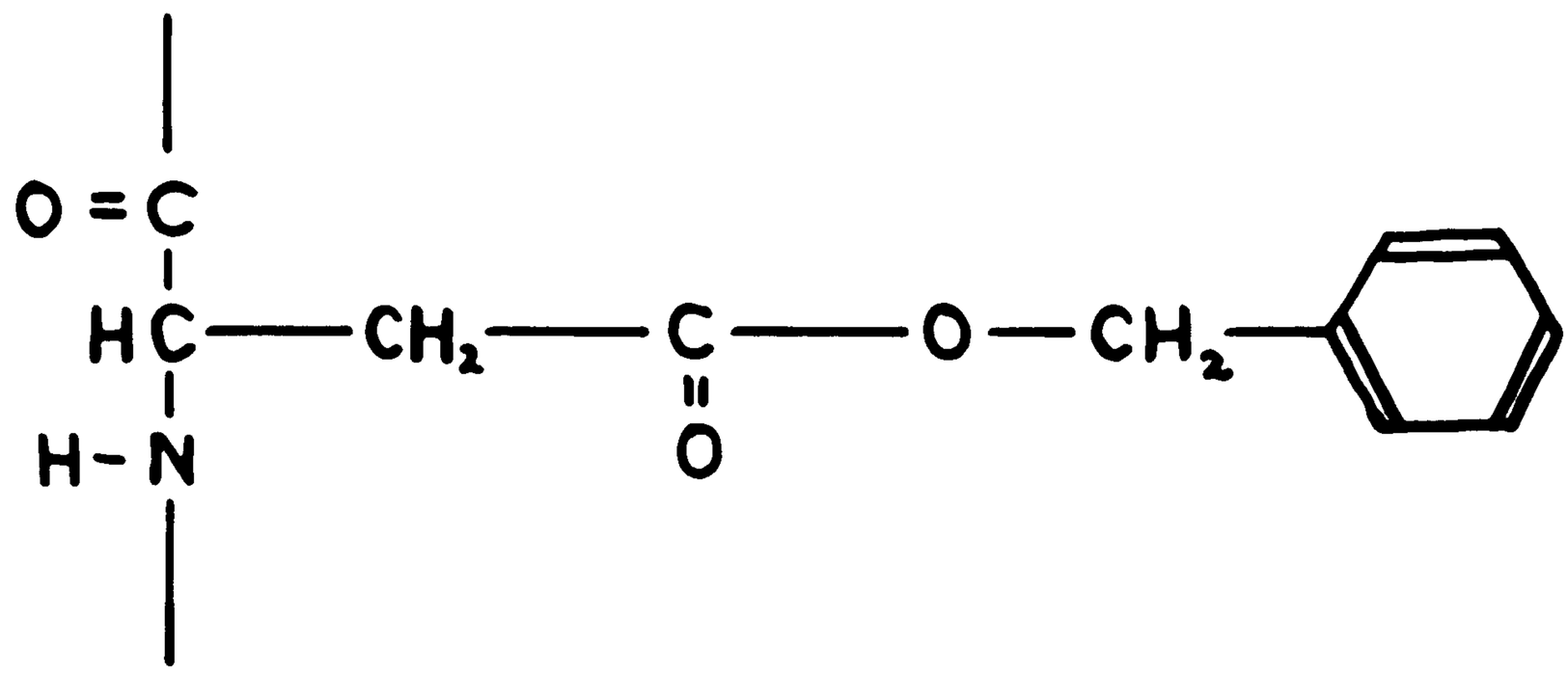

In solvents such as dichlorethylene, chloroform and metacresol, its conformation at room temperature is that of a α helix with a left-handed sense.[1]

Dielectric dispersion studies[2,3,4,5] have described its electric properties purely in terms of a permanent moment, largely attributable to the hydrogen bonds in the CO-NH linkage.

Although many electro-optic studies have been carried out on the related polypeptide poly - γ - benzyl - l - glutamate (PBLG)[6] few workers have investigated PBLA. Charney et al.[7] were unable to observe electric dichroism transients and attributed this behaviour to either a random or a particularly fortuitous orientation of the side chains. Yamaoka[8] observed both birefringence and optical activity

transients of PBLA in chloroform, ascribing the electric field dependence of the birefringence to molecules having both permanent and induced moments.

In this study measurements have been made on chloroform and metacresol solutions, the high molecular weight samples of PBLA being insoluble in dichloroethylene.

Two sets of measurements, A and B, were made, and to avoid confusion these will be presented separately with their own results and discussion.

Materials PBLA samples of molecular weight 178,000, 230,000 and 395,000 were purchased from Pilot Chemical Co. (Lot no's A-17, A-23, A-25 respectively) and used without further purification. All measurements were made on the 230,000 molecular weight sample except where stated otherwise. The solvents employed were obtained from BDH Chemicals Ltd. and were of analar grade. Chloroform was used without further purification. Metacresol was used both in its yellow, slightly oxidised form, represented here as MCO and in its clear pure state after vacuum distillation, here referred to as MCD.

Measurements A

Experimental

Solutions of PBLA in chloroform and MCO of concentration 0·05% to 0·5% were individually prepared. Slight warming was required to dissolve the polymer, and all solutions were filtered through 5 μm M.F. millipore filters before use.

The qudratic optical system with light of wavelength 5461 Å and cell 1 were employed. All measurements were made at the prevailing room temperature of 25 ± 2° C. Measurements were made on the solvents themselves and their contribution was subtracted from the observed phase difference. To observe the rapid transient decay, a photomultiplier load resistance of 10 KΩ was chosen. The lowest value of the phase difference observed was approximately 7×10^{-2} radians. No allowance was made for the cell stray phase whichwas typically 7×10^{-3} radians.

Pulse generator 2 was used. Pulses of duration 0·7 msec and of maximum amplitude 6 kV were obtained, and because the pulse generator was used incorrectly (see Chapter 4) the magnitude of each pulse fell by a total of 15%.

Results and Discussion

The sensitivity of the apparatus, as used here, did not allow an accurate assessment of the Kerr constant of chloroform to be made. A literature value of $-3{\cdot}2 \times 10^{-7}$ cm statvolt^{-2} was therefore employed in the calculations. MCD produced an easily observable effect which accurately obeyed Kerr's law with a Kerr constant of $1{\cdot}7 \times 10^{-6}$ cm statvolt^{-2}.

A typical transient obtained with PBLA in chloroform is shown in Fig. 1. Values of phase difference and electric field strength necessary to construct Graph 1 were obtained by measuring the relevant transient amplitude at the termination of the field pulse. Because considerable saturation

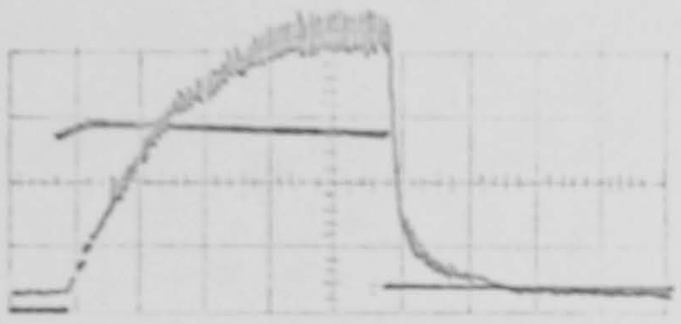

FIG. 1

PBLA in $CHCl_3$

concentration 0·2 %

field strength $4·5 \times 10^3$ V/cm

duration 0·5 msec

δ solution $1·1 \times 10^{-1}$ radians

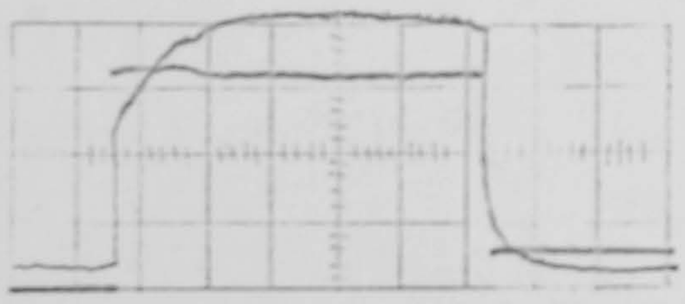

FIG. 2

PBLA in MCO

concentration 0·05 %

field strength $2·0 \times 10^4$ V/cm

duration 0·56 msec

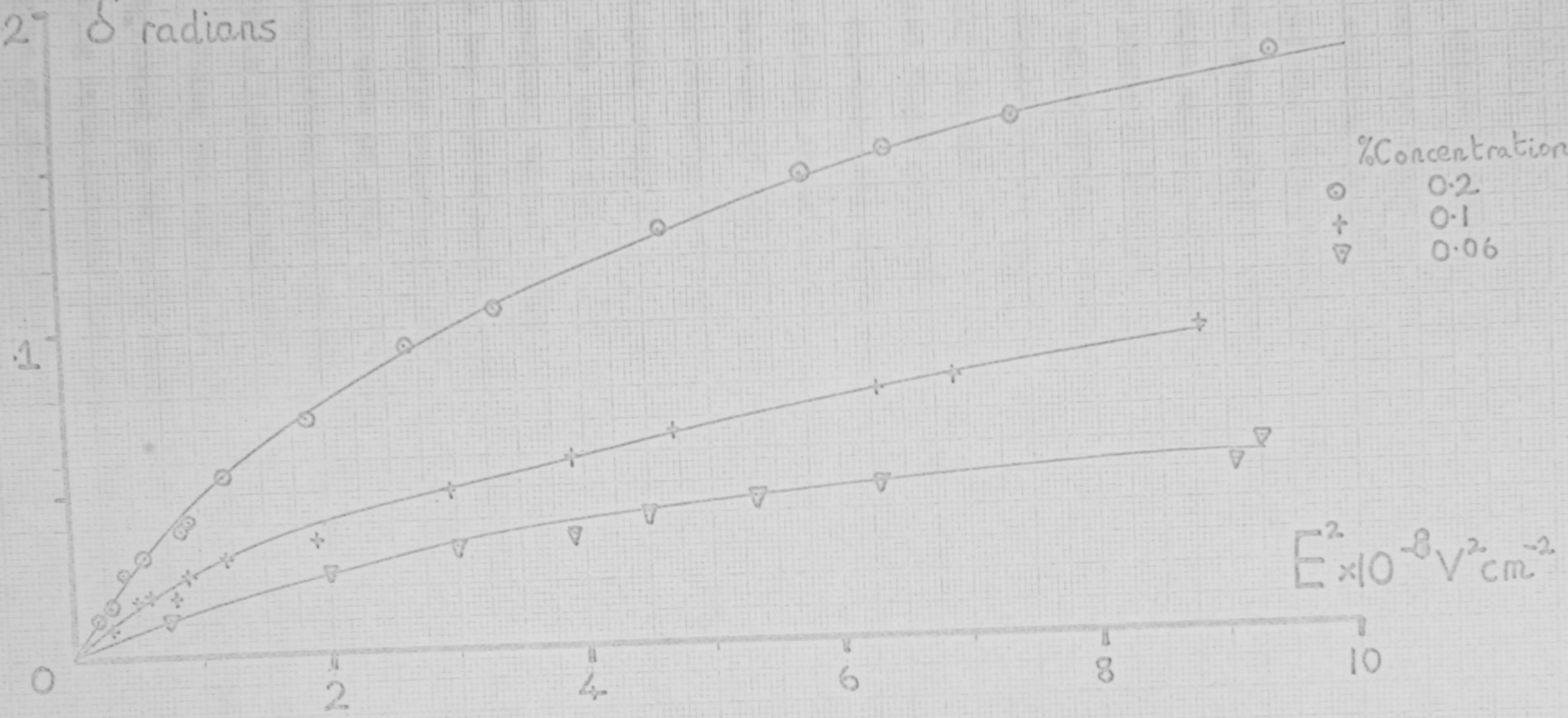

GRAPH 1 δ VERSUS E^2 (PBLA in CHLOROFORM)

of the effect occurred, the curve fitting procedure of O'Konski (see Chapter 2, ref. 6) was employed to determine the electrical properties of PBLA. The experimental plot required for this procedure is shown in Graph 2. The two sets of experimental data shown did not coincide.

This was a result of three factors: the presence of a stray phase difference which was not corrected for in the final calculations, the errors typically invloved in the measurement of the quantity δ/E^2 with this equipment, and finally the use of the quantity δ/E^2 obtained at the lowest applied field strength as the value $(\delta/E^2)_{E\to 0}$.

Moreover the experimental values did not truly coincide with steady state values. However, the solid curve representing the average of the two experimental curves is almost identical in all respects with that obtained by Yamaoka[8] in an analogous study on a sample of 336,000 molecular weight.

The best fit of the experimental solid curve to the theoretical master curves (see Graph 3 and Fit B) showed that PBLA has a permanent dipole moment only, in agreement with dielectric measurements[2] and frequency dispersion measurements made on PBLA in m-cresol by the present author; but in contradiction with Yamaoka's interpretation.[8] The validity of this latter interpretation will be discussed later.

Using the values obtained from this fit μ^1 was determined to be 2,300 Debye with an error of ± 300 Debye taking into account the spread of experimental data. The degree of polymerisation of the polymer, which is equal to the molecular weight divided by 205, was $1{\cdot}15 \times 10^3$. The

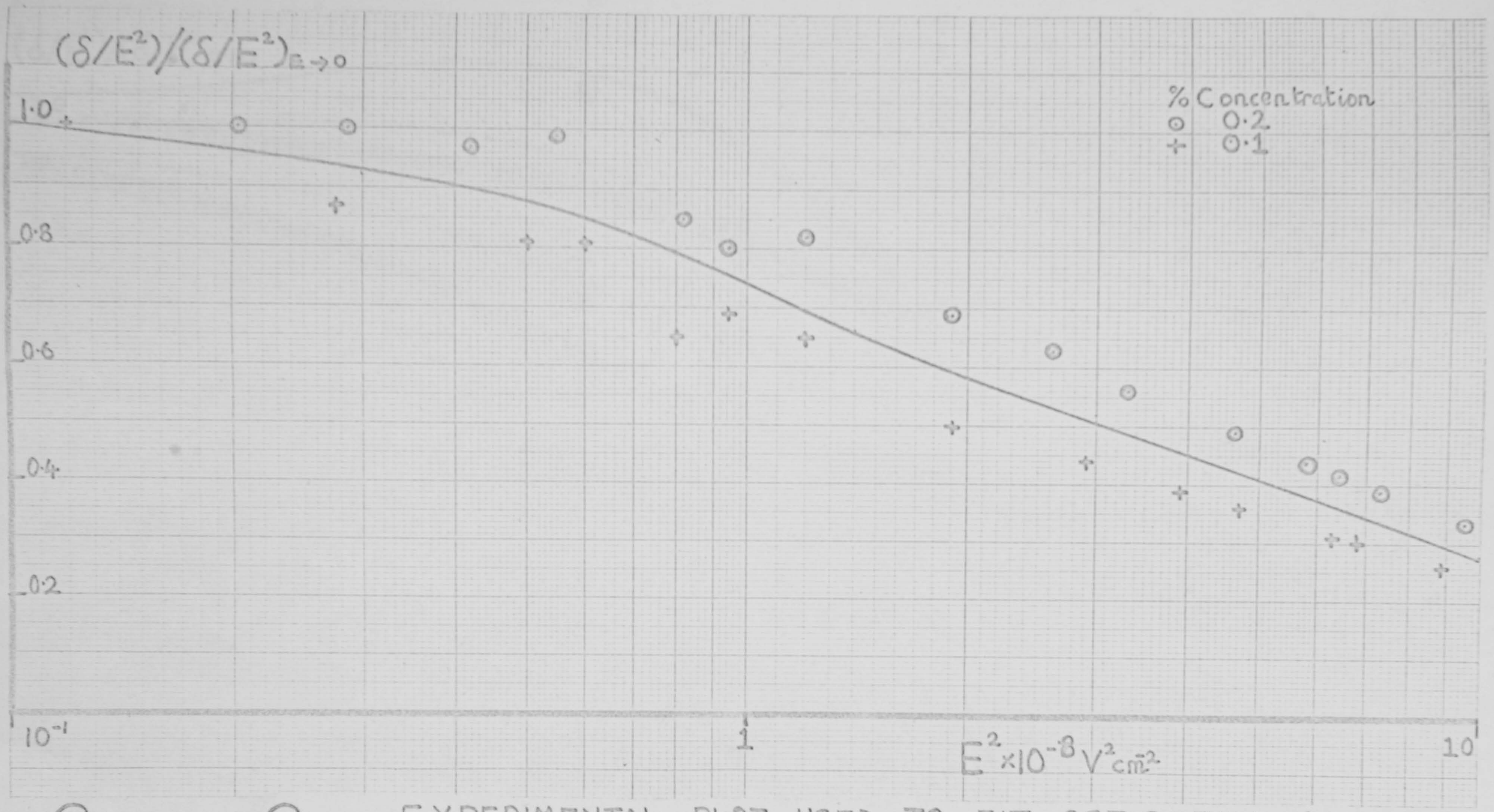

GRAPH 2 EXPERIMENTAL PLOT USED TO FIT SATURATION OF BIREFRINGENCE TO THEORETICAL CURVES.

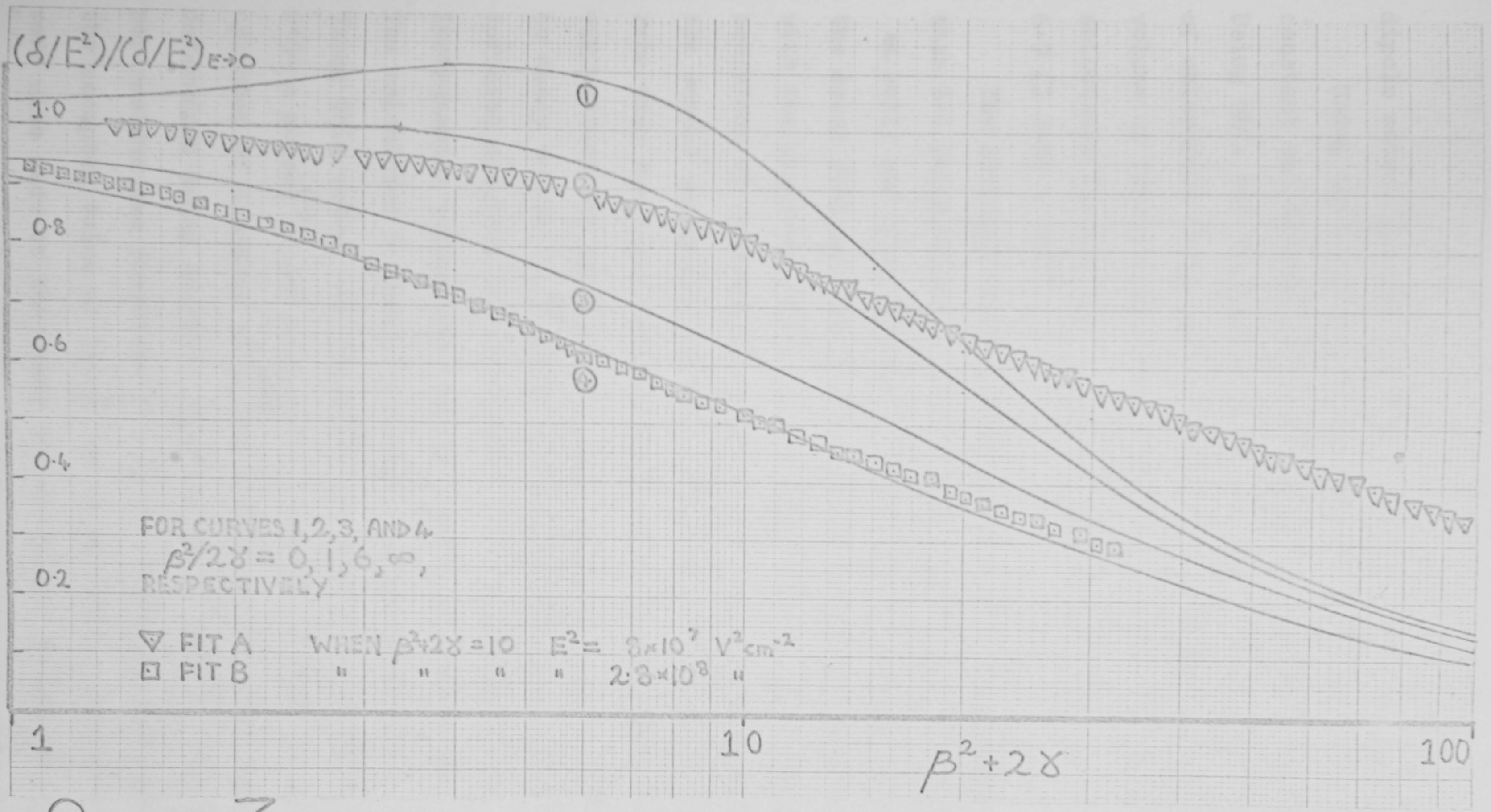

GRAPH 3 FIT OF EXPERIMENTAL PLOT TO MASTER CURVES.

dipole moment per residue was therefore 2·0 Debye/residue.

Using the limiting values of δ/E^2 the intrinsic Kerr constant was determined to be 3·0 ± 1·0 x 10^{-3} $cm^4 gm^{-1} statvolt^{-2}$. Using this and the above value for μ^1, the refractive index of chloroform 1·45, and a value for the partial specific volume of PBLA in chloroform of 0·77 $cm^3 gm^{-1}$ (9) the optical anisotropy factor, $\beta_1 - \beta_2$, was determined to be 6·7 (± 2·0) x 10^{-4}.

The residual dipole moment found here is somewhat smaller than 3·6 Debye/residue theoretically predicted(1,3) for an α helix and experimentally determined elsewhere. However the decay analysis yielded a monomer length in good agreement with the accepted value, as is shown below. The non-linear behaviour of logarithmic plots of the decay illustrated that the sample was polydisperse. The small variation in the decay rate over the concentration range studied indicated that aggregation was negligible. The time taken for a transient to decay to the $1/e^{th}$ point was determined for a solution of infinite dilution to be 11 μsec. On correction for an instrumental relaxation time of 1 μsec this value was 9 μsec. The calculated diffusion constant was therefore 9·3 x $10^3 sec^{-1}$. Using this value, the viscosity of chloroform at 25°C, 0·54 c poise;(10) and assuming a molecule of PBLA to be a cylinder of diameter 15 Å,(2) the length of the molecule was determined using Burger's equation to be 1500 Å. The length per residue was therefore 1·3 Å, in reasonable agreement with the accepted value of 1·5 Å for an α helix. Measurements were also made on the other two molecular weight samples of concentration 0·2% and the results obtained are compared with

those on the 230,000 molecular weight sample in Table 1.

x 10^3 M.W.	$\times 10^{-3}$ K	τ exp
178	6·3	11
230	9·0	18
395	7·5	8

TABLE 1.

The values obtained for the high molecular weight sample suggest that either the molecular weight is in error or that the helical chain is extremely flexible.

For PBLA in NCO and at a concentration of 0·05% the contribution of the solvent was appreciable (see Fig. 2). The intrinsic Kerr constant was determined to be $4{\cdot}0\ (\pm\ 0{\cdot}5) \times 10^{-3}$ cm^{4}gm^{-1}statvolt.$^{-2}$ Decay analysis yielded a value of the experimental relaxation time at infinite dilution of 11 μsec. Using a value for the viscosity of 15 c poise[10] at 25° C a length per residue of 0·44 Å was determined. This latter value is particularly small and little confidence is placed in its validity, for the following reason. During an attempt to determine accurately the molecular weight of the 230,000 sample by light scattering it was found that metacresol attacks Millipore type MF filters. A solution which fluoresced quite strongly in the green was produced. The possibility that the behaviour of

the contaminant attributed to the low value for the residual length cannot therefore be neglected.

Measurements B.

Experimental

PBLA was dissolved in distilled metacresol, MCD, by warming the solutions to 50° C in a water bath. Solutions were not filtered.

The linear optical system with white light and cell 3 with the PTFE electrode mounting were now employed. The quarter-wave plate used was calibrated at 5461 Å. Phase differences as low as 6×10^{-3} radians were observed without the need to allow for the cell phase difference, which was 2×10^{-3} radians. An 'equivalent' wavelength of 5,000 Å can be used with the limitations imposed by the discussion in Chapter 3.

D.C. pulses of duration greater than 5 msec were obtained using P.G.3. Pulses of up to 2 kV could be safely applied in this manner, but above 800 V relay bounce distorted the decay transients. A.C. pulses were obtained using P.G.4 with the 'Airmec' amplifier.

All measurements were made at a room temperature of $25 \pm 2^{\circ}$ C.

Results and Discussion

A Kerr constant of MCD of $1{\cdot}7\ (\pm\ 0{\cdot}1) \times 10^{-6}$ cm statvolt^{-2} was determined, and was equal to that obtained with MCD.

Similar to the situation encountered with the calibration measurements performed on nitrobenzene this value is smaller than the only other reported figure,[11] of 2·4 x 10^{-6} cm statvolt^{-2}.

A typical d.c. transient obtained with a solution of concentration 0·1% is shown in Fig. 3. Up to the maximum field strength of 3,500 V/cm, Kerr's law was obeyed within experimental error. A specific Kerr constant of 6·3 (± 0·2) x 10^{-3} cm^{4}gm^{-1}statvolt^{-2} was determined. Because O'Konski's method could not be used in this case, a value of $b^2/2\theta$ equal to 1 was determined using the area method of Watanabe.

Decay analysis yielded relaxation times consistent to 2·0 (± 0·5) x 10^{-4} sec, which were equivalent to a value of D of 8·3 (± 3·0) x 10^2 sec^{-1}, and hence a length per residue of 0·9 Å.

Corresponding results obtained with a solution of concentration 0·3% were for the specific Kerr constant 7·5 x 10^{-3} cm^{4}gm^{-1}statvolt^{-2}, for D 1·4 (± 0·4) x 10^3sec^{-1}, and hence a residual length of 0·8 Å.

A.C. pulses of frequency from 20 Hz to 20 kHz were applied to the 0·3% solution, and typical transients are shown in Figs. 4A and @B. It is a significant point that little distortion of the optical pulse shape and base line occur even with pulses of 0·1 sec duration. The dispersion of birefringence with frequency is shown in Graph 4.

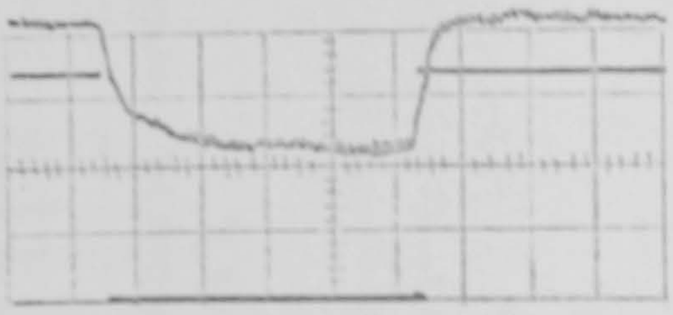

PBLA in MCD

concentration 0·1%

field strength $3·3\times10^{3}$ V/cm

duration 8 msec

$\delta_{solvent}$ $7·0\times10^{-3}$ δ_{solute} $2·8\times10^{-2}$

FIG 3

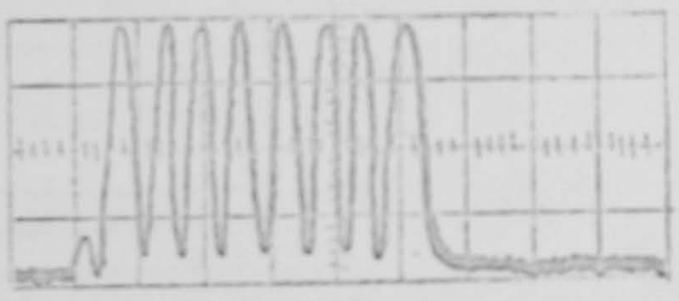

PBLA in MCD

concentration 0·3%

field pulse not shown but of

r.m.s. strength $3·3\times10^{3}$ V/cm

and frequency

60 Hz for fig a.

20 KHz for fig b.

FIG 4a

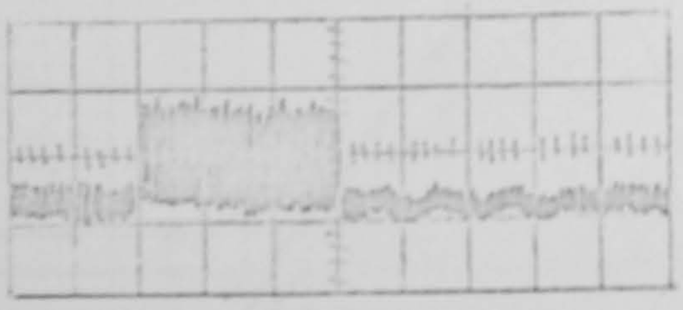

FIG 4b

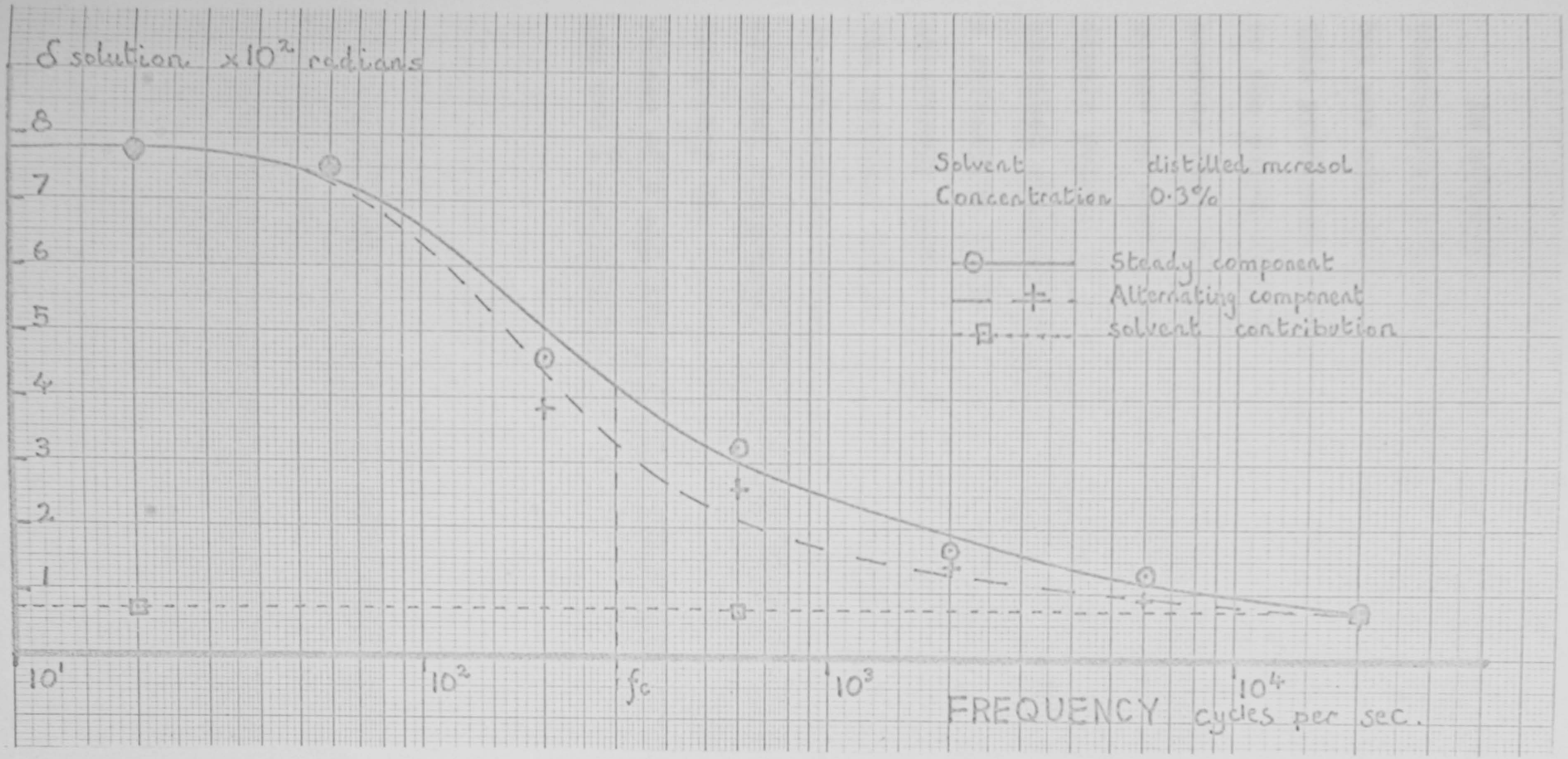

GRAPH 4 FREQUENCY DISPERSION

An attempt was made to fit the experimental data to the theoretical curves of Thurston and Bowling (see Chapter 2), but was not successful. The dispersion was slightly broader than predicted theoretically, and this was attributed again to the polydisperse nature of the sample. It was concluded however that because the high frequency contribution of the solute is small, PBLA effectively has only a permanent dipole moment in m-cresol. Using the specific Kerr constant obtained with the 0·1% solution (i.e. $6{\cdot}3 \times 10^{-3} cm^4 gm^{-1} statvolt^{-2}$) a refractive index of 1·54 and the value of the optical anisotropy factor previously determined (i.e. $6{\cdot}7 \times 10^{-4}$), the residual dipole moment was determined to be 1·7 Debye. An estimation of particle size was also obtained from the critical frequency, f_c, as indicated on Graph 4. This frequency was $3{\cdot}0 (\pm 0{\cdot}5) \times 10^2$ c sec^{-1}. The corresponding values of D and the residual length were $9{\cdot}4 (\pm 1{\cdot}6) \times 10^2 sec^{-1}$ and 0·9 Å respectively.

Final Discussion

The reduction of the experimental data into values of the dipole moment and length per residue has not yielded results in accord with those expected for an α helix. It is probable that this finding can be directly attributed to the distribution of particle size in the sample. The values of the molecular weight, the diffusion constant, and total dipole moment quoted above are average values. Moreover each average does not correspond to the same statistical weighting. The molecular weight is a viscosity average. As recently shown by Schweitzer and Jennings[12] the diffusion constant of a rigid rod with a permanent moment along the symmetry axis corresponds to a Z + 1 and a weight average at limiting low and high electric field strengths respectively. (Exactly the same situation was encountered by Watanabe[6] who analysed the decay transient in a completely different manner.) The author is not aware of the appropriate average for the dipole moment. Moreover to determine the residual values above, different averages have then been compared.

Nonetheless two significantly different values of the residual length were determined in the two solvents. The values were 1·3 Å in chloroform and 0·9 Å in m-cresol. In view of the above discussion it is not possible to conclude that PBLA has an α helical structure in either solvent. No conclusive evidence has been found here to suggest the cause of the different values. Flexibility, aggregation and solvation have been considered as follows.

PBLA is slightly more flexible in m-cresol than it is in chloroform, but its helical content at 25° C is high, and of the order of 95%.[3,13] A measure of the effect of this higher degree of flexibility can be gained from the work of Watanabe et al[14] on the helix to coil transition of PBLG. In agreement with that work the value of $D Z_o$ is greater in the solvent, giving rise to higher flexibility, ($D Z_o$ = 50 in chloroform, $D Z_o$ = 140 in m-cresol). However the magnitude of the variation is consistent with PBLA having a helical structure in chloroform and a random coil structure in m-cresol. This situation can be rejected also on the grounds of the small variation in intrinsic Kerr constant observed.

Aggregation of PBLA in chloroform has been observed[13] but at an unspecified concentration. The 60% variation in relaxation time over the concentration range observed for the chloroform solutions would not generally be taken as an indication of the continued formation of aggregates.

Finally, solvation effects have been tentatively suggested[9] to give rise to the variation of intrinsic viscosity of PBLA in m-cresol and dichloroethane. It is unlikely that such a large variation in $D Z_o$ as observed here could be accounted for by such effects.

It is perhaps interesting to note that many workers[3,4,5] have not attempted to verify that their relaxation data can be accounted for with the 'known' properties of the α helix.

The intrinsic Kerr constant was also smaller for m-cresol solutions. That value, on correction to a wavelength

of 5461 Å, was 5·8 (± 0·2) x 10^{-3} cm^4 gm^{-1} $statvolt^{-2}$ in comparison to 9·0 (± 1·0) x 10^{-3} cm^4 gm^{-1} $statvolt^{-2}$ in chloroform. Such a difference need be attributed to no more than the variation of the optical anisotropy factor with solvent refractive index. Flexibility and aggregation need not therefore be considered. This conclusion has been drawn from the work of Tsvetkov et al[15] on PBLG in mcresol and dichlorethane (refractive index = 1·44) who determined the ratio [K] DCE / [K] mc to be as high as 2·5.

The electrical properties of PBLA have been interpreted purely in terms of a permanent moment orientation. (It is true that Watanabe's area method did suggest a value of r equal to one, but this has generally been considered a poor method of determining the value of r.) Yamaoka,[8] however, fitted his experimental values for the saturation of birefringence to the curve $B^2/2\gamma = 1·25$ and obtained a value of 1·7 Debye for the residual dipole moment. The present author's results could be used to simulate almost exactly the situation attained by Yamaoka, and this is shown as Fit A on Graph 3. It can be seen that for values of $E^2 > 1 \times 10^8 V^2 cm^{-2}$ the experimental data does not fit any of the theoretical curves. Yamaoka suggested that this behaviour might be attributed to three factors;

1) inadequacy of O'Konski's theory, 2) polydispersity and 3) molecular conformation changes at high fields. He correctly discounted the effects of solvent birefringence but neglected to mention the possible effects of the optical rotation introduced by this helical polypeptide. In this

work a typical value for the rotation was 1.3×10^{-3} radians for a 0.1% solution in cell 1, and therefore was probably negligible.

It is the contention of the present author that none of Yamaoka's suggestions need to be considered. Yamaoka's experimental data can readily be fitted to the theoretical curve for a pure permanent moment, and Fit B of Graph 3 simulates this situation almost exactly. Above values of E^2 equal to 8×10^7 $V^2 cm^{-2}$ an exact fit can be made. Below this value Yamaoka's experimental data is 5% greater than theoretically predicted. Not only has more of the data been accurately fitted but the discrepancy at low fields can easily be attributed to the experimental errors outlined above. This is so, even though Yamaoka reduced the effects of stray birefringence by employing the linear detection system. With such a fit Yamaoka's value of the residual dipole moment would have been 1.3 Debye, smaller than his original value!

Concluding Remarks.

The residual length of PBLA in mcresol and chloroform has been observed to be 0.9 Å and 1.3 Å respectively. A residual dipole moment of approximately 2.0 Debye was determined from the saturation of birefringence. The data could not be fitted to the 'known' properties of an helix, nor was there a plausible single explanation for the difference in residual lengths observed. The errors implicit in performing the saturation of birefringence curve fitting procedure of O'Konski were outlined and used to justify the

statement that the present results and those of Yamaoka are best interpreted purely in terms of a permanent dipole orientation mechanism.

Suggestions for further studies.

A study of the helix to coil transition of PBLA in mcresol using a.c. fields would be of current interest. The dielectric dispersion measurements of Wada[4] and Marchal[5] were in disagreement and this was attributed by Marchal to electrode polarisation processes. This explanation could readily be tested with birefringence measurements which, because of the high fields employed, are relatively unaffected by electrode polarisation.

To eliminate all possible effects of polydispersity it is necessary either to selectively choose a monodisperse sample or produce one by rather laborious fractionation processes.[16]

References

1) Fasman (G.D.), 'Poly - α - Amino Acids', Marcel Dekker Inc. N.Y. 1967.

2) Erenrich (E.H.), Scherage (H.A.) Macromolecules 5, 747, 1972.

3) Wada (A.) et Al. Biopolymers 11, 587, 1972.

4) Wada (A.) Chem. Phys. lettr. 8, 211, 1971.

5) Marchal (E.) Chem. Phys. lettr. 12, 9, 1971.

6) Watanabe (I.), Yoshioka (K.), Review article in 'Physical Principles & Techniques of Protein Chemistry' Ed. S.J. Leach, Academic Press, 1969.

7) Charney (E.) et Al. J. Am. Chem. Soc. 92, 2657, 1970.

8) Yamaoka (K.) Ph.D. Thesis, Univ. of California, 1964, University Microfilms Inc. 4 - 13, 124.

9) Shecter (E.) et Al. J. Chim. Physique, 1179, 1972.

10) Handbook of Chemistry and Physics, 48th edn. Chemical Rubber Co. Cleveland, Ohio, 1967.

11) International Critical Tables V.7, P. 109.

12) Schweitzer (J.), Jennings (B.R.), Biopolymers 11, 1077, 1972 and Biopolymers 12, 2439, 1973.

13) Hayashi (Y.) et Al, Biopolymers 8, 403, 1969.

14) Watanabe (I.) et Al. Biopolymers 2, 91, 1964.

15) Tsvetkov (V.N.) et Al. Vysokomolekul Svedin, 1965?.

16) 'Characterisation of Polymers' Ed. N.M. Bikales, Pub. Wiley - Interscience 1971.

CHAPTER 6

Birefringence study on a polymer surfactant system

Introduction

The polymer, polyvinylpyrrolidone (hereafter referred to as PVP) is an homopolymer of Nvinylpyrrolidone and because of

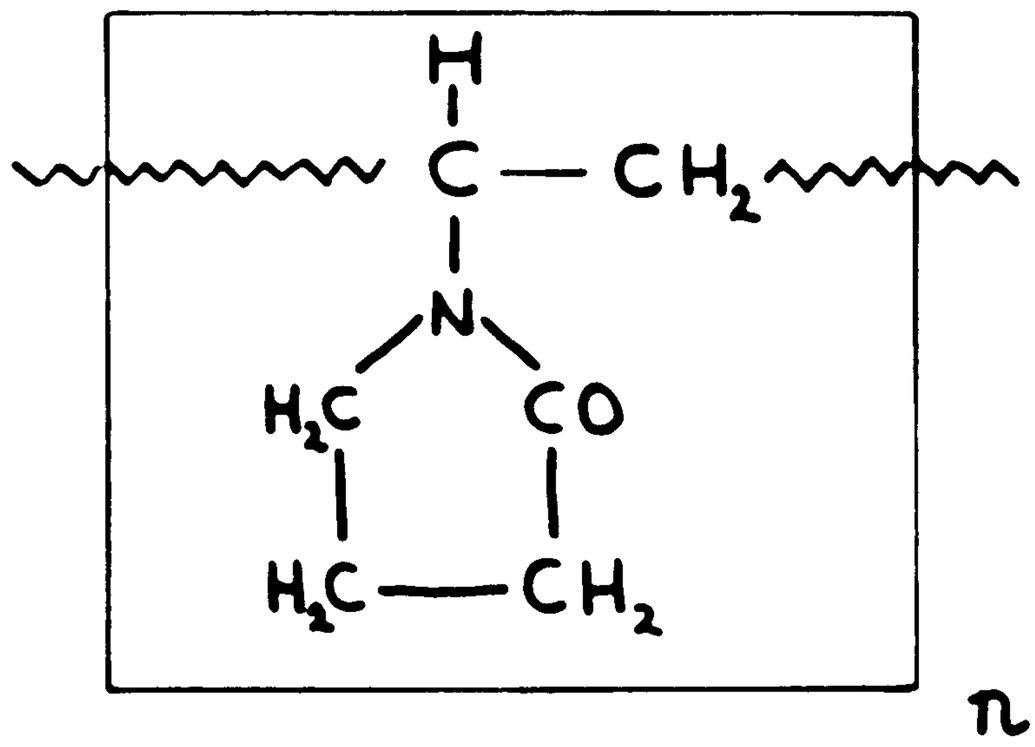

its complexing and detoxifying capabilities is widely used in the pharmaceutical industry. Its basic structural properties have been widely observed[1,2,3] but studies relating to its electric properties are rare.[4] It is a non-ionic, random coil polymer having dipoles present in the short side chains.

The surfactant, sodium dodecyl sulphate (hereafter referred to as SDS) is a typical anionic detergent.[5] In aqueous solution and below the critical micelle concentration (c.m.c.), 8·2 mm/litre (1 mm = 1 millimole), it exists in a dissociated form consisting of sodium ions Na^+ and dodecyl sulphate ions $CH_3(CH_2)_{11}SO_4^-$ (abbreviated DS^-). Above the c.m.c. it forms micelles having a spherical core of DS^- ions surrounded

by an ion atmosphere of Na^+ ions.

It is known that DS^- ions complex with PVP to form a polyelectrolyte.[6,7]

The purpose of the present study was to determine if this behaviour could be observed and secondly to investigate the dependence of the effect on SDS concentration.

Apart from electro-optic dichroism measurements made on dye complexes,[8] few electro-optic studies have been specifically made on polymer-surfactant systems.[9]

Experimental

The samples were kindly prepared by Dr. I.D. Robb (Unilever Research Laboratories, Port Sunlight) as follows:-

PVP of molecular weight 700,000, obtained from B.D.H. Ltd., was made up to a 2% aqueous solution and dialysed against permanganate distilled water. SDS (B.D.H. Specially Pure grade) was added to the PVP stock solution to produce a series of samples having a SDS concentration of 0 to 25 mm/l.

Due to the stability of PVP solutions, measurements were made up to a month after preparation.

Linear detection with a quarter wave plate calibrated at 5461Å was used with white light but no corrections were applied to the observed phase differences (an equivalent wavelength of 5,000Å can be used with the limitations imposed by the discussion in Chapter 3). The photomultiplier load resistance was 10 kΩ so that phase differences as low as 1×10^{-3} radians and decay times of the order of 1 μsec could be observed.

Cell 3 was employed with the Tufnol electrode arrangement, with an electrode spacing of 2 mm. D.C. pulses of duration 0·5 msec and height 10kV were applied using pulse generator 2. A.C. pulses were also applied using the Airmec amplifier and relay box arrangement.

All measurements were made at the prevailing room temperature of $25 \pm 2^{o}C$.

Measurements were also made on solutions of SDS itself to determine its contribution to the PVP/SDS Kerr constant.

Results

PVP alone

Prior to these measurements, transients obtained using commercial grades of PVP without purification (kindly supplied by G.A.F. Ltd. Manchester) indicated by their sporadic behaviour that the above removal of ionic impurities by dialysis was necessary.

A typical transient obtained using the present sample and voltages as high as $2{\cdot}4 \times 10^4$ V/cm is shown in Fig. 1. The initial fast rise was due to the solvent and hence set the limiting concentration of PVP to 2%. Measurements made on water obtained from an Elgestat still yielded an average value of the Kerr constant of $2{\cdot}9 \times 10^{-7}$ cm statvolt^{-2} in good agreement with the value obtained for true distilled water.[10] The solution accurately obeyed Kerr's law up to a field strength of $2{\cdot}4 \times 10^4$ V/cm, yielding a value of the Kerr constant of $9{\cdot}6(\pm 0{\cdot}12) \times 10^{-7}$ cm statvolt^{-2}. The Kerr constant of PVP and the specific Kerr constant were therefore $6{\cdot}7(\pm 0{\cdot}1) \times 10^{-7}$ cm statvolt^{-2} and $3{\cdot}4(\pm 0{\cdot}1) \times 10^{-5}$ cm^{4}gm statvolt^{-2} respectively.

SDS alone

For any one of the representative experimental SDS concentrations, Kerr's law was not obeyed. Neither was there any systematic variation of the effect with concentration. The height of any one transient obtained was at the most equivalent to a Kerr constant five times greater than that of

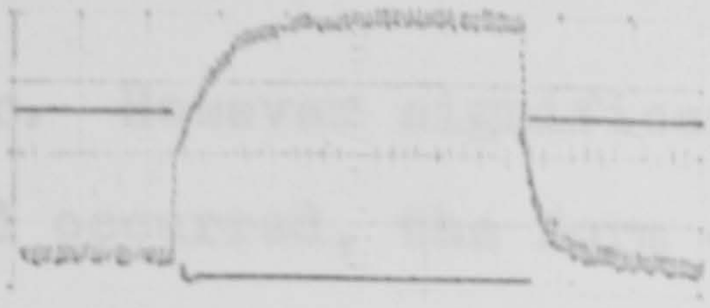

E = 1.08×10^4 V/cm
δsolute = 2.2×10^{-2}
δsolvent = 1.1×10^{-2}

timebase = 0·1 msec/division

Figure 1 PVP (alone)

a.

E = 1.94×10^3 V/cm
δsolute = 3.95×10^{-2}
Both values at maximum height

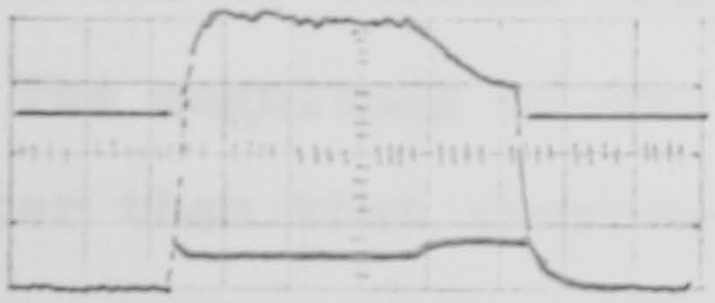

b.

E = 4.39×10^3 V/cm
δsolute = 1.90×10^{-1}
Both values at maximum height

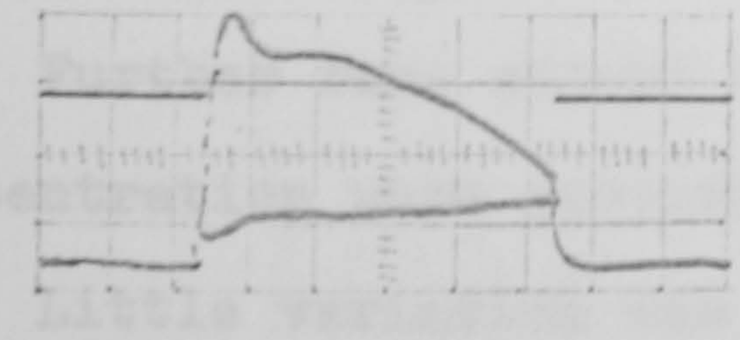

c.

E = 9.01×10^3 V/cm.

timebase = 0·1 msec/division

Figure 2 PVP with 8 mM/ℓ SDS

water. However significant distortion of the applied electric field occurred, the form of which depended on the magnitude of the field applied and not on the concentration of SDS present.

PVP and SDS

The behaviour of the electric field showed no marked difference from that with SDS alone. See Fig. 2 abc.

The response of the solutions to the electric field can be summarised as follows:- three pulses could be rapidly applied without untoward distortion of the optical response. On the application of many pulses, bubbles formed on the electrodes and the solution between the electrodes turned yellow due to thermal degradation of the PVP.

The magnitude of the optical response was, however, much greater than that observed previously. Measurements were made on transients as shown in Fig. 2 a and 2 b at the maximum height of the optical response. The resulting electric field dependence obeyed the Kerr law (see Graph 1), the Kerr constant obtained depending markedly on the concentration of SDS,(see Graph 2).

Further runs showed that the results at any one SDS concentration were accurately reproduceable.

Little variation was observed in the decay characteristics of the optical pulse. On PVP alone curvature of the decay log plot was obtained (see Graph 3).

The useful application of a.c. pulses in the frequency range 20 to 2 x 10^3 Hz was impeded by virtue of the low

GRAPH 1
δ VERSUS E^2

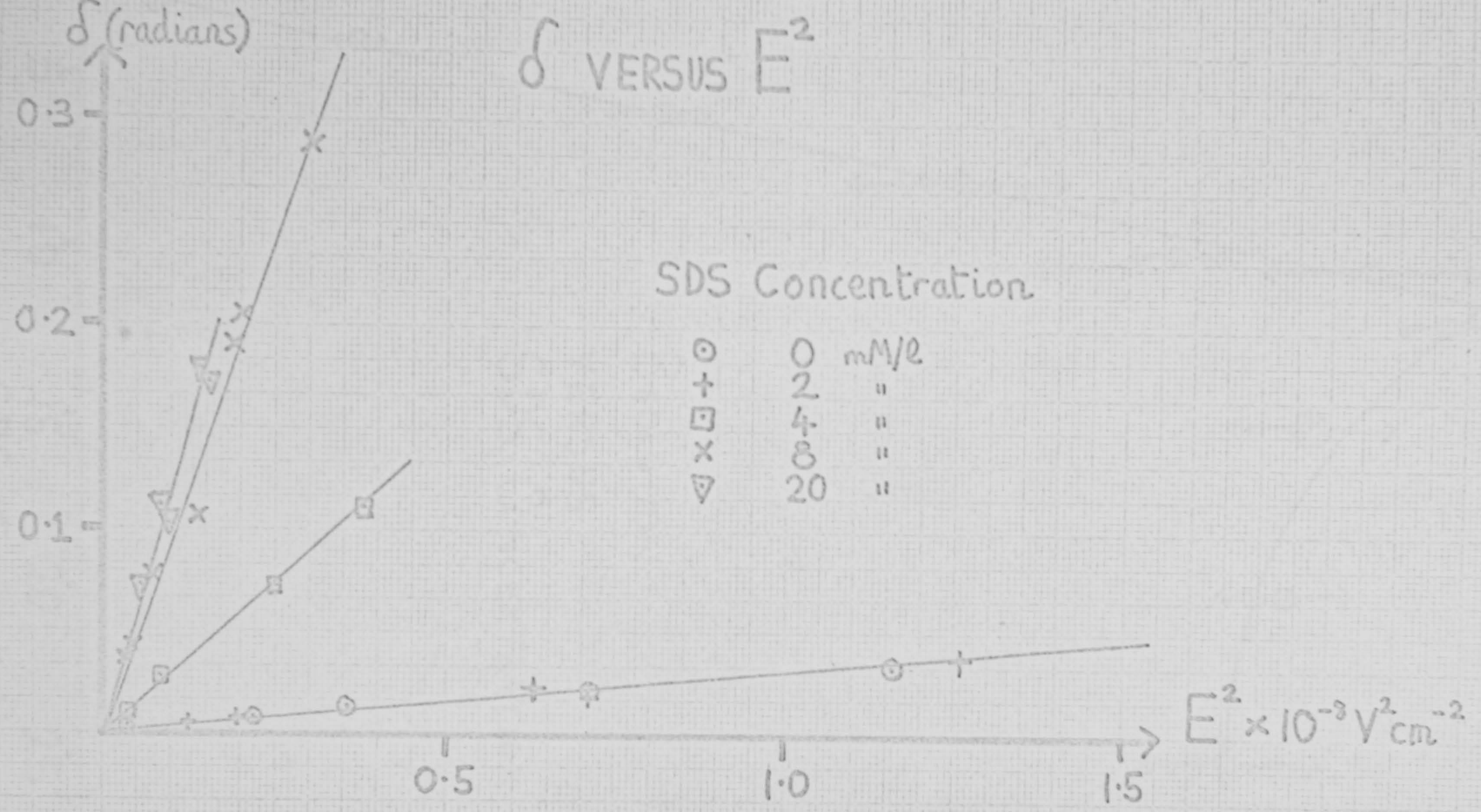

GRAPH 2

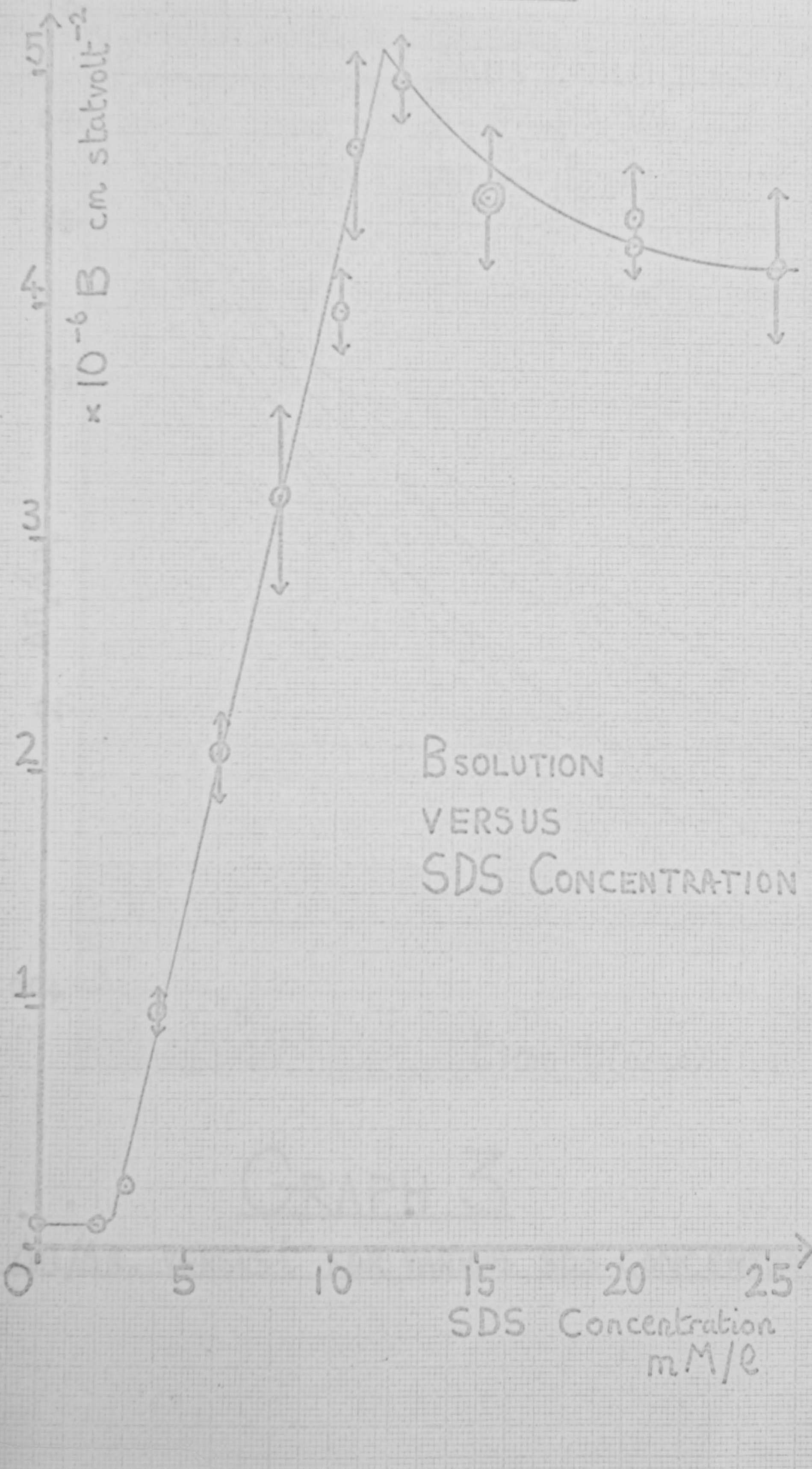
σ_1
4
3
2
1
$\times 10^{-6}$ B cm statvolt^{-2}
B SOLUTION
VERSUS
SDS CONCENTRATION
0
5
10
15
20
25
SDS Concentration
mM/e

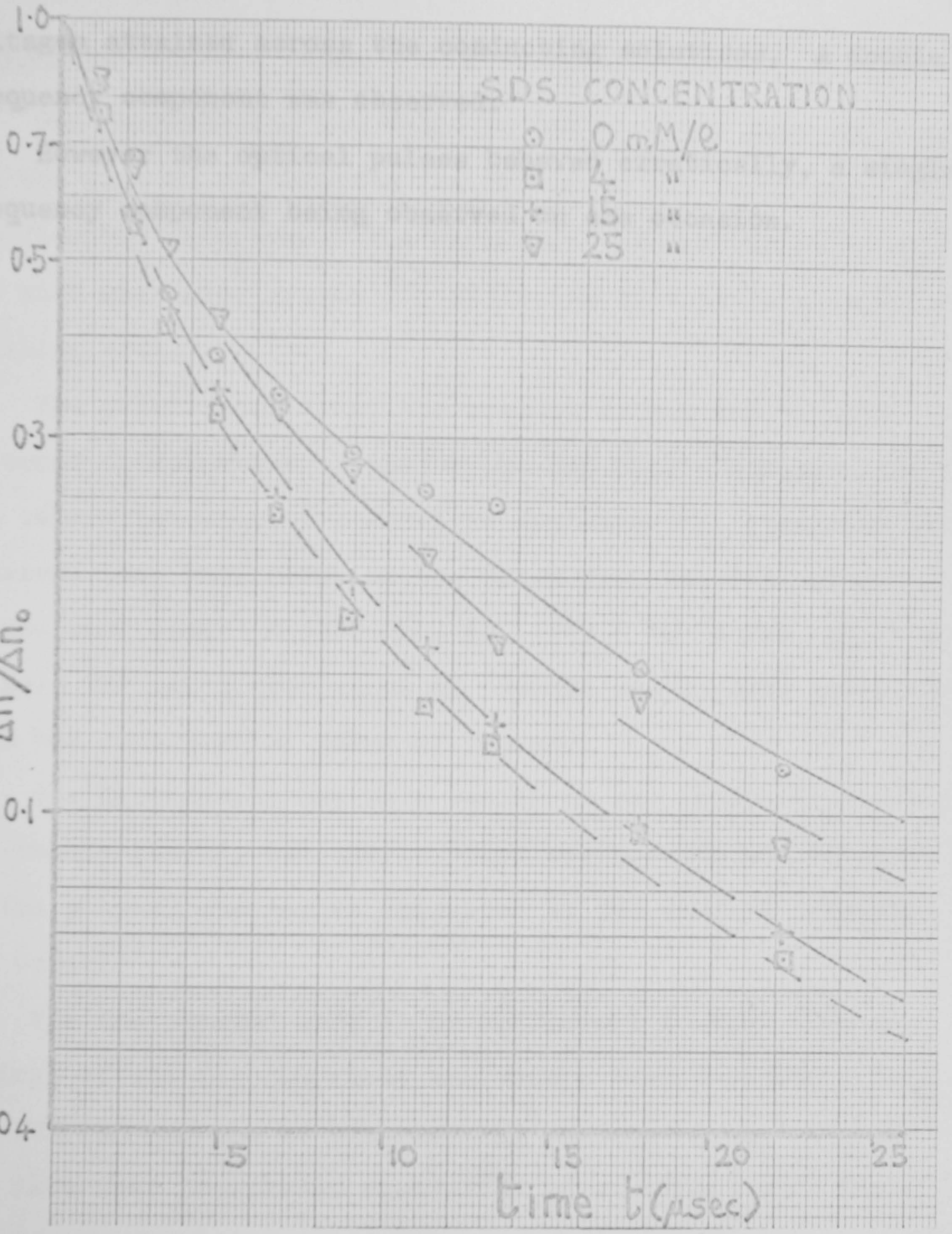

GRAPH 3

Δn/Δn₀ VERSUS t FOR VARIOUS SDS CONCENTRATIONS

voltages attained across the conducting solutions. A double frequency component was observed.

However the optical pulses behaved erratically, a single frequency component being observed on one occasion.

Discussion

The exeptionally low value of the specific Kerr constant and the fast decay observed for PVP alone are indicative of its flexible structure. The dependence of the viscosity of PVP with molecular weight[20] indicates that it is a non-free draining coil.

The polydispersity of the present sample was unknown. In order to determine if Stockmayer and Baur's equation for the relaxation time of a non-free draining coil predicted the observed long time slope of the decay plot the following values were used: M 700,000, $[z]$ $1{\cdot}7 \times 10^{2}$ ml/gm, z_0 9×10^{-3} poise. The calculated value of 18 μsec was in good agreement with the experimental value of 33 μsec.

The discrepancy may be a result of the inapplicability of the theory itself, the sample polydispersity or entanglement of the polymer chains, as suggested by the work of Nishijima and Oster.[3]

For the present work it is sufficient to know that the optical effect for SDS alone was always less than 20% of that of the PVP/SDS samples of the same SDS concentration. However the fact that transients equivalent to an effect five times greater than that of water were observed, appears to be more indicative of the conductance of the solutions and not of the structure of SDS.[11] Apart from this, changes in the steady light level were presumably due to heating effects in the cell.

The most drastic effect of the SDS was to distort the pulse

shape. Tests showed that this was due only to the large currents passing through the switching valves of the pulse generator and not to any intrinsic property of the conductance of the solutions.

From the change in the value of V_o (see Fig. 4 Chapter 4) before and after application of the pulse, it was deduced that the resistance of the cell was 75 Ω, when containing 20 mm/l of SDS. Using the resistivity relationship[12] the conductance of the SDS solutions was therefore determined to be less than 6×10^{-4} $Ohm^{-1}cm^{-1}$.

Since one was dealing with highly conducting solutions several effects could possibly have occurred:-

Joule heating can give rise to an increase in temperature of the solution. Using typical values obtainable in the present work 10 amps at 10^3 V for 5×10^{-4} sec, 5 joules of energy dissipated in the small volume of liquid between the electrodes could have given rise to an increase in temperature of 1.5^{o} C.

The movement of charge could be quite substantial.[11] A free sodium ion, for instance, can travel a distance of 6×10^{-4} cms. when placed in a field of strength 5×10^3 V/cm for 5×10^{-4} sec. The mobility of large ions and charged molecules is similar. Heller[13] suggested that the resulting electrophoretic orientation would result in the phase difference being partially dependent on the first power of the field. At field strengths greater than 10^4 V/cm the Wien effect can also occur.[12,14] The results here did not require either effect to be considered for their interpretation.

The movement of charge to the electrodes can result in electrode polarisation and electrolysis. The formation of a layer of charged ions on the electrodes results in a drop in the applied voltage across the actual solution. The actual drop is however only of the order of a few volts.[12] The removal or injection of ions caused by electrolysis would obviously result in changes of composition of the solution. In the present case, in which steel electrodes were used, it is probable that oxygen and hydrogen were formed at the electrodes whilst sodium ions were not discharged.

Due to the fact that measurements were repeatable, despite the use of different numbers of pulses, and by the fact that an E^2 relationship was observed, the results of the PVP/SDS samples have been interpreted solely in terms of molecular orientation in an electric field.

Three distinct regions of behaviour occurred in the PVP/SDS system, this being in agreement with the same[7] and similar polymer-surfactant systems.[15,16]

In the range 0 to 2 mm/l of SDS no change was discernible in either the Kerr constant or the decay plot. No interaction between PVP and SDS apparently occurred in this region.

From 2 mm/l to approximately 11 mm/l of SDS a rapid increase in Kerr constant was evident. Intuitive reasoning would suggest that the DS^- ions attached themselves to the uncharged PVP polymer chain to form a polyelectrolyte. Flexible polyelectrolytes, as well as rigid polyelectrolytes, have large Kerr constants.[14,17] This is in agreement with other studies.[15,18] The large change which should therefore

have occurred in the induced dipole moment did not manifest itself in the shape of the optical transient. The time required for saturation of the transient was, however, smaller than that observed for PVP alone.

As far as the author is aware no theories are at present capable of interpreting the Kerr constant of a flexible molecule to which bound ions are attached and around which a counterion cloud exists.[19]

It is probable that a change in the optical anisotropy of the chain occurred as well as the induced electric moment per unit length. Noting that the Kerr constant was a linear function of SDS concentration and that the work of Fishman and Eirich[7] suggested that the uptake of ions also occurs linearly, it would appear that the Kerr constant is linearly related to the charge held on the chain.

By virtue of the electrostatic repulsion of the attached DS^- ions one would expect the polymer chain to take on an extended shape. The increase in intrinsic viscosity of the polymer complex would necessarily lead to a longer relaxation time for rotation of the whole coil in accordance with Stockmayer and Baur's equations. Indeed all the relaxation times corresponding to different modes of segmental vibration should increase. In consequence the induced birefringence should decay more slowly. In fact, as shown in Graph 3, in the region under discussion the opposite behaviour occurred. Nonetheless the slope of the decay plots at long times corresponding to whole chain rotation was no different, within experimental error, from that of PVP alone.

Above 11 mm/l of SDS a rapid change in slope of Graph 2 occurred, the Kerr constant even decreased in value. Correspondingly no marked change in the relaxation curves occurred. If one is to identify this region then it must be one in which DS^- ions no longer complex with the polymer but cluster together to form micelles.

Jones,[15] investigating the polyethylene oxide - SDS system, estimated a similar second transition point as being the sum of the critical micelle concentration and the amount of SDS needed to saturate the polymer chain. He assumed that the hydrocarbon tail of the DS^- ions lay flat along the chain. A similar situation had been envisaged by Frank et Al[18] with PVP/dye complexes. Assuming therefore a PVP monomer length of 2 A^o and a DS^- ion length of 16 A^o, 22mm/l of SDS would be required to saturate the polymer chains in a 2% solution. The second transition point should therefore be approximately 30 mm/litre. One could interpret the experimental result in terms of a binding efficiency of only 15%.

Fishman and Eirich have suggested[7] however that the critical micelle concentration is a decreasing function of PVP concentration. A linear extrapolation of their rather meagre results yields a negative e.m.c. for the PVP concentration used here!

The degree of binding suggested here would appear to be rather low. This result possibly indicates that only the outer extremities of the compact random coil were capable of interacting with the SD^- ions.

As stated little changes occurred in the relaxation times, although at 25 mm/l of SDS the observed curve had returned to that of PVP alone. This behaviour and the fall off in the Kerr constant might possibly be indicative of a supposed[7,15] interaction between the SDS micelles and the polymer surfactant complex. Conversely the increased number of sodium counterions in the vicinity of the charged flexible chain might give rise to this effect.

The fall in Kerr constant could certainly not be explained by further binding of single surfactant molecules to the complex.

It is interesting to note that Gravsholt[21] observed three transition points in the behaviour of the conductance of a PVP/SDS sample. The first and third transitions he interpreted in the manner of Jones. He did not however suggest any mechanism giving rise to the second transition point near to 10 mm/l of SDS.

Conclusion

The Kerr effect has clearly defined three regions of interaction between SDS and PVP.

Interpretation of the results could only be attempted on a very broad qualitative basis, and was not altogether satisfactory. The large variation in Kerr constant showed that a polyelectrolyte had formed, but the second transition point indicated a small degree of ion binding. The small change in the decay transient to faster relaxation times could not be interpreted in terms of expansion of the coil.

Nonetheless the very rapid assimilation of experimental data compared with the equilibrium dialysis measurements of former experimenters[7] and the possibility that much knowledge can be gained about the Kerr effect of flexible polyelectrolytes in general, indicates that future measurements are worthwhile.

Suggestions for future work

The high conductance of detergent solutions indicates that d.c. pulse work is limited to molecules having fast relaxation times. In order to determine that ion-cloud formation actually takes place, reversing pulses and a.c. pulses should be of greater use[8] than d.c. pulses.

For the present system the variation of the form of Graph 2, in particular the position of the second transition point, with the molecular weight and concentration of the polymer, is of interest.

Flow birefringence measurements should also be made to determine the dependence of the optical anisotropy of the PVP chain on SDS concentration.

The observation of the behaviour of non-ionic surfactants,[6] using the Kerr effect, would appear to be of little use. It is the polyelectrolyte nature of the complex which is readily detected.

Moreover the action of an ionic surfactant on a rigid macromolecule could receive better treatment with existing Kerr effect theories.

References

1) Miller (L.E.), Hamm (F.A.), J. Phys. Chem. 57, 110, 1953.

2) Frank (H.P.), Levy (G.B.), J. Polymer Sci. 10, 371, 1952.

3) Nishijima (Y.), Oster (G.), J. Polymer Sci. 14, 337, 1956.

4) Weyl (D.A.), Neale (S.M.), Dielectrics 1, 22, 1963.

5) McBain (J.W.) 'Colloid Science' Pub. D.C. Heath & Co. 1950.

6) Breuer (M.M.), Robb (I.D.) Chem. & Industry, 530, 1972.

7) Fishman (M.L.), Eirich (F.R.) Polym. Prep. A. Chem. Soc. Div. Polym. Chem. 10, 746, 1969.

8) Paulson (C.M.), O'Konski (C.T.) Polym. Prep. A.C.S 7, 1175, 1966.

9) Stoylov (S.P.), Petkanchin (I.) J. Coll. Int. Sci. 40, 159, 1972.

10) Orrtung (W.H.), Meyers (J.A.) J. Phys. Chem. 67, 1905, 1963.

11) Bjornstahl (Y.) Phil. Mag. 2, 701, 1926.

12) Milazzo (G.) 'Electrochemistry' Elsiner 1963).

13) Heller (W.) Rev. Mod. Phys. 14, 390, 1942.

14) Nakayama (H.), Yoshioka (K.) J. Pol. Sci. 3, 813, 1965.

15) Jones (M.N.) J. Colloid Sci. 23, 36, 1967.

16) Nagaki (M.), Ninomiya (Y.) 37, 87, 1964.

17) Yoshioka (K.), O'Konski (C.T.) J. Poly. Sci. A-2. 6, 421, 1968.

18) Frank (H.P.) et Al, J. Phys. Chem. 61, 1375, 1957.

19) Hornick (C.), Weill (G.) Biopolymers 10, 2345, 1971.

20) Brandup & Immergut, Polymer Handbook. Pub. Interscience 1966.

21) Gravsholt, Chim. Phys. Applied Prat. Ag. Surface

cr. Congr. Inst. Deter. 1968. V 2. p.993.

CHAPTER 7

An electro-optic study on the bacterium Escherichia coli.

Introduction

Escherichia coli (E. coli) is a typical bacterium whose shape and size can be approximately represented by a prolate ellipsoid of axial ratio 2 and major dimension 2 μm.[1]

The behaviour of living bacteria in electric fields has been widely studied; in concentrated suspensions pearl chain formation can occur.[2] Dielectric dispersion measurements have indicated the electrical properties of the cell membrane,[3,16] and high voltages have been used to kill bacteria by irreversibly damaging the membrane.[4]

The present birefringence study on E. coli was performed to complement the electro-optic light scattering study on the same bacterium by Dr. V. Morris of this group. However, it will be shown that the only effect of the electric field was to change the amount of light transmitted by the suspensions of this bacteria.

An experimental procedure will be given which convincingly proved that the changes were a result of the manner in which the bacteria scattered light out of the forward direction of the beam and not to anisotropic absorption of light energy. For the first time Rayleigh Gans light scattering theory has been used to predict the magnitude of the intensity changes. This approach allowed estimates of the size, shape and direction of the electric

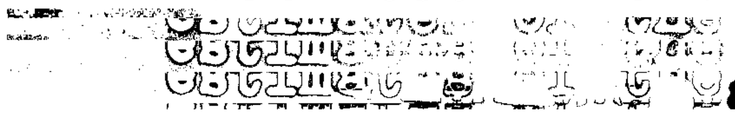

acteria to be made. The conclusions are to

be compared with those obtained from existing electro-optic theories.

Previous electro-optic dichroism measurements performed by Tolstoi et Al[6] and scattering measurements of Stoylov[5] led to contradictory conclusions. This work for the first time will prove that those results are not a consequence of the observation of apparently different optical effects.

Primarily consider the required equations and theory.

Theory

The reduction in intensity of a light beam passing through a suspension of randomly orientated particles is described by the Beer - Lambert law

$$I = I_o \, 10^{-Al} \qquad (1)$$

where I_o is the intensity of the incident beam,
I is the intensity of the transmitted beam,
l is the thickness of the absorbing medium,
and A is the absorbance of the medium.

When light passes through a solution of molecules which absorb light energy anisotropically, the value of the absorbance depends on the orientation of the molecules (and therefore the direction of the applied electric field) and the plane of vibration of the incident linearly polarised light. It has been recently[7] shown that

$$A_{Th} = A + \Delta A$$

$$A_{Tv} = A - \tfrac{1}{2}\Delta A$$

$$A_{Tu} = A + {}^{\Delta A}/_{4} \qquad (2)$$

$$A_{Lh} = A_{Lv} = A_{Lu} = A - \tfrac{1}{2}\Delta A$$

where T (L) indicates the direction of the light path to be at 90° (0°) relative to the applied field.

v (h) indicates the plane of vibration of the linearly polarised light to be at 90° (0°) relative to the direction of the transverse field.

u indicates the use of unpolarised light

and the combination of symbols represents the relevant combination of field direction and orientation of the polarised light.

When reduction in transmitted intensity results from light scattered out of the forward direction the Beer - Lambert law is expressed in the form

$$I = I_{o} \exp (- Tl) \qquad (3)$$

where T is the turbidity of the solution.

Turbidity is therefore related to values of absorbance by the equation

$$T = 2{\cdot}3\ A \qquad (4)$$

The applicability of Rayleigh-Gans theory in determining the light scattered from particles as large as bacteria has been discussed by Koch.[8,9] He has shown that at least for randomly orientated bacteria use of that theory introduces little error into the determination of turbidity. Hence

$$T = k \int_{0}^{\pi} P(\theta) (1 + \cos^{2}\theta) \sin\theta \, \partial\theta \qquad (5)$$

where θ is the angle between a unit vector $\hat{s}$ representing

the scattered ray and a unit vector $\hat{s}_o$ representing the incident ray.

$P(\theta)$ is the particle scattering factor.

k has the value[8]

$$\frac{4\pi^3}{9} \left(\frac{dn/dc}{n_o}\right)^2 \frac{q^2 \nu}{\lambda'^4} \qquad (6)$$

where

λ' is the wavelength of the incident light in the medium,

q is the anhydrous mass of material in a single particle,

ν is the number of particles per unit volume,

n_o is the refractive index of the suspending medium

and $\frac{dn}{dc}$ is the specific refraction index increment.

The variation of T with wavelength is given by the equation[10]

$$-\frac{\partial \log T}{\partial \log \lambda} = 4 - \frac{\partial \log Q}{\partial \log \lambda} = 4 - B \qquad (7)$$

where

$$Q = {}^3/_8 \int_0^{\pi} P(\theta)\,(1 + \cos^2\theta)\,\sin\theta\, d\theta$$

B is a function of $P(\theta)$ and is therefore dependent on the size and shape of the scattering particle.

The variation of T on application of an electric field is the result of changes occurring in $P(\theta)$. The form of $P(\theta)$ for completely orientated and completely random ellipsoids in the Rayleigh region has been given by Roess and Shull.[11]

Consider ellipsoids of principal axes a, b, b;

For full orientation

$$P(\Theta)_{orientated} = 9\left(\frac{\sin k - k\cos k}{k^3}\right)^2 \qquad (8)$$

where $K = \frac{4\pi b}{\lambda'} \sin \Theta/2 \,(\sin^2 \phi + p^2 \cos^2 \phi)^{\frac{1}{2}}$ (9)

The factor 9 is included to normalize $P(\Theta)$ at $\Theta = 0$.

p, equal to a/b, is the axial ratio ($p < 1$ oblate $p > 1$ prolate)

ϕ is the angle between the axis, a, of the ellipsoid and the scattering vector $\hat{s} - \hat{s}_o$.

Using simple vector algebra it can readily be shown that ϕ is a simple function only of Θ, when a is parallel to $\hat{s}_o$.

For this case,

$$\phi = 90 - \Theta/2 \qquad (10)$$

For random orientation.

$P(\Theta)$ is determined by integrating over all values of ϕ.

$$P(\Theta)_{random} = \frac{1}{4\pi} \int_0^{\pi} 9\left(\frac{\sin k - k\cos k}{k^3}\right)^2 2\pi \sin\phi \, d\phi \qquad (11)$$

The relative change in light intensity when random ellipsoids are completely orientated with their axis, a, parallel to the direction of the unpolarised light beam is therefore

$$\frac{\Delta I_{max}}{I_s} = \frac{e^{-T_o l} - e^{-T_R l}}{e^{-T_R l}} \qquad (12)$$

where T_o is the turbidity of the orientated ellipsoids,

T_R is the turbidity of random ellipsoids,

I_s is the steady light intensity reaching the detector,

and ΔI_{max} is the maximum change in I_s as is produced on application of an electric field sufficient to cause saturation of the effect.

In essence the form of transient changes in turbidity can be determined using existing electric light scattering theories for rod shaped molecules.[12] In particular on removal of the field

$$\frac{\Delta T(t)}{\Delta T(t=0)} = e^{-6Dt} \qquad (13)$$

The change in turbidity $\Delta T(t)$ is determined from the recorded photographic trace using the formula

$$\Delta T(t) = -\frac{1}{e} \ln \left(\frac{\Delta I(t)}{I_s} + 1\right) \qquad (14)$$

Experimental

Samples of E. coli, sealed in capsules at liquid nitrogen temperatures were supplied by the Microbiological Research Establishment, Porton Down, and kindly prepared for use by Dr. Morris. A capsule was warmed gently to room temperature and its contents dispersed in glass distilled water. This suspension was then centrifuged at 2,000 g for 20 minutes. The supernatant was removed and the sediment resuspended in dust-free distilled water. This process of centrifugation and resuspension was repeated six times. The final suspension was further diluted and used for measurements within eight hours.

Electric light scattering measurements were made on suspensions of concentration approximately 10^7 bacteria/ml by Dr. Morris.

Electric birefringence measurements were made by the author on the same suspension using the linear detection system. The analyser was offset to 6^{o}, cell 3 was employed, and white light was used to increase the sensitivity of the system. D.C. and A.C. field pulses of magnitude 600 V. r.m.s. and duration 1 sec. were applied to the suspensions using the Wareham amplifier in series with the relay box which was manually switched. The voltage offset device was connected between the photomultiplier and oscilloscope to avoid distortion of the optical pulse.

Changes in the light transmitted by the suspensions were observed using a typical linear dichroism arrangement. The author's optical apparatus was used with the quarter wave-plate and analyser removed. A cell constructed by Dr. Bailey, formerly of this group, was used for transverse and longitudinal field measurements[13] (see equation 2).

On the basis of preliminary experiments a wavelength of 4,400 A^{o} and suspension concentration of approximately 10^{8} bacteria/ml were chosen to give relatively large changes in light intensity with little noise.

The absorption spectrum of this suspension was obtained in the region 2,000 to 8,500Å using a Perkin - Elmer 402 ultra-violet spectrophotometer.

All electric field measurements were made at a room temperature of 25 ± 2^{o} C.

Results and Discussion

Birefringence Transients were not observed. Phase differences, if produced, were therefore less than 10^{-4} radians per cm. of suspension. Transient light scattering measurements had already shown that the bacteria were fully orientated at fields of 200 V/cm., suggesting that the bacteria as a whole are optically isotropic. Optically anisotropic components present in the cell have therefore a symmetric distribution in the cell membrane and are randomly orientated in the fluid body of the cell.

At concentrations greater than 10^7 bacteria/ml it was evident that absorption changes accounted for the observed transients, although calculations were not performed to determine if birefringence was also present.

Electric Dichroism measurements.

The application of A.C. pulses produced typical electro-optic transients (see Fig. 1 a c). However the action of d.c. pulses was often to produce consistent but erratic behaviour (see Fig. 1 d). Repeated observations showed that this was a function of the particular suspension and more evidently the type of electrodes employed. For this reason longitudinal measurements, producing normal transients, (see Fig. 1 b) were preferred for observation of the field dependence (see Graph 1) and frequency dependence (see Graph 2) of the transmitted light intensity.

In order to determine the nature of the absorption changes, transverse and longitudinal measurements were performed.

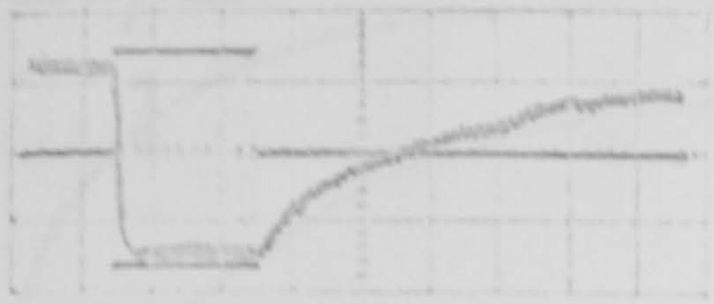

a.

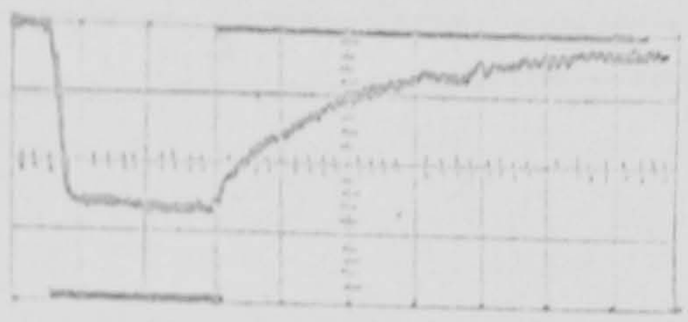

b.

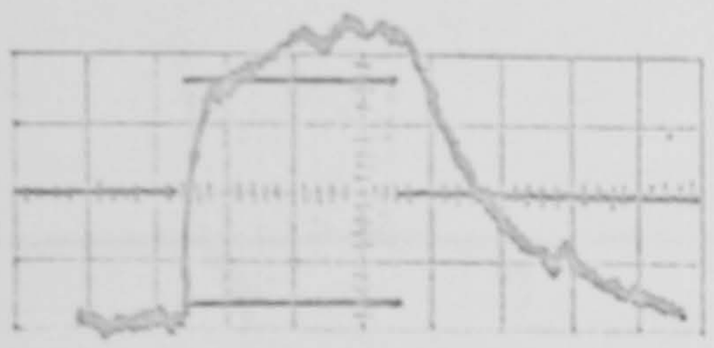

c.

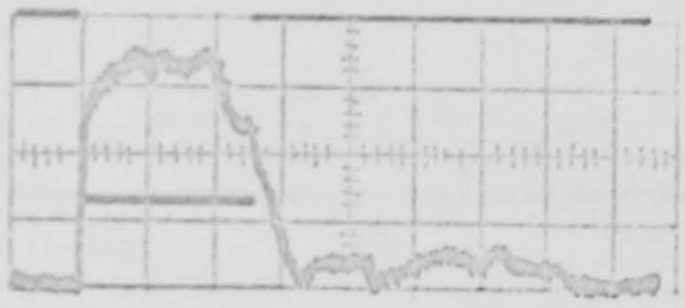

d.

FIG. 1

longitudinal measurements figs. a, b.
transverse measurements figs. c, d.
Applied field strength $\simeq$ 100 $V_{R.M.S}$/cm.
A.c. field frequency 1 KHz.
time scale 0·5 sec/division.

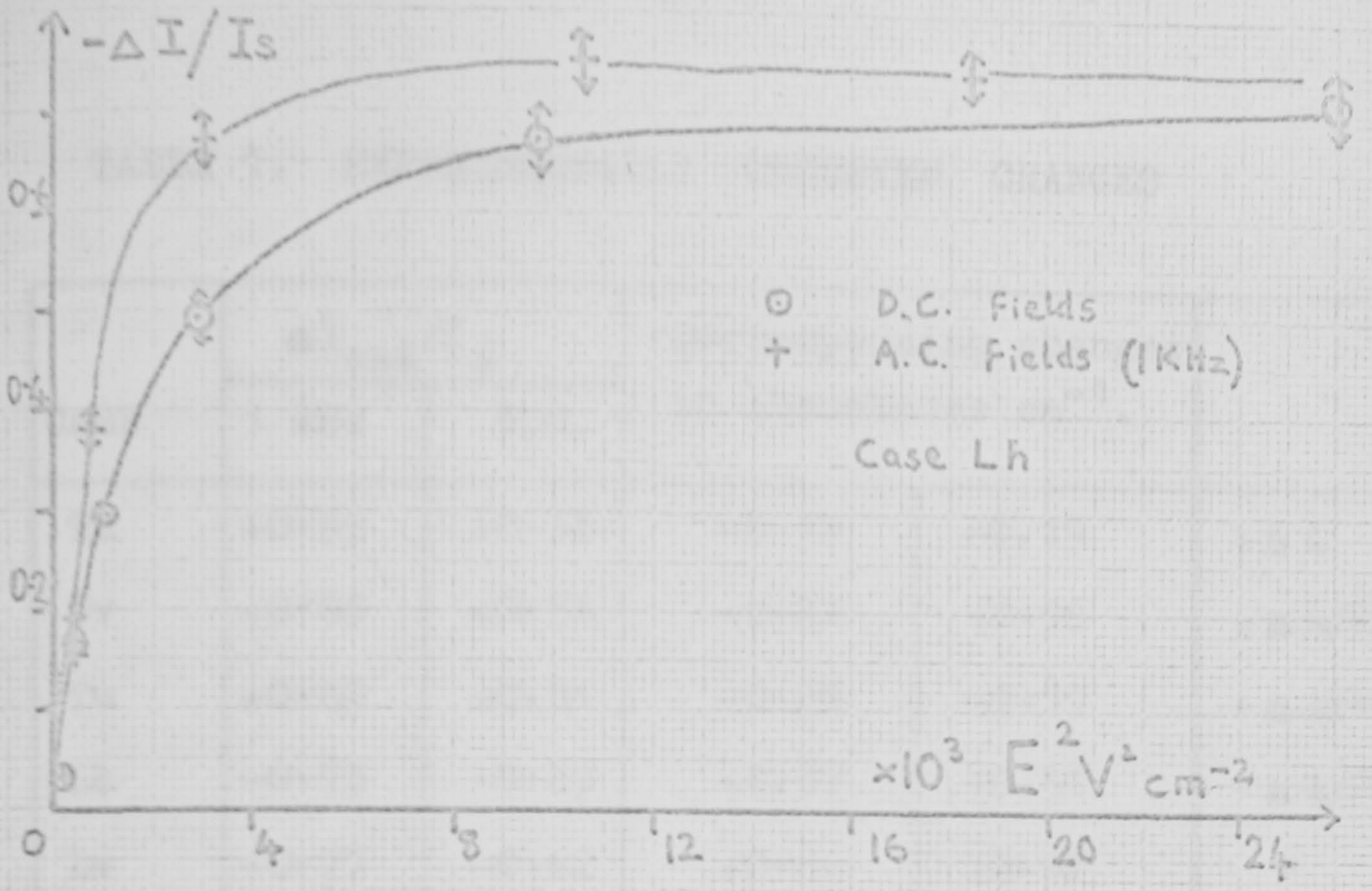

GRAPH 1

FIELD DEPENDANCE OF THE INTENSITY CHANGES

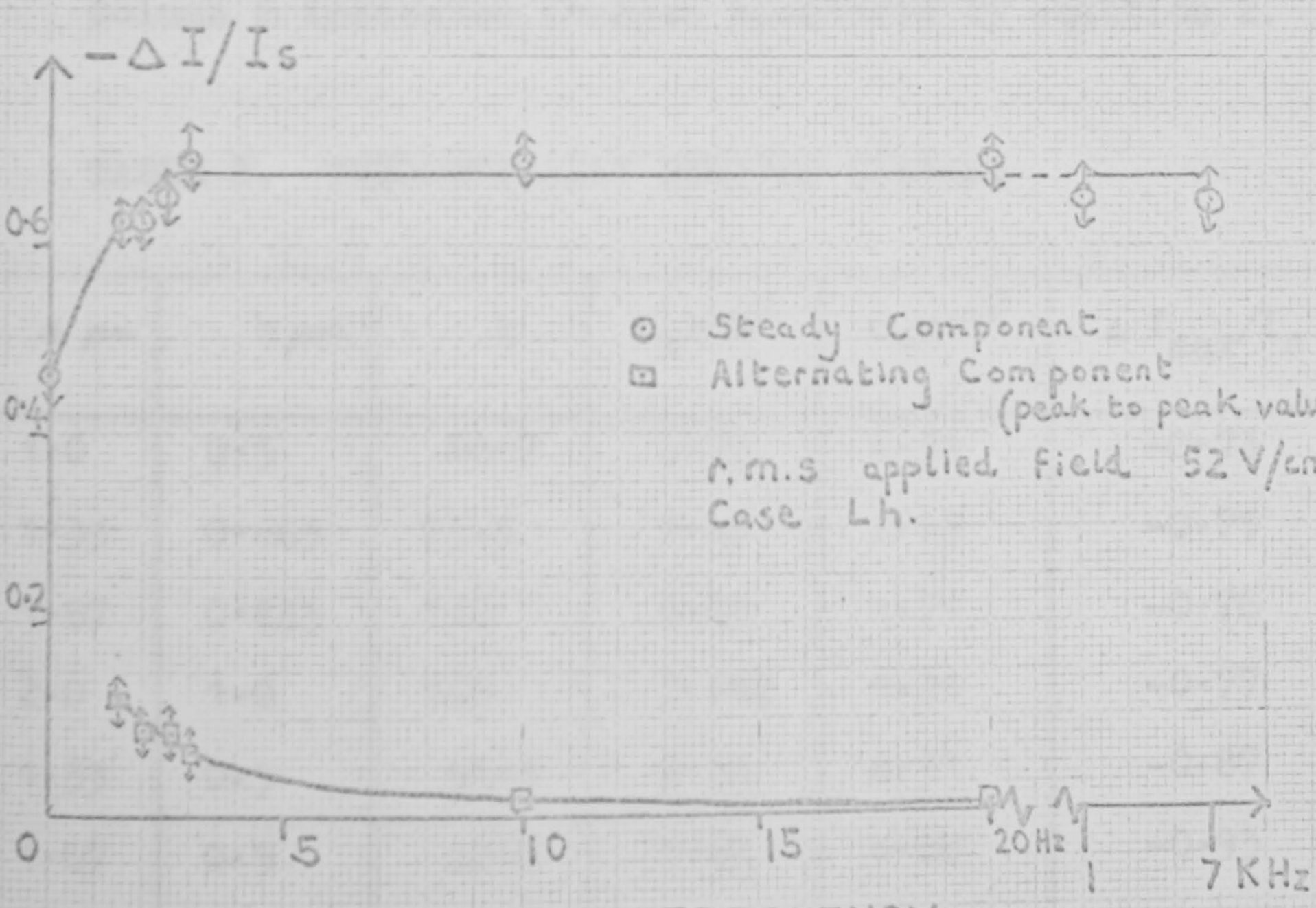

GRAPH 2

RELATIVE CHANGE IN LIGHT INTENSITY V. FREQUENCY
NOTE CHANGE IN FREQUENCY SCALE.

TABLE 1. EXPERIMENTALLY OBSERVED CHANGES

CASE	$\Delta I_{max}/I_s$ 1 kHz	$\Delta I_{max}/I_s$ D.C.	Corresponding changes in absorbance cm^{-1}.		
Th	+0·55	+0·56	-0·19	-0.19	$+\Delta A$
Tv	+0·55	+0·53	-0·22	-0·18	$-\Delta A/2$
Tu	+0·60	+0·54	-0·20	-0·19	$+\Delta A/4$
Lh	-0·73	-0·69	+0·57	+0·51	$-\Delta A/2$
Lv	-0·77	-0·62	+0·64	+0·42	"
Lu	-0·75	-0.66	+0·60	+0·47	"

A_{random} = 0·52 cm^{-1} $E_{R.M.S.}$ = 270 V/cm

Column 6 indicates changes predicted by equation 2.

TABLE 2. THEORETICALLY DERIVED CHANGES

a μm	b μm	k	$Q_r x10^2$	$Q_o x10^2$	$\Delta I_{max}/I_s$
1·0	0·5	40·9	2·92	4·51	-0·73
1·33	0·665	71·5	1·67	2·65	-0·75
1·67	0·835	112	1·07	1·71	-0·76
2·0	1·0	160	0·747	1·21	-0·77
1·33	0·5	51·3	2·33	4·31	-0·87
1·67	0·5	62·0	1·93	4·08	-0·93
2·00	0·5	72·3	1·65	3·88	-0·96

A_{random} = 0·52 cm^{-1} λ = 0·44 μm

n = 1·33 l = 2·0 cms. case a parallel to light beam

Table 1 summarises the values of $\Delta I_{max}/I_s$ obtained for d.c. and a.c. field pulses. It is evident that equation 2 does not predict the changes observed. Indeed the spectrophotometer plot (Graph 3) indicates only one marked absorption band at 2,100 A^o, well away from the wavelength 4,400 A^o used in this study. Both results suggest that light scattering is the principal cause of beam attenuation at 4,400 A^o.

To examine the possibility of Rayleigh Gans theory predicting the magnitude of the observations two sets of calculations were performed:-

<u>To determine the variation of absorbance with wavelength</u>

using equation (7), a computer program was written to evaluate the integral $\int_0^{\pi} P(\theta)_{random} (1 + \cos^2\theta)\sin\theta \, d\theta$ for various wavelengths. The results for an ellipsoid of semi-axes 1 μm 0·5 μm 0·5 μm are plotted on Graph 4. The slope of the straight line passing through these points equalled 1·95 ± 0·03. The theoretical value of $d \log A / d \log \lambda$ was therefore -2·05 ± ·03. The experimental values of A and λ obtained from the spectrophotometer plot , also shown on Graph 4, fitted a straight line relationship in the wavelength range 3,000 to 8,000 A^o such that $d \log A / d \log \lambda$ equalled - 1·7 ± 0·1. Further calculations for the prolate ellipsoids used in the construction of Table 2 could not account for the discrepancy. Indeed the value of B is very insensitive to quite large variations in particle size and shape and can never be greater than 2·0.

Other experimental values reported are -2·28 by Koch,[8] and -1·51 by Fikman.[14] Koch attributes his high value to

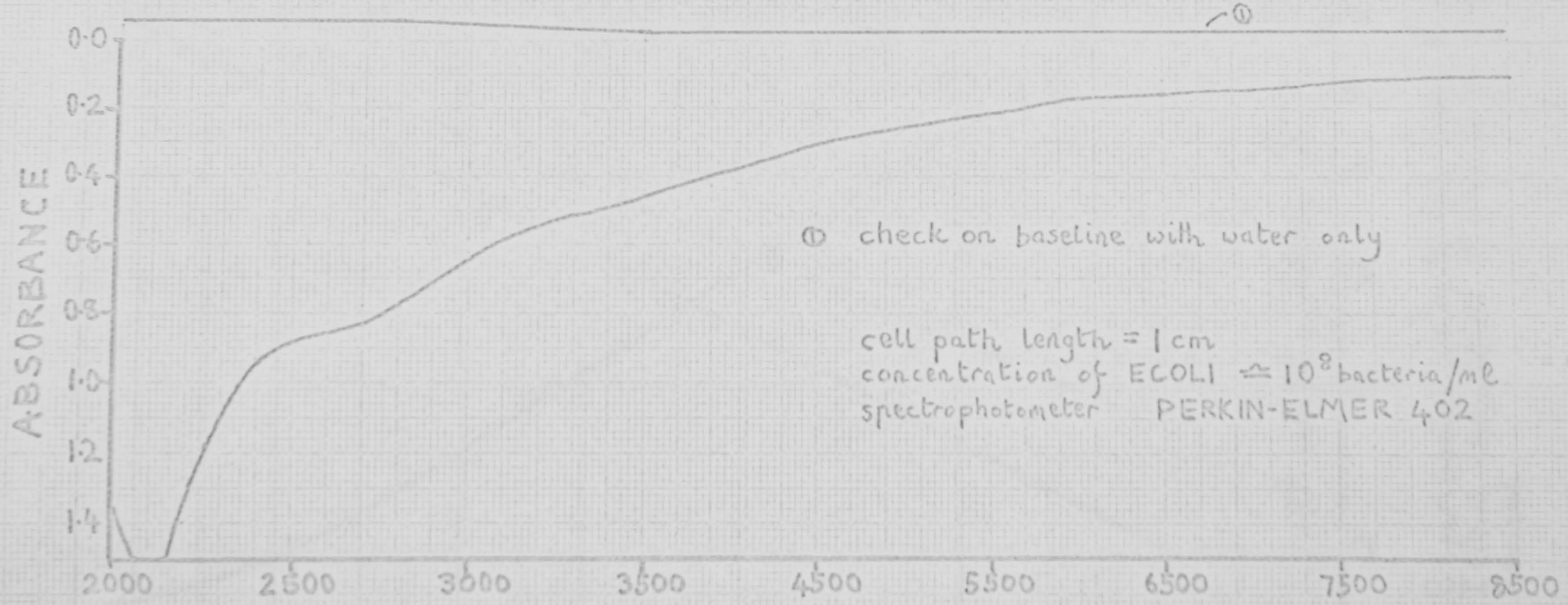

GRAPH 3 . ABSORPTION SPECTRUM OF ECOLI

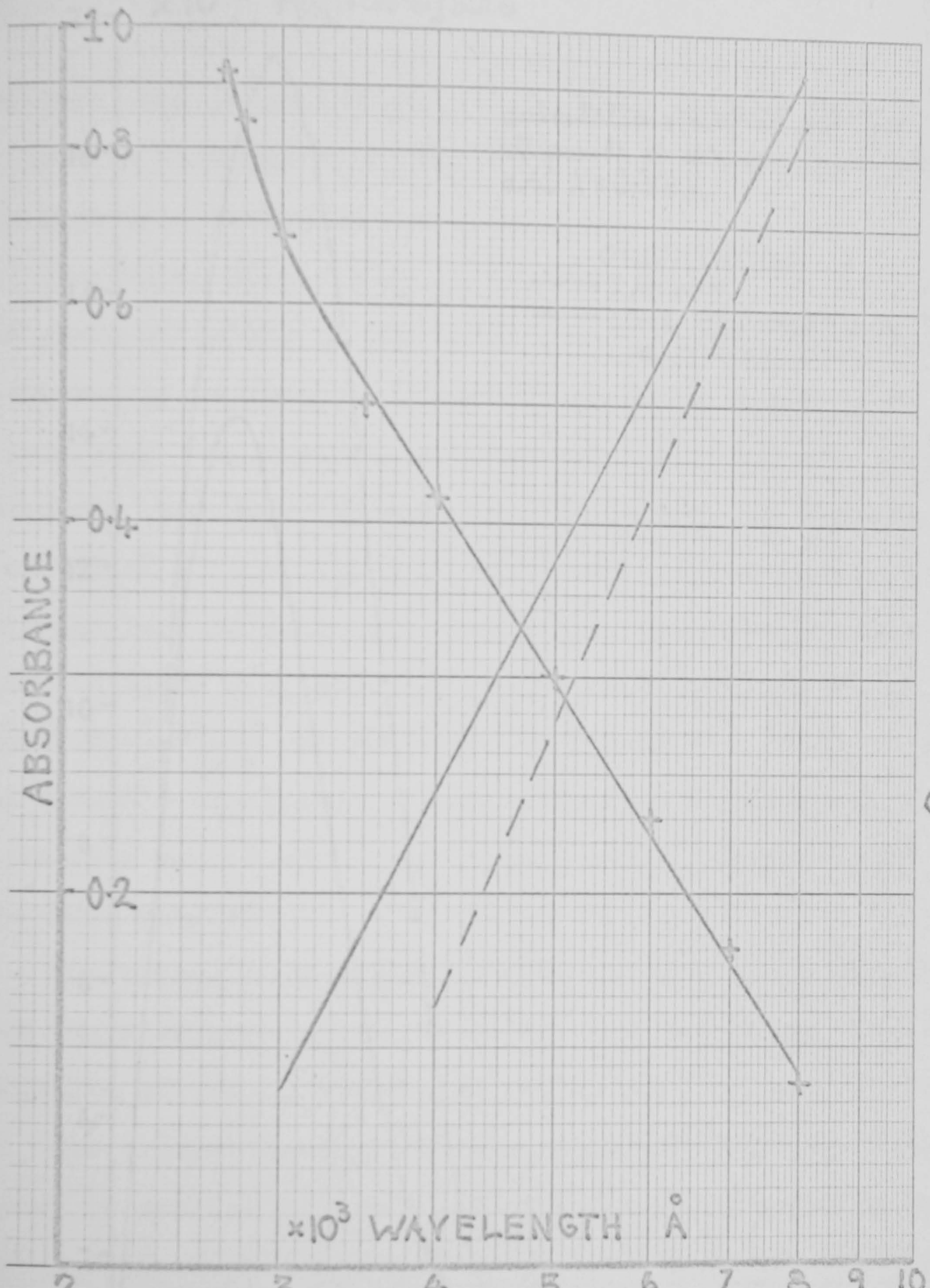

+——+——+ Experimental values of absorbance v. wavelength
——— Initial computation of form of Q v. wavelength
— — — — Revised " " " " " "

GRAPH 4

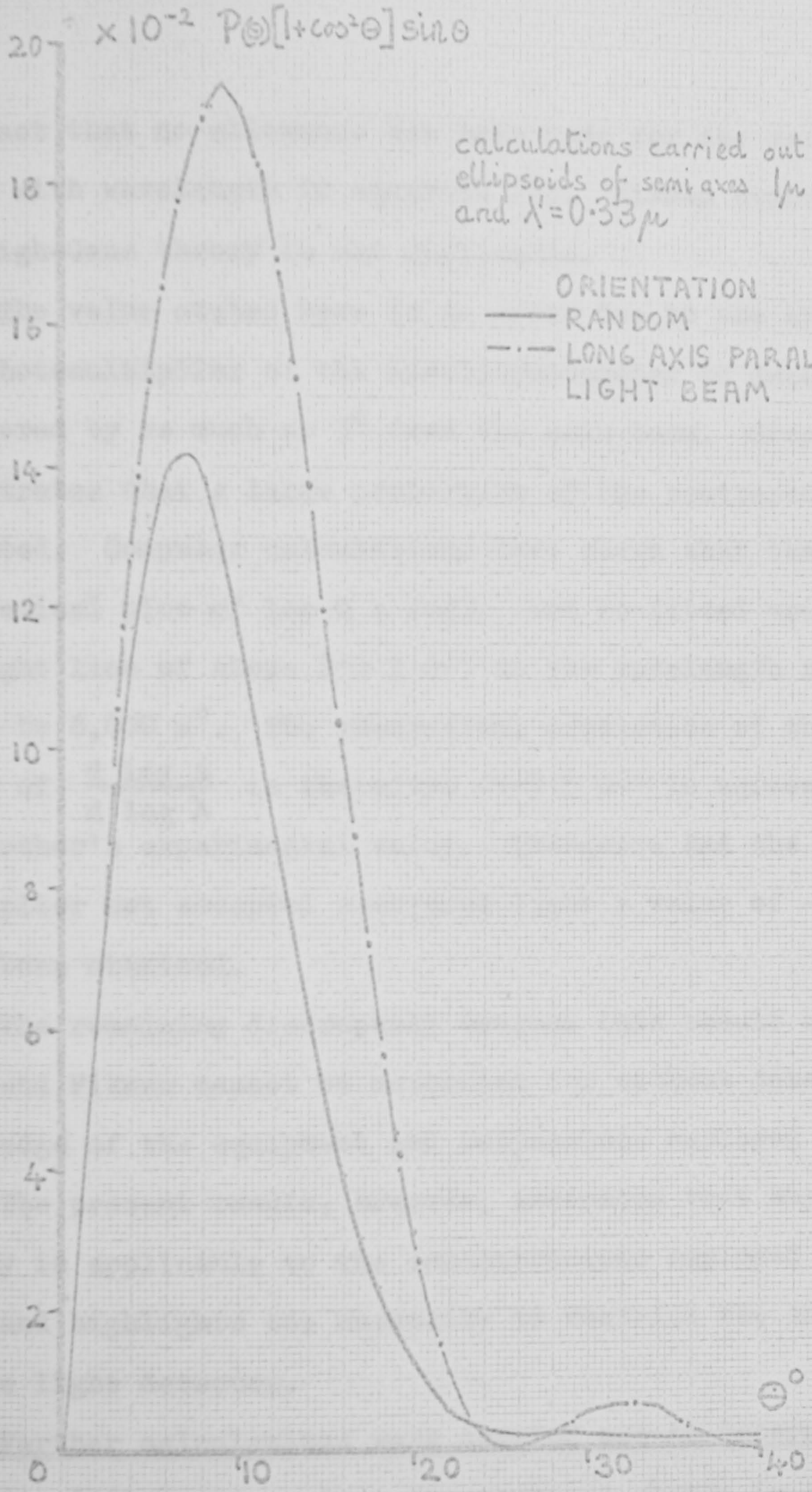

GRAPH 5

THE ANGULAR DISTRUBUTION OF SCATTERED LIGHT.

the fact that no allowance has been made for the variation of dn/dc with wavelength in equation (7). Fikman states that Rayleigh-Gans theory is not applicable.

The value stated here is in error due to the ability of the photomultiplier of the spectrophotometer to detect light scattered by as much as 5^{o} from the main beam. Graph 5 illustrates that a large proportion of the scattered light is detected. Computer calculations have shown that the revised theoretical plot of log Q v log λ can be fitted using a straight line of slope $2 \cdot 3 \pm 0 \cdot 1$ in the wavelength range 4,000 to 8,000 A^{o}. The theoretical prediction of the observed value of $\frac{d \log A}{d \log \lambda}$ is therefore $-1 \cdot 7 \pm 0 \cdot 1$ in agreement with the author's experimental value. Therefore had the photomultiplier not accepted scattered light a value of -2·05 would have been obtained.

The remaining discrepancy between this result and those of Koch and Fikman cannot be accounted for without detailed knowledge of the equipment and suspensions employed by them.

The present result, however, indicates that Rayleigh-Gans theory is applicable to the concentrations employed in this work and highlights the necessity to restrict the angular size of the light detector.

Further calculations were carried out to determine if equation (12) could predict the observed change in intensity for either the T_u or L_u cases (see Table 1). In order to determine the magnitude of the change it was necessary to evaluate the constant k. Through lack of accurate knowledge of dn/dc, ρ, and ν, equation (6) could not be used. k was

evaluated using the value of the absorbance as measured using the electro-optic system. Here a collimating slit and the position of the photomultiplier were such that light scattered through angles more than 1^{o} was not detected. The value of absorbance measured was 0·52 cm. at 4,400 A^{o}. The flow diagram F1 illustrates the method of determining $(\Delta I_{max}/I_s)_{theoretical}$ in a program written by the author, the results of which are given in Table 2. The agreement in the sign of $(\Delta I_{max}/I_s)_{theoretical}$ with that of $\Delta I_{max}/I_s$ for the experimental case L_u shows that the major axis, a, of the bacteria is aligned along the direction of the light beam and hence the applied electric field. For the case of a.c. pulses of frequency 1 kHz only the induced moment operates to orientate the bacteria. It is therefore possible to say that the induced moment is along the direction of the major axis of the bacteria. A comparison of the magnitude of these two quantities allows an estimate of the theoretical dimensions to be made.

$$a = 1{\cdot}33\ \mu m$$

$$b = c = 0{\cdot}67\ \mu m$$

However, the 5% error possible in the experimental value indicates that whereas the shape of the bacteria can be ascertained with accuracy the actual dimensions quoted here cannot. Nonetheless the values stated above are in agreement with the 'known' estimates and the values obtained from the decay analysis presented later. There is little doubt therefore that Rayleigh-Gans theory accounts for the observed changes despite the lack of simple equations to determine the

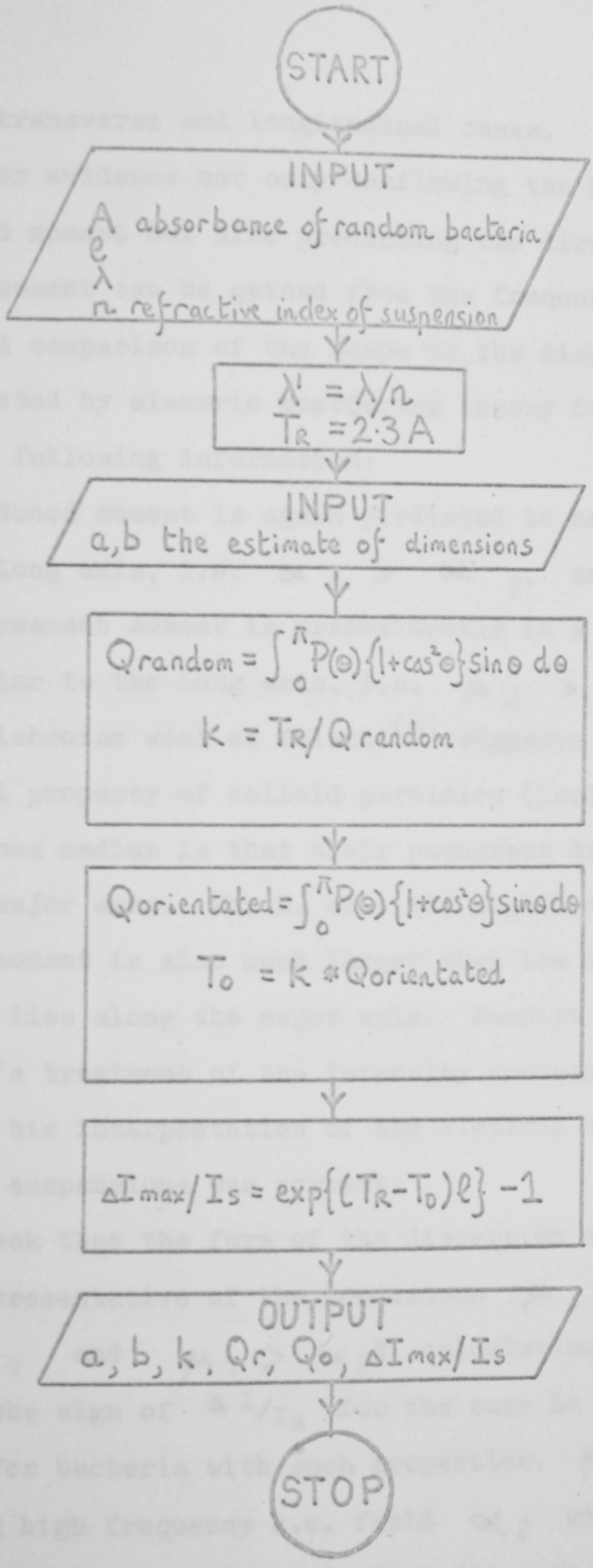

FLOW DIAGRAM 1

remaining transverse and longitudinal cases.

Further evidence not only confirming the direction of the induced moment but also predicting the direction of the permanent moment can be gained from the frequency dispersion, Graph 2. A comparison of the shape of the dispersion with that predicted by electric scattering theory for long rods yields the following information:

(1) The induced moment is again predicted to be predominantly along the long axis, i.e. $\alpha_1 > \alpha_2$, and

(2) The permanent moment is predominantly in a direction perpendicular to the long axis, i.e. $\mu_2 > \mu_1$.

The dichroism work of Tolstoi[6] suggests that a fundamental property of colloid particles (including bacteria) in an aqueous medium is that their permanent dipole moment is along the major axis. For E. coli the magnitude of the permanent moment is also much larger than the induced moment which also lies along the major axis. Despite the shortcomings of Tolstoi's treatment of the intensity changes there is little doubt that his interpretation of the electric moments of his particular suspensions was correct.

To check that the form of the dispersion observed here was not representative of the conditions $\mu_1 > \mu_2$, $\alpha_2 > \alpha_1$ and $\mu_1 > \alpha_2 E$ calculations were made to show that the sign of $\Delta I/I_s$ for the case Lu could not be predicted for bacteria with such properties. For a fully orientating high frequency a.c. field α_2 would be along the direction of the field, and the major axis of the ellipsoids

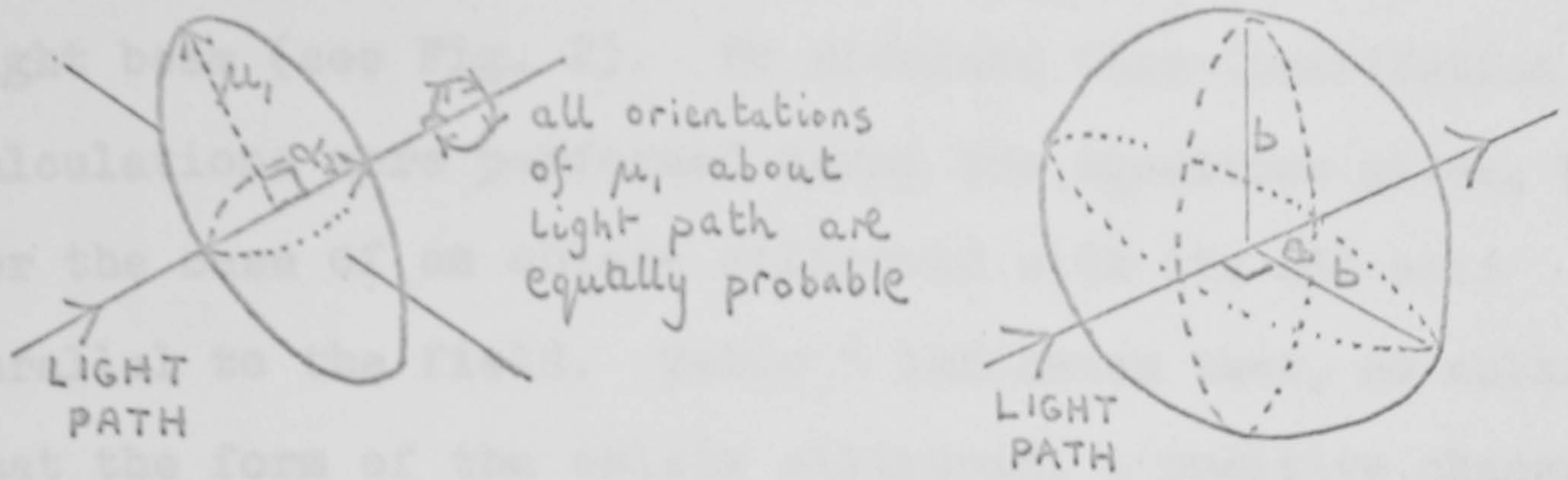

a b

Figure 2 a. possible orientation in 1KHz longitudinal field
b. simulation employed for purpose of calculations

a	b	$\Delta I_{max}/I_s$
0·1	1·0	+3·33
0·5	1·0	+1·22
0·9	1·0	+0·17

Theoretical changes predicted using simulation

TABLE 3

could take any orientation in a plane perpendicular to the light beam (see Fig. 2). To simulate this distribution calculations were performed using the equations given, but for the case of an oblate ellipsoid with its odd axis parallel to the field. Table 3 indicates that, no matter what the form of the oblate ellipsoid, a positive change in intensity should be observed. This is not in accordance with the experimental result.

Confirmation of the predicted size and shape was obtained from the decay analysis. A series of transients for transverse and longitudinal a.c. fields showed that the time taken for the effect to fall to the $^{1}/_{e}$ point was reproduceable to $0{\cdot}9 \pm 0{\cdot}4$ secs (see Graph 6). The relaxation time of the transverse measurements appeared to be slightly greater than that of the longitudinal measurements, whereas the longitudinal decay plots appeared to be more curved. Normal transients observed with d.c. pulse fields yielded plots lying in the limits shown. When curvature of such plots existed this was ascribed to the polydisperse nature of the sample.

It might be thought that two diffusion constants are necessary to describe the transient decay, corresponding to motion of the ellipsoids about the transverse and symmetry axes. Birefringence transients do not manifest the latter type of motion. Ridgeway[17] attributed this behaviour to the invariance of the physical phenomena on orientation of the ellipsoid about the symmetry axis. Provided therefore that scattering matter is distributed symmetrically about the long

GRAPH 6

DECAY OF TURBIDITY

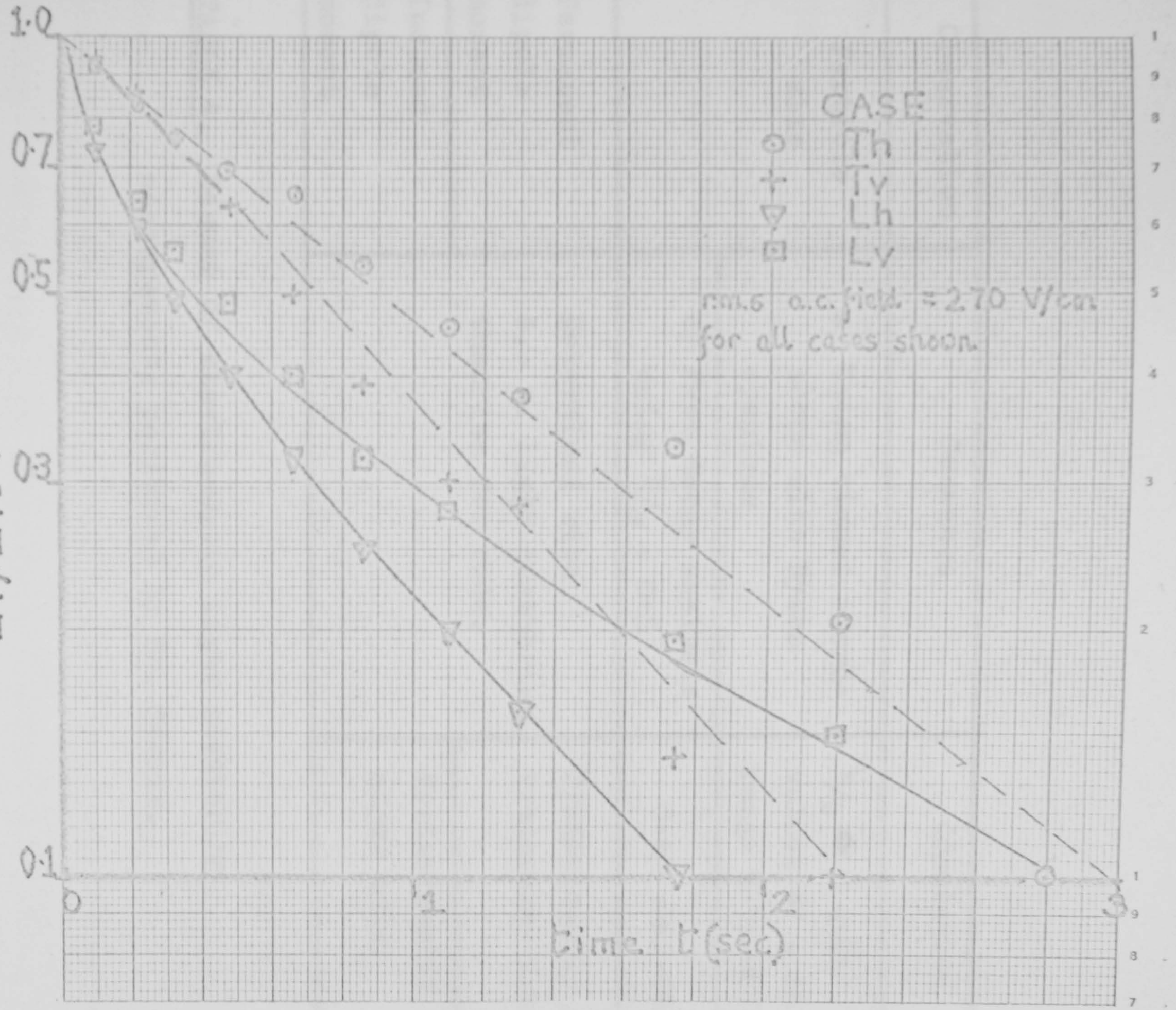

Observation	Comments	Conclusion
Particle size	a) Using visual microscope with Dyson eyepiece	$a/b \triangleq 2$ with values of a in range 0·58 → 1·58 μm.
	b) From decay analysis using $b/a = 0·5$	0·65 → 1·28 μm
Permanent dipole moment	Determined with e.- o. light scattering theories for rods.	Predominantly along transverse axis.
Induced dipole moment		Predominantly along major axis.

TABLE 4. Resumé of electro-optic light scattering measurements performed by Dr. Morris.

axis of the ellipse, the decay of turbidity will also be dependent only on the former type of motion.

Assuming a value of 2 for the axial ratio, the use of Perrin's equation (see Ch. 2, equ. 12) produced the following values:-

$$a = 1{\cdot}3(\pm\ 0{\cdot}2)\mu m \qquad b = c = 0{\cdot}65(\pm\ 0{\cdot}1)\ \mu m$$

in excellent agreement with those previously obtained.

The results of Dr. Morris on the same bacterial suspensions, but of lower concentration, can be seen in Table 4.

Conclusions, including suggestions for further study.

At a concentration of 10^7 bacteria/ml birefringence transients were not observable, i.e. $\Delta n < 10^{-9}$. However, Bateman[15] has suggested that in some circumstances redistribution of refracting material may result in bacteria becoming birefringent. An electro-optic study might be useful in observing this phenomena.

At higher concentrations the observed dichroism changes could not be described by equations related to the absorption of light energy. Rayleigh Gans theory however predicted:-

1) The dependence of the absorbance on wavelength without the need for the additional considerations suggested by Koch.

2) That the bacteria align themselves parallel to a fully orientating a.c. field.

3) That the magnitude of the intensity changes were consistent

with bacteria of the shape of a prolate ellipsoid with semi-axes of length 1·33 μm and 0·67 μm.

The latter values were confirmed by analysis of the decay transients. In addition it would seem reasonable to suggest that the two sets of experimental observations could be used to determine unequivocally both the shape and size of bacteria. It should be remembered however that real bacteria are neither exact ellipsoids nor monodisperse.

The direction of the induced moment was confirmed using an electro-optic light scattering theory developed for long thin rods. The direction of the permanent moment was predicted, using this theory, to be predominantly along the transverse axis. Estimation of the magnitude of the dipole moments should also be attempted in further work.

The experimental method is a substantial improvement over that employed by Tolstoi.[6] A polariser is not required and, if the photomultiplier aperture is reduced, a normal commercial spectrophotometer[13] could be used to record directly changes in terms of turbidity values.

Moreover electro-optic dichroism and scattering measurements on the same bacteria have yielded results consistent with those of Stoylov[5] and in disagreement with those of Tolstoi.[6]

References

1) Gunsalus (I.C.), Stanier (R.Y.) "The Bacteria", vol. 1, Academic Press 1960.

2) Teixeira-Pinto (A.A.) et Al, Experimental Cell Research 20, 548, 1960.

3) Schwan (H.P.) Adv. Biol. Med. Phys. 5, 147, 1957.

4) Sale (A.J.H.), Hamilton (W.A.) Biochimica et Biophys Acta 148, 781, 1967.

5) Stoylov (S.) et Al, Doklady. Akad. Nauk. S.S.S.R. 180, 1165, 1968.

6) Tolstoi (N.A.) et Al, "Research in Surface Forces", ed. B.V. Dervagin, vol. 3, 49-65, 1971.

7) Foweraker (A.), Jennings (B.R.) Applied Optics, August 1973.

8) Koch (A.L.) Biochim Biophys Acta, 51, 429, 1961.

9) Koch (A.L.) J. Theoret. Biol. 18, 133, 1968.

10) Doty (P.), Steiner (R.F.) J. Chem. Phys. 18, 1211, 1950.

11) Roess (L.C.), Shull (C.G.), J. Appl. Phys. 18, 309, 1947.

12) Stoylov (S.P.), Advances in colloid and interface science, 3, 45, 1971.
(This is a review of birefringence, dichroism and light scattering measurements made on colloids including bacteria.)

13) Baily (E.D.), Jennings (B.R.), Applied Optics 11, 527, 1972.

14) Fikman (B.A.), Biofizika 8, 380, 1963.

15) Bateman (J.B.), J. Colloid Interface Sci. 27, 458, 1968.

16) Cartensen (E.L.), Biophys J. 7, 493, 1967.

17) Ridgeway (D.), J. Am. Chem. Soc. 88, 1104, 1966.

CHAPTER 8

Concluding Remarks

Transient electric birefringence measurements have been made using both the linear and quadratic optical systems. A detailed account of the author's equipment and its alignment was given in Chapters 4 and 3 respectively. It was suggested that with this equipment the linear detection system be used, thereby minimising the effects of stray birefringence and variations in the light source output. The equipment was most accurately employed in the observation of phase differences from 1×10^{-3} to 2 radians. The performance of both quadratic and linear optical systems was tested by the standard use of nitrobenzene. The values of the Kerr constant differed with each other by approximately 15% and were on average 30% smaller than the generally accepted value. The latter result was attributed to the purity of the nitrobenzene; a factor commented on by previous workers.

A new rapid method of data handling and analysis has been developed and found to function satisfactorily. It consisted of a transient recorder interfaced to a tape punch with computer processing of the recorded transients. A useful development of this equipment might be to directly link the transient recorder to a computer and provide a teletype link so that the experimenter could also simultaneously input information. However the additional expense of such a

system would be relatively enormous. Moreover the present system and program are sufficiently complex to remove the drudgery out of data analysis and only the interpretation of the experimental results remains. Future development of the equipment as suggested would therefore be an unnecessary extravagance compared with the minimal gains.

Three macromolecular systems were studied by the author.

In Chapter 5 both a.c. and d.c. voltage pulses were applied to a polypeptide, Poly - β - benzyl - l - aspartate in chloroform and metacresol. The saturation of birefringence in d.c. fields was used to determine the electrical properties of PBLA in chloroform. It was shown that errors in estimating the limiting value required for that procedure can lead to substantially different interpretations of the electrical properties. It was concluded that Yamaoka's measurements and the present results could best be treated in terms of a permanent dipole orientation.

The values of the residual moment and length were not in agreement with values expected for an α helix. It was suggested that the error lay in the polydisperse nature of the sample. A number of optimistic attempts by electro-optics workers have been made to use the decay characteristics to determine the distribution of particle size in a poly-disperse sample. It is the view of the author that electro-optic methods as used here will never succeed in this aim. To interpret results in terms of residual values it is necessary to use monodisperse samples. The more complex

problems of polydispersity are best treated using other methods (see reference 16 of Chapter 5).

An interesting application of the Kerr effect to a highly conducting system was made in a study of an anionic surfactant, sodium dodecyl sulphate, on a flexible polymer, polyvinylpyrrolidone. This is the first report, to the author's knowledge, of electro-optic measurements on such a system. A particularly marked variation in Kerr constant was observed. It clearly showed three regions of behaviour similar to those observed using other techniques. However no such changes were observed in the decay characteristics. Other methods have suggested that the polymer chain expands on adsorbing dodecyl sulphate ions; it would appear therefore that the decay of birefringence was here dependent on the motion of short individual chain lengths and not on the chain as a whole. Unfortunately no more than empirical observations could be made, and this has practically always been the situation when flexible macromolecules have been studied with the Kerr effect. It is unlikely that meaningful quantitative measurements can be made on such a system without considerable effort. A rigid macromolecule should therefore be chosen for future surfactant work. Moreover, pulse fields were employed to minimise the effects of joule heating, electrolysis and electrophoresis. When conducting systems are studied the problem of determining the internal field strngth acting on the individual molecules also arises. Much work needs to be done before these problems will be fully appreciated.

Another novel aspect of this work was the realisation that changes in turbidity accounted for the observed electro-optic effects with suspensions of the bacteria E.coli. Existing electro-optic theories and Rayleigh-Gans light scattering theory were both successfully employed to give the correct size and shape of the bacteria. Unlike the measurements of some previous workers it was shown that the results were in accord with electro-optic light scattering measurements.

In conclusion electro-optic methods, especially transient electric birefringence, have been used with varying degrees of success in the study of many macromolecular systems. But, although the subject has been in existence for a century, much work has still to be done if it is to be universally employed. In particular, methods of dealing with poly-dispersity, flexibility and conducting solutions need to be revised if they are to be relevant to the sophisticated problems of current interest.

It is the hope of the author that this thesis has made a worthwhile contribution to the realms of macromolecular science, through the development of this physical method.

ACKNOWLEDGEMENTS

This work was done under the supervision of Dr. B.R. Jennings, to whom I am particularly indebted for his continuous advice, encouragement and friendship

The first year of this work was performed at Queen Elizabeth College, London University. I thank Prof. R.E. Burge for the facilities I employed there, and all the staff of the Physics Department for their generous help.

For the remaining two years I thank Prof. C.A. Hogarth for the specious facilities provided at Brunel University.

I thank all the Physics staff, and particularly the workshop staff for constructing the Kerr cells.

In addition but none the less I thank Mr. Geoffrey Ford and the Electronics workshop staff for designing and constructing the hydrogen thyratron pulse generator.

Applied Research Laboratories (Luton) for questions answered regarding the (transient recorder - tape punch) interface which they designed and constructed.

Those members of the university computing centre, in particular Mrs. Margaret Clifton, for producing a system enabling the transient recorder data tape to be read.

Dr. V. Morris for many discussions regarding the work on his bacteria.

Finally I thank the Science Research Council for the award of a research studentship during the whole of the past threee years.

Appendix 1.

Published Work

Transient recorder display for electro-optical studies of macromolecules.

By P.J. Rudd and B.R. Jennings.

Laboratory Practice 22, 535, August 1973.

Electric birefringence for the study of polymer-surfactant interactions. The polyvinylpyrrolidone - sodium dodecyl sulphate system.

By P.J. Rudd and B.R. Jennings.

Accepted for publication in the Journal of Colloid and Interface Science.

The first of these papers is included directly below, and should be read in conjunction with the work in Chapter 4.

Transient recorder display for electro-optical studies of macromolecules

P. J. Rudd and B. R. Jennings

Physics Department, Brunel University, Uxbridge, Middlesex

The recent interest in macromolecules in solution has resulted in the development of many optical techniques. In particular, light scattering (Stoylov, 1971; Jennings, 1972), optical rotation (Tinoco and Hammerle, 1956; Jennings and Baily, 1970), birefringence (Yoshioka and Watanabe, 1969; O'Konski, 1969) and dichroism (Yoshioka and Watanabe, 1969) have all been the basis of novel electro-optical experiments. The electro-optic method is fundamentally an observation of the change in an optical property of a solution which accompanies the orientation of the solute macromolecules when subjected to an electric field. It is advantageous to apply the field as a single-shot pulse. Electrophoretic effects are then reduced, the method can be made very rapid and particle relaxation effects can be observed.

With pulsed fields the optical properties of the solution change in a transient manner which approximates to an exponential rise to a steady state condition, followed by an exponential decay as the solute particles revert to a random array after the termination of the field. The maximum amplitude of the transient is related to the optical and electrical properties of the solute while the decay generally follows the equation (Benoit, 1951)

$$Z(t) = Z(o) \exp(-6Dt) \quad \ldots\ldots\ldots\ldots\ldots\ldots (1)$$

for a rigid, monodisperse solute. Here Z represents the amplitude of the optical property under study and t the time measured from the instant of termination of the electric pulse when the optical effect has value Z(o). The rotary diffusion constant D is conveniently obtained from the co-ordinates of the transient decay by evaluating the slope of a plot of log Z(t) /Z(o) vs. t . If the solute is polydisperse the most reliable procedure is to analyse the initial slope of such a plot. For extended particles, of length l, D is a function (Perrin, 1934) of (l^{-3}) and hence is useful for particle size determination.

Generally an optical apparatus is used which manifests the transient change in the optical property as a transient fluctuation of the light intensity reaching a photomultiplier detector. Typical of this procedure is the electric birefringence arrangement, described elsewhere (Yoshioka and Watanabe, 1969; Jerrard *et al*, 1969; O'Konski, 1969). With no applied field the crossed analyzer and polarizer allow only stray light to reach the detector. In the electric field particle alignment results in a birefringent solution. This changes the linearly polarized to elliptically polarized light, whence light penetrates the analyzer. The output signal $\triangle V$ from the photodetector is then proportional to the *square* (Jerrard *et al*, 1969) of the birefringence ($\triangle n$). The rapid detector response is displayed on an oscilloscope and photographed.

Analysis of such photographs has normally consisted of projecting the negative onto a large grid and reading off the co-ordinates. These are then manipulated into the log plot (O'Konski, 1969), and D obtained with some 2 per cent precision. The method is so laborious and slow that both optical scanning (Busch *et al*, 1972) and electronic simulation (Itzhaki, 1966; Brown and Jennings, 1970) methods have been developed. Both extensions provide a much quicker analysis of the data but still require the obtaining and handling of a photographic negative.

The recent commercial availability of *transient recorders* has enabled us to build a system for direct analysis of the optical transient, which obviates the photographic process. The digital output from the recorder can be fed indirectly to a computer for complete processing.

The present note gives details of the system, demonstrates its suitability for current macromolecular studies and indicates future improvements.

Apparatus and procedure

The prerequisites of the complete data handling system were that both the recording procedure and the analysis of the recorded data be rapid. These requirements enable the experimenter to follow the experiment and hence to manoeuvre the conditions during the course of the study. In addition to experimental rapidity, one needs to determine accurately the applied field strength and a time origin of the decay process. It is also desirable that the applied field and the optical response be recorded and displayed simultaneously.

The transient display has been established around a low cost Biomation model 610B transient recorder. Figure 1 is a schematic diagram of the display used in conjunction with an electric birefringence apparatus. It is emphasized that the display is equally suitable for other transient effects from macromolecular solutions.

A transient recorder is capable of converting the transient electric input signal directly from the photomultiplier into a series of digital numbers by a high speed analogue-to-digital converter. This sequence of numbers is stored in a constantly circulating memory and can be fed out for processing. Alternatively it can be reconverted to analogue form and passed to a continuous display (such as an oscilloscope or pen recorder) should a permanent visual record be required. For electro-optic experiments one needs an external signal to trigger the recorder. This is obtained from the generator of the electric pulse. The recorder is used in a pretrigger mode, in which recording commences before the pulse is applied. The model 610 can sample at 128 points in the whole, or a selected portion of, the transient optical response provided the photomultiplier output is less than 50 V amplitude and the observed duration is 100 μs or more. Each sample is stored in the form of a six-bit binary word with an accuracy of plus or minus one binary bit.

The 128 word output is forwarded *via* an interface (Figure 2), kindly developed by Applied Research Laboratories of Luton, to a Facit type 4070 tape punch. This outputs with tape having an eight track ISO standard punch hole configuration. The first six tracks contain the transient recorder read out. The other two are punched manually and have been adapted to allow rejection

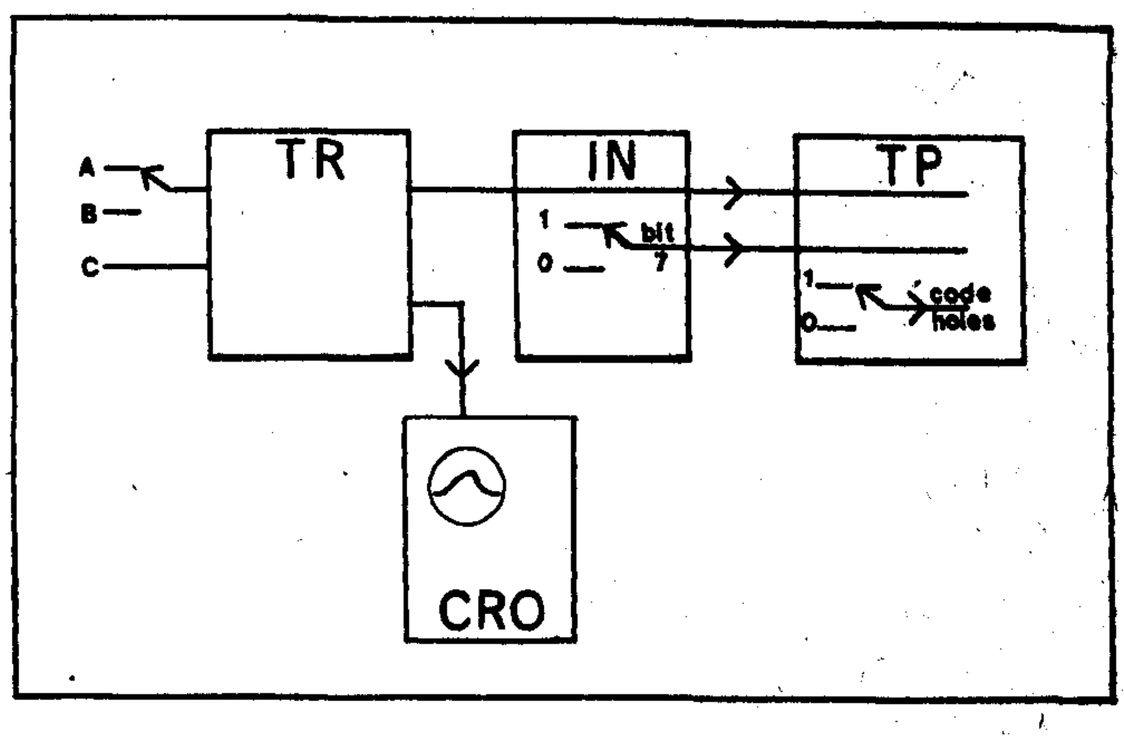

Diagram of the data logging system. Inputs A, B and C, represent the optical response from the photomultiplier, attenuated sample of the applied field and a trigger pulse from the generator respectively. The symbols represent the following: TR – transient recorder, IN – interface, TP – tape punch and CRO – oscilloscope.

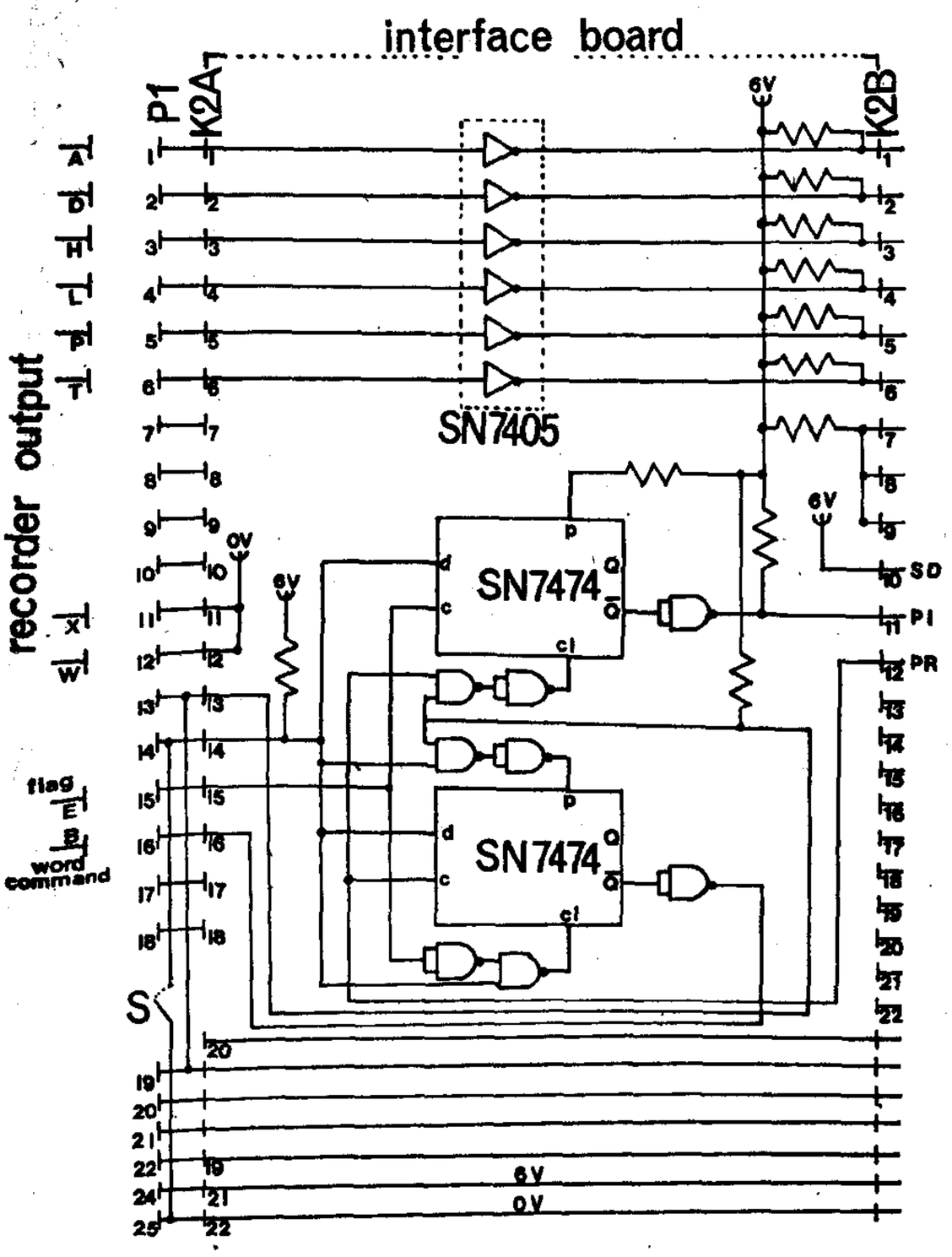

Figure 2. Circuit diagram for the interface. Alphabetical connections are to the recorder using the same plug symbols as the recorder manufacturer. The twelve interface output connections are on the right of the diagram. See text for details of the electronic components. Terminal connections are indicated by d (data), c (clock), cl (clear), p (preset), Q and $\bar{Q}$.

of the digital information on completion of an experiment. The interface is compact and all of its components are standard packages. The hexagonal inverters are in a single SN 7405 N unit and two SN 7400 D units contain the eight 'nand' gates. Both edge triggered flip-flops are found in a single SN 7474 unit. All units are standard from Texas Instruments. The 6 and zero volt supplies for these units are obtained from pins K2A/21 and /22 respectively. All the pull-up resistors are high stability of value 3.3 kΩ. Operation of switch S renders the tape punch inoperative. For the sake of simplicity the additional circuitry, which allows track 7 to be punched manually, has not been shown in Figure 2.

A disadvantage of the model 610 recorder is that it can only accept a single channel or signal. To record both the optical transient and the applied field one must apply the field twice to the solution and measure the optical response and the field consecutively. A data tape is output, which depicts these two responses. Details of the experimental and recorder settings are available on a series of punch computer cards.

Tape and cards are fed directly to an ICL 1906 computer, together with a suitable Algol program. The compatibility of 8 hole tape with the computer input capabilities should be carefully considered. Magnetic tape could be used as an alternative. The complete computer analysis first compares the applied pulse and the optical transient to evaluate the beginning of the transient decay. The amplitude at this point corresponds to the steady state value of the optical response (in this case, related to the optical birefringence Δn). Correction is then made for solvent and stray birefringence contributions, determined in a previous experiment on the solvent alone. Each point on the decay curve is then converted into a birefringence value and curve fitted by a standard matrix method to give the initial slope (and hence D) for the decay process. Tables and graphs of Δn, the initial slope (S) and the square of the field strength (E^2) form the final output.

Performance

The system admirably meets the requirements for speed of manipulation and analysis. It eliminates the necessity for photographing the transients and yet allows one to do so, after a visual inspection of the transient, should an analogue record be required.

The limitations on the molecular diffusion constants that can be measured and the precision in the molecular parameters evaluated, are a direct reflection of the transient recorder characteristics. Firstly the resolution of the record to plus or minus one binary bit corresponds to a 3 per cent uncertainty in recorded amplitudes of E^2 if the full six bit word capacity is employed. Secondly there is uncertainty in the time *origin* of plus or minus one in the 128 samples of the sweep. This is important in the location of the start of the decay process, and is the reason why the applied pulse is required as a fiducial event. It gives an approximate decay time origin. The computer programme has been designed to search around this value for the position of sudden amplitude change in the transient response. The final error in the initial slope depends upon the trace noise and the decay rate relative to the sample interval. The third limitation of this particular recorder is the restriction to a single channel. Whereas it is unlikely that the pulse generator characteristics change between the two pulses, uncertainty would be eliminated if a two channel transient recorder could be used. Such a recorder has recently come on to the market (Table II).

An appraisal of the system was made through two experiments. Both involved the recording and analysis of birefringence transients using (a) the transient recorder and computation and (b) the conventional procedure of photographing the oscilloscope trace and analyzing it by projecting the negative onto a grid. The first experiment was on liquid nitrobenzene at a wavelength of 546 nm with pulsed fields up to 13 kV cm^{-1} and a duration of 2 ms. Laboratory grade nitrobenzene was used. The birefringence corresponds to a very clean, noise-free trace. Typical responses are shown in Figure 3 and comparative results are given in Table I for the steady-state amplitudes of the transients, determined using both the rapid recorder and the tedious C.R.O.

Table I

Comparison of the transient recorded data with the oscilloscope and manual analysis.

birefringence ($\Delta n \times 10^7$)		E^2 ($V^2cm^{-2} \times 10^{-7}$)		δ *per cent*
CRO	*TR*	*CRO*	*TR*	
3.58	3.46	1.89	1.88	2
6.75	6.51	3.73	3.90	8
9.64	10.04	5.06	4.99	— 5
13.71	17.85	7.65	7.51	— 3
30.45	30.28	18.00	17.80	— 1

δ represents the discrepancy $\left[\frac{\left(\frac{\Delta n}{E^2}\right)_{CRO} - \left(\frac{\Delta n}{E^2}\right)}{\left(\frac{\Delta n}{E^2}\right)_{CRO}}\right] 100$

Table II

Commercial transient recorders, known to the authors.

Type	*Inputs*	*ADC bits*	*Samples per sweep*	*Pretrigger sampling times*
B610	1	6	128	100 μs—5s
B610B	1	6	256	200 μs—10s
B802	1	8	1024	1,000 μs—20s
DL905	1	8	1024	200 μs—10s
B8100	2 single	8	2024	20 μs—20,000s
	2 dual	,,	1012 per channel	200 μs—20,000s

B and DL refer to Biomation and Data Laboratories respectively, while ADC is the analogue to digital conversion.

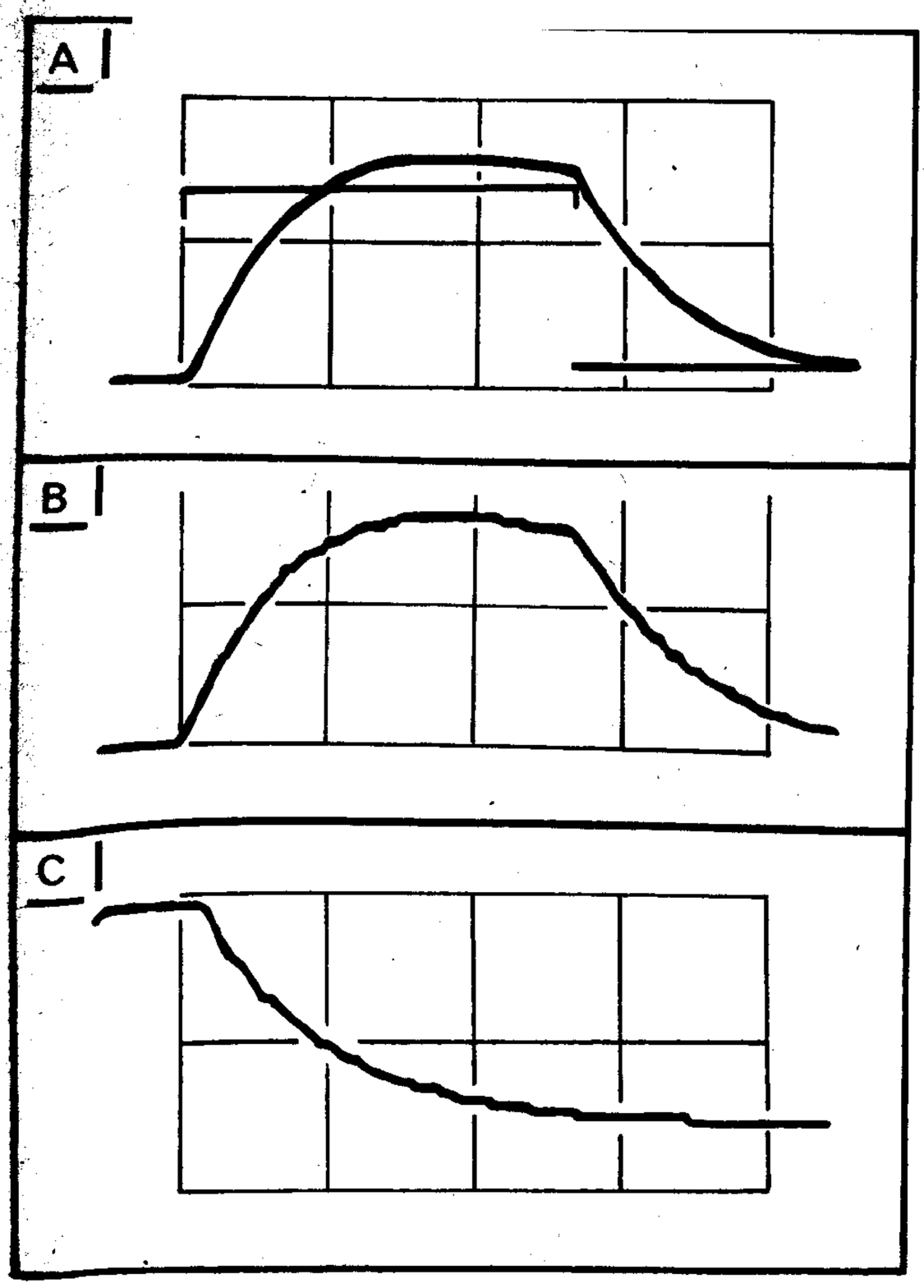

Figure 3. Transient responses with little noise.
A; Using oscilloscope with no recorder,
B; Oscilloscope display of analogue output from recorder,
C; as B, but for a recorded sweep of the decay alone.

and projection methods. The amplitude data have been transposed directly into $\triangle n$, the apparent birefringence (Jerrard *et al*, 1969). The average discrepancy in δ (see Table I for definition) was 3 per cent. The small liquid molecules relax too rapidly for D to be determined. The finite decay rate evident in Figure 3 was due to the photomultiplier time constant. It can easily be adjusted to the high value here by changing the photomultiplier loading. The transient recorder and the laborious log plot procedures indicated values of the time constant within 6 per cent of each other. This would correspond to a discrepancy in molecular dimensions of less than 2 per cent.

The second experiment was on a 1 per cent solution of the polypeptide polybenzyl-L-glutamate (PBLG) in ethylene dichloride (EDC). This system is typical of that studied by transient electro-optics. The molecule is a somewhat stiff helix in this solvent and the trace is more noisy that that of Figure 3. Fields of 0.2 ms duration and up to 17 $kVcm^{-1}$ amplitude were applied. Such fields exceeded the region of Kerr's law (where $\triangle n$ is proportional to E^2). With this more noisy system the two procedures for detection and analysis differed by an average of 5 per cent in δ. The initial slopes, and hence D, agreed within 7 per cent. As the log plot ordinate (Z(t)/Z(o)) descreased below a decade, the discrepancy widened, owing to the inability of the recorder to resolve accurately the base line of the transient. However it is the initial slope that gives the reliable and most useful data (Schweitzer and Jennings, 1972).

Conclusions

Data logging equipment in the form of a transient recorder, interface and tape punch can be incorporated easily into any apparatus for transient electro-optic experiments on macromolecular solutions. Using the low-cost Biomation 610 transient recorder, transients of greater than 100 μs could be handled with little loss in precision over the conventional, laborious method of photographic analysis. The above mentioned time limit suggests that molecules with approximate dimensions of 100 nm and above may be studied. Even without full on-line computer facilities, the very comprehensive analysis of the transients was undertaken in a time unequalled by conventional methods. Such a facility should prove invaluable in extending the transient electro-optic methods beyond the realm of static molecular characterization. One should be able to follow the time dependent changes in molecular dimensions and properties which accompany conformation changes.

The performance of the analytical system should improve with the development of faster and more versatile transient recorders with dual channel input. It should be noted however that dual channel operation lengthens the minimum sweep time, as with the recently introduced Biomation model 8100 recorder. In dual mode operation transients of 200 μs can be handled. This is slower than the model used here. In *single* mode operation the model 8100 has a sweep time of 20 μs which is much faster than that used in this study. Such speeds would enable rigid macromolecules of some 10 nm size to be studied.

Table II lists the instruments known to the authors which are currently available commercially.

Acknowledgements

Both authors express thanks to Applied Research Laboratories Ltd., of Luton, for constructing the interface and supplying the transient recorder and to Messrs. Kodak Ltd. for assistance in the purchase of the tape punch. One author (PJR) thanks the Science Research Council for a studentship.

References

Benoit, H. (1951). *Ann. Phys., Paris*, **6**, 561.
Brown, B. L. and Jennings, B. R. (1970). *J. Phys. E.*, **3**, 195.
Busch, G. E., Jones, R. P., Topp, M. R. and Rentzepis, P. M. (1972). *Rev. Sci. Instr.*, **43**, 777.
Itzhaki, R. F. (1966). *Proc. R. Soc.*, **B164**, 75.
Jennings, B. R. (1972). Ch. 13 in 'Light Scattering from Polymer Solutions', M. Huglin (Ed), Academic Press, London.
Jennings, B. R. and Baily, E. D. (1970). *Nature*, **228**, 1309.
Jerrard, H. G., Riddiford, C. L. and Ingram, P. (1969). *J. Phys. E.*, **2**, 761.
O'Konski, C. T. (1969). *Encycl. Polym. Sci. Technol.*, **9**, 551.
Perrin, F. (1934). *J. Phys. Radium, Paris*, **5**, 497.
Schweitzer, J. and Jennings, B. R. (1972). *Biopolymers*, **11**, 1077.
Stoylov, S. P. (1971). *Adv. Coll.* and *Inter. Sci.*, **3**, 45.
Tinoco, I. and Hammerle, W. G. (1956). *J. Phys. Chem.*, **60**, 1619.
Yoshioka, K. and Watanabe, H. (1969), in 'Physical Principles in Protein Chemistry' p. 335; Academic Press, N.Y.

Appendix 2.

Quantity	One c.g.c. unit	S.I. equivalent
E	statvolt cm^{-1}	$3{\cdot}00 \times 10^{2}$ Vm^{-1}
B	$cm\ statvolt^{-2}$	$1{\cdot}11 \times 10^{-7}$ mV^{-2}
K	$cm^{4} statvolt^{-2} gm^{-1}$	$1{\cdot}11 \times 10^{-10}$ $Kgm\ m^{4}V^{-2}$
$g_1 - g_2$	dimensionless	1
$\alpha_1 - \alpha_2$	cm^{3}	$1{\cdot}11 \times 10^{-16}$ $F\ m^{2}$
	debye = 10^{-18} esu	$3{\cdot}34 \times 10^{-30}$ $C\ m^{2}$
viscosity	poise = 1 gm $cm^{-1} sec^{-1}$	1 poise
wavelength	$\mathring{A}$	0·1 n m

c.g.s. to S.I. conversion table.